ISSN 2759-1417

BULLETIN OF THE LABORATORY FOR ZERO-CARBON ENERGY

VOL.4
2025

Laboratory for Zero-Carbon Energy (ZC)
Institute of Innovative Research
Tokyo Institute of Technology

BULLETIN OF THE LABORATORY FOR ZERO-CARBON ENERGY

(Formerly, BULLETIN OF THE LABORATORY FOR ADVANCED NUCLEAR ENERGY)

Abbreviation of the "**BULLETIN OF THE LABORATORY FOR ZERO-CARBON ENERGY**" is **"BULL. LAB. ZC. ENERGY"**

All communications should be addressed to the editor, Laboratory for Zero-Carbon Energy, Institute of Integrated Research, Institute of Science Tokyo (Tokyo Kagaku Daigaku), 2-12-1-N1-16, O-okayama, Meguro-ku, Tokyo 152-8550, Japan.

TEL. +81-3-5734-3052, FAX. +81-3-5734-2959, E-mail bulletin@zc.iir.titech.ac.jp

http://www.zc.iir.titech.ac.jp/

BULLETIN OF THE LABORATORY FOR ZERO-CARBON ENERGY
BULL. LAB. ZC. ENERGY, Vol.4, 2025

CONTENTS

Research staffs of
THE LABORATORY FOR ZERO-CARBON ENERGY,
INSTITUTE OF SCIENCE TOKYO
AS OF 2025 JAPANESE FISCAL YEAR

Director

Yukitaka Kato	Professor

Future Energy Division

Junichiro Otomo	Professor
Takehiko Tsukahara	Professor
Yoichi Murakami	Professor
Toshiyuki Yokoi	Professor
Hiroki Takasu	Associate Professor
Riku Enomoto	Assistant Professor
Shigehiko Funayama	Assistant Professor
Ryoji Kanno	Institute Professor

Nuclear Energy Division

Toru Obara	Professor
Yoshinao Kobayashi	Professor
Hiroshi Sagara	Professor
Noriyasu Hayashizaki	Professor
Yoshihisa Matsumoto	Professor
Katsumi Yoshida	Professor
Hiroshi Akatsuka	Associate Professor
Chikako Ishizuka	Associate Professor
Mizuki Uenomachi	Associate Professor
Tatsuya Katabuchi	Associate Professor
Hiroshige Kikura	Associate Professor
Masatoshi Kondo	Associate Professor
Koichiro Takao	Associate Professor
Hiroaki Tsutsui	Associate Professor
Masahiko Nakase	Associate Professor
Jun Hasegawa	Associate Professor
Shintaro Yasui	Associate Professor
Shota Ikeda	Assistant Professor
Naokazu Idota	Assistant Professor
Kentaro Urata	Assistant Professor
Yoshiki Kimura	Assistant Professor

Other Faculties

Masahiro Okamura	Specially Appointed Professor
Yosuke Shiratori	Specially Appointed Professor
Jun Sugimoto	Specially Appointed Professor
Kenji Takeshita	Specially Appointed Professor
Keigo Akimoto	Specially Appointed Professor
Hiroshi Asano	Specially Appointed Professor
Chikako Iwaki	Specially Appointed Professor
Ken Koyama	Specially Appointed Professor
Takao Nakagaki	Specially Appointed Professor
Tsuyoshi Fujita	Specially Appointed Professor
Atsushi Morihara	Specially Appointed Professor
Ayumi Ito	Specially Appointed Associate Professor
Hanna Hubarevich	Specially Appointed Associate Professor
Chi Young Han	Specially Appointed Associate Professor
Tomohiro Okamura	Specially Appointed Assistant Professor
Tadashi Narabayashi	Visiting Professor
Hidekazu Asano	Visiting Professor
Yuma Miyaoka	Research Administrator

Technical Staffs

Isao Yoda	Senior Technical Specialist
Kazuo Takezawa	Technical Specialist
Ken-ichi Tosaka	Technical Specialist
Atsushi Nezu	Technical Specialist

I. Research Reports

I-1 Development of particle accelerators and manufacturing human resource

Noriyosu Hayashizaki and Shota Ikeda

1. Multi-ion beam acceleration test using a heavy-ion therapy injector with high stability

Multi-ion therapy is a treatment method that uses various ion beams with different charges and masses, not limited to carbon ions. It is expected to achieve higher therapeutic efficacy than conventional heavy-ion cancer therapy. For example, in the hypoxic regions inside tumors that are highly resistant to radiation, beams of heavier ions such as oxygen or neon can be used to inflict more lethal damage on the DNA of cancer cells, while carbon ion beams can be applied to other areas. Conversely, for cancers that are more sensitive to radiation, the use of lighter ions such as helium can help reduce damage to the surrounding healthy tissues.

Therefore, multi-ion irradiation technology, which employs various ion beams according to tumor characteristics, holds great promise for further improving the treatment outcomes of heavy-ion therapy. In this study, we conducted beam acceleration tests with carbon and helium ions to establish multi-ion acceleration technology for an improved heavy-ion therapy injector, and evaluated the beam characteristics of each ion.

In the carbon ion (C^{4+}) acceleration test, various parameters such as beam current, emittance, and energy distribution were measured and compared with design values. As a result, a C^{4+} beam current of 150 μA was achieved, confirming stable acceleration at a practical level.

In the helium ion production test, we optimized the ECR ion source operating conditions and evaluated the production efficiency of the He^{2+} beam. It was found that the highest He^{2+} beam current was obtained under the conditions of a gas flow rate of 0.13 sccm and a microwave power of 275-300 W. Next, in the He^{2+} beam acceleration test, the beam transmission and energy distribution were measured, confirming that a He^{2+} beam current of 158 μA was successfully accelerated to an energy level comparable to that of the C^{4+} beam.

2. Liquid lithium flow demonstration for the design of a high intense LINAC based neutron source [1]

High intensity accelerator-driven neutron sources with a free surface liquid lithium (Li) target system are widely being designed and developed because heat dissipation under high beam power is easier compared to a solid target and there is no need to periodically replace the target. However, a linear accelerator must be operated under ultra-high vacuum ($<10^{-5}$ Pa) to avoid beam loss with the residual gas and keep the designed performance. On the other hand, a liquid Li target system should be handled under much lower vacuum ($>10^{-3}$ Pa) to avoid Li boiling.

We assembled a 1/10 scale experimental setup of the high energy beam transport section of the advanced fusion neutron source accelerator and demonstrated the design with a liquid Li loop system. Although the outgassing was higher than expected, differential pumping of 10^{-4} and 10^{-2} Pa was experimentally demonstrated under Li flow.

3. A collaborative project between Science Tokyo, technical high school and KOSEN for developing manufacturing human resource and promoting STEAM education.

In recent years, Japan has been facing a chronic labor shortage, and the lack of science and engineering graduates from high schools has become a particularly serious issue. The job openings-to-applicants ratio for the students of technical high schools has been increasing year by year. Technical high schools play an important role in developing Japan's manufacturing human resources, yet it is said that students at these schools have few opportunities to see, experience, and learn about cutting-edge science and technology firsthand.

This project aims to establish a unique collaborative model between Science Tokyo, technical high schools and National institute of technology (KOSEN) for expanding the base of manufacturing human resource, mainly through cooperation focused on "Project Study" within "Curriculum Guidelines". In addition, we have been organizing STEAM education and Science Tokyo and high school collaborative lectures, introducing students at technical high schools to advanced science and technology centered on our research activities.

In FY2024, this project was selected for Science Tokyo's "Support Program for the Promotion of Science Education (Project to Broaden the Base of Manufacturing Human Resources and Promote STEAM Education)". As part of this initiative, Science Tokyo and high school collaborative lecture was held at NAGANO Technical High School, targeting second-year students in the course of electrical and electronic engineering. A senior researcher from the National Institute of Advanced Industrial Science and Technology (AIST) was also invited as a lecturer.

Furthermore, the students of NAGANO Technical High School presented a poster session on the activities of this project at the 2025 Shinshu Science Camp "Shinshu Science Meeting".

Acknowledgments

The collaborative project between Science Tokyo, technical high school and KOSEN for developing manufacturing human resource and promoting STEAM education is partially supported by AirTrunk and Fujitsu Limited.

References

[1] Takashi Ebisawa, et al.; e-Journal of Surface Science and Nanotechnology 23, 296-305 (2025).

I-2 GXI VISION 2050 for Sustainable society

Yukitaka Kato, Takao Nakagaki, Yuma Miyaoka, Keigo Akimoto and Kenji Takeshita

1. Green Transformation

Four years have passed since the Japanese government announced in October 2020 that it would achieve carbon neutrality (CN) by 2050, and the government has been revitalizing the Green Transformation (GX) movement that will lead to economic growth. The Japanese government's policies are timely, and we hope for future progress and development for Japan.

At the G7 Ministers' Meeting on Climate, Energy and Environment in April 2024, it was stated that Japan is one of the few countries that has achieved "on track" with respect to the Nationally Determined Contribution (NDC) of the Paris Agreement. However, this is largely due to the decline in energy consumption caused by the slump in domestic production in energy-intensive industries, and as the economic downturn caused by COVID-19 recovers and power consumption continues to increase due to the rapid increase in data centers, further emission reductions may entail even greater cost burdens.

Institute of Science Tokyo's Green Transformation Initiative (Science Tokyo GXI, GXI)[1,2] (Mission Realization Acceleration Funding Project of Ministry of Education, Culture, Sports, Science and Technology, 2022-2026) aims to realize GX technologies to achieve CN through open innovation in collaboration between industry, government, academia and the public sector.

GXI activities to date have confirmed that the technologies possessed by Japanese companies and universities are excellent and that their potential for social contribution is very large by international standards. In addition, GX technologies that are emerging and progressing in each organization are judged to have a high potential to contribute to Japan and the world. Therefore, based on the activities of the GXI and taking into consideration the above situation, GXI published a position paper with an eye towards 2050, at the time of drafting Japan's 7th Strategic Energy Plan, named as GXI VISION 2050 – Affordable* transition to carbon neutrality in the prospect of social inertia**– in September 2024 [3].

*Affordable :

It means affordable and fully acceptable, and is mainly used in the context of the price of goods and services, economic burden, etc. Here, it refers to an attitude that does not simply pursue cheapness or low barriers to introduction, and is used in a broad sense, not just in economic terms.

**Social Inertia :

This concept originated in psychology and sociology, and refers to resistance to social change or maintaining the status quo in a community, etc. Here, by analogy with mechanical inertia proportional to mass, it is not limited to the above concept in modern communities and organizations, but also refers to the difficulty of rapid change due to various factors such as infrastructure that is assumed to be used for a long time, huge production facilities, and complex and overall huge supply chains, and the concept is used to extend to social systems in general.

2. Three Pillars in the VISION

The picture of GXI VISION 2050 proposed by Science Tokyo GXI is shown in Fig. 1. We claim that the following three technological pillars are important to achieve CN by realizing GX.

(1) Ensuring sufficient zero-carbon energy: To ensure affordable and sufficient zero-carbon energy as a primary energy source, it is important to make renewable energy mainstream as well as to utilize nuclear power.

(2) Ensuring rational capacity and adjustment capabilities of energy storage systems: In making renewable energy the mainstream, we assert the importance of a system (ESMOS, Energy Storage Mix Optimization System) that rationally integrates and optimizes various energy storage technologies.

(3) Strengthening GX through carbon recycling: The establishment of carbon recycling-based industries through carbon value chains between different industries is important as a GX technology

Based on the GX technologies described in the paper, we hope that industry, government, academia, and citizens will work together to achieve carbon neutrality through an affordable transition that takes into account social inertia.

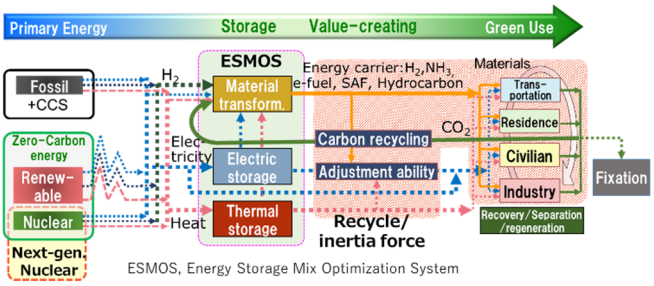

Fig. 1 The GX society trend that Science Tokyo GXI aims for to achieve CN and the technologies that should be strengthened in GXI VISION 2050 to realize it [3]

References

1. Science Tokyo GXI, https://www.gxi.iir.titech.ac.jp/about/
2. Y. Kato; Base Sekkei Shiryo, Kensetsu Kogyo Chosakai, Tokyo, Journal of Nuclear Materials, No. 127, 36-38(2025)
3. GXI VISION 2050, Science Tokyo GXI (2024), https://www.gxi.iir.titech.ac.jp/research/gxi-vision-2050/

I-3 Metallurgy for zero-carbon iron/steelmaking process and energy systems

Yoshinao Kobayashi

1. Introduction

Toward realization of Zero Carbon society, it is essential to establish the material creation process with carbon neutral loop and secure safety energy supply systmems . We are targeting the realization of carbon neutral iron-making process as a carbon-circulating green industrial system, utilization of scrap steel with the countermeasure copper shortness as material circulating process, as well as contribution to the development of thermodynamics of nuclear chemistry to promote safe and prompt decommissioning of Fukushima Daiichi Nuclear Power Plant in combination with OECD/NEA based projects

2. Carbon-neutral iron-making process

In the conventional ironmaking process, blast furnace has been centered upon as the most efficient molten metal production process that our race has ever devised. During this process, iron oxide in iron ore is reduced by carbon in cokes inevitably produces CO_2 fully exhausted to the environment. Direct iron ore smelting reduction process[1] also emits CO_2 produced molten iron oxide reduction process originated from the usage of coal with impurities such as phosphorus and sulfur, the same goes for blast furnace process. To solve these problems, direct steelmaking by CO gas blowing reduction is newly proposed, under the scheme of Science Tokyo GXI(Green transformation initiative) [2], which has been launched on the platform of Laboratory for Zero-Carbon Energy. In this proposed process, CO gas blowing from the bottom of furnace reduces iron oxide dissolved in the molten slag to resultantly produce CO_2. Emitted CO_2 gas which can be reduced by electrolyzation using zero-carbon energy to revert back to CO, which can be used as reducing gas again for bottom blowing. In this loop, emission of CO_2 gas is virtually zero, where, carbon is circulating as if playing a quasi-catalytic role continuously producing metallic iron. Differently from conventional ironmaking process starting from coal, impurity is not included in principle because recycled CO does not contain any other element, possibly resulting in steelmaking process without refining.

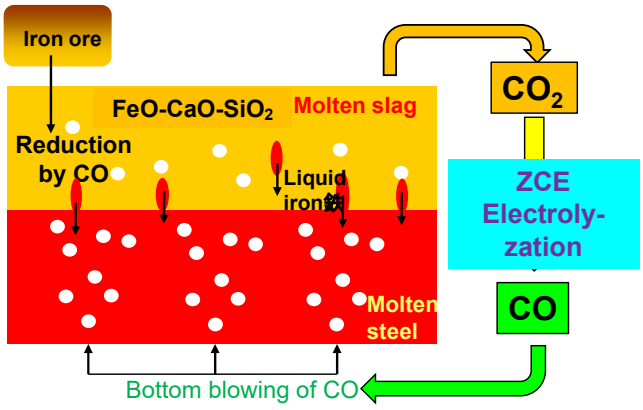

Fig.1 Conceptual cross section of ZC ironmaking process

3. Steel scrap recycling process

The accumulated amount of steel once having come on to the market is increasing in the world including that still in service as well as that beyond end-of-life. Rotary flow returning back from this accumulation to crude steel production as iron resource would be important factor to reduce CO_2 emission, essentially because steel scrap has been already reduced to metal, with no need of iron oxide reduction process inherently accompanying CO_2 emission. Steel scrap usually contain nobler element than iron such as copper, bringing about characteristic problem of copper embrittlement which is crucial in viewpoint of processability. To avoid this problem originated from copper, many types of countermeasure has been taken up and tried for application. Among them, copper sulphide precipitation has been paid growing attention to suppress the above problem by stabilizing copper as solid phase separated from matrix, which may weaken the factor for formation of copper enriched liquid phase induced by preferential oxidation of iron [3]. Experimental study was implemented to mainly investigate the critical cooling rate for the precipitation of copper sulphide in our laboratory. On the basis of the observational results on cross section of the as-cast or heat treated sample with variation in experimental condition, several tens kelvin per second would be probable value for the critical cooling rate[4]. Enlargement of usage of steel scrap for crude steel production should be important issue in viewpoint of hybridization of iron-steelmaking process.

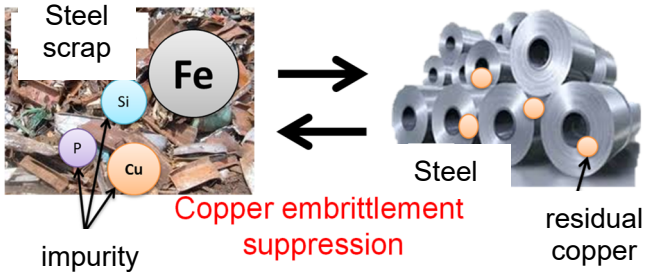

Fig.2 Condensation loop of copper in steel scrap

Reference

1. T. Kitagawa: *Tetsu-to-Hagané*, Vol.88, p.432, (2002)
2. http://www.gxi.iir.titech.ac.jp/index.php#gxi
3. Z. Liu, Y. Kobayashi, K. Nagai, Jian Yang and M. Kuwabara: *ISIJ International*, 46, 744-753 (2006)
4. Y. Kobayashi:; *The 183rd ISIJ Meeting* Mar. 2022.

I-4 Recognition and Repair of DNA Double-strand Breaks: From Molecular Mechanisms to Cancer Therapy and Radioprotection

Yoshihisa Matsumoto, Mikio Shimada*

1. Background

Ionizing radiation (IR) causes various biological effects, including the genesis and cure of cancer, through induction of DNA damages. DNA double-strand break (DSB) is considered the most deleterious type of DNA damage among those which are induced by IR. Understanding the molecular mechanisms of the recognition and repair of DNA damages will bring us further advance in cancer therapy and radioprotection.

DNA-dependent protein kinase (DNA-PK), Ataxia telangiectasia mutated (ATM) and ATM- and Rad3-Related (ATR) are structurally related protein kinases (enzymes to phosphorylate proteins) and members of phosphatidyl-inositol 3-kinase-like kinases (Fig. 1). DNA-PK and ATM act as the sensors for DSBs and ATR acts as the sensor for single-stranded DNA, which appears in ongoing DNA replication and repair. These protein kinases are shown to phosphorylate over 1,000 proteins and thought to orchestrate DNA repair and other cellular responses, such as cell cycle checkpoint and apoptosis. A transcription factor p53 activates the expression of a great number of genes, which are required for cell cycle checkpoint and apoptosis.

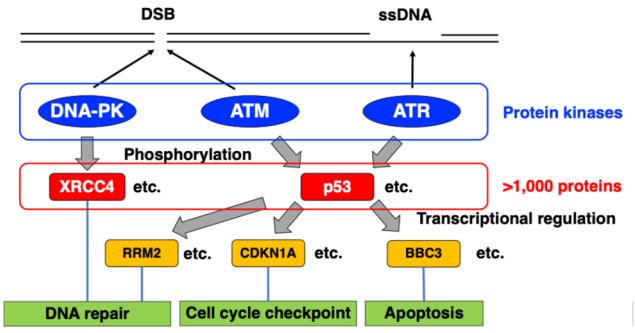

Fig. 1 Overview of cellular response to DNA damage.

Now four pathways to repair DSBs are known in eukaryotes (Fig. 2): non-homologous end joining (NHEJ), alternative end joining (A-EJ), single strand annealing (SSA) and homologous recombination (HR). Among them, NHEJ and HR play major roles in human.

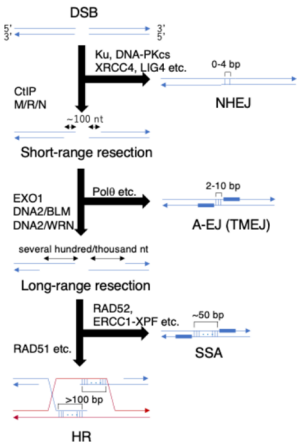

Fig. 2 Four pathways for DSB repair (Right).

2. Molecular mechanisms for the recognition and repair of DSB: the targets and roles of DNA-PK in NHEJ

We have studied the mechanisms for the recognition and repair of DSBs, especially focusing on DNA-PK. DNA-PK consists of the catalytic subunit (DNA-PKcs) and Ku70-Ku80 heterodimer and is thought to play a pivotal role in NHEJ with DNA ligase IV, XRCC4, XLF and PAXX. Despite lines of evidence indicating that the kinase activity of DNA-PKcs is essential for NHEJ, the target(s) and role(s) of phosphorylation remain unclear for three decades (1). After our first report of XRCC4 phosphorylation by DNA-PK in response to DSBs (2), we and others have identified at least six phosphorylation sites in XRCC4 by DNA-PK. We have generated phosphorylation-specific antibodies correspond-ing to all of these six phosphorylation sites and reported that Ser260 and Ser320 are phosphorylated by DNA-PK in cellulo (3,4). Notably, four out of six phosphorylation sites are located in XRCC4 extremely C-terminal (XECT) region, which is unique to and highly conserved in vertebrates (5) (Fig. 3). As DNA-PKcs is absent in most of invertebrate species, it is surmised that XECT region might have emerged simultaneously with vertebrates to sophisticate the regulation of NHEJ by DNA-PK. This interplay might also have evolved highly adaptive immune system by diversification of antibodies through V(D)J recombination.

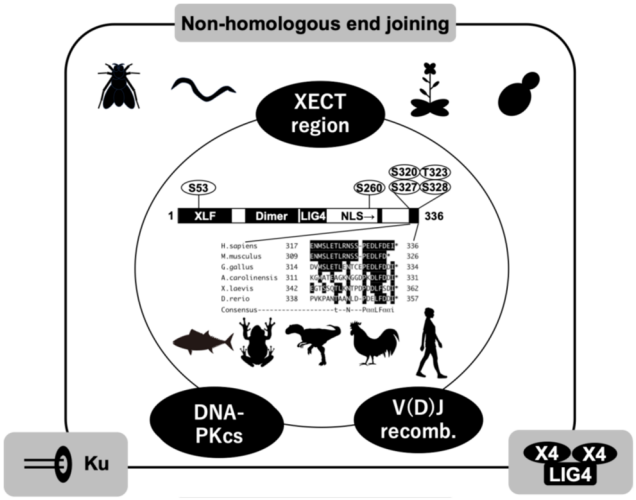

Fig. 3 Significance of interplay of DNA-PK and XRCC4 through XECT region from an aspect of vertebrate evolution.

*Present affiliation: Radiation Effects Research Foundation (since July 1, 2025)

To deepen further the understanding of DSB repair, we are analyzing the function and regulation of proteins involved in the processing of DNA ends (adapting the structure of DNA ends for ligation) such as polynucleotide kinase phosphatase (PNKP) (6-8) and aprataxin (APTX) (9).

3. Possible medical application: 1. Individual Difference in DSB Repair Ability through NHEJ and Radiosensitivity

Mutations in the genes involved in NHEJ were found in human patients exhibiting immunodeficiency, microcephaly and/or growth defect, indicating that NHEJ is essential for the development, particularly, in immune and neuronal systems (10,11). There is increased attention to the variation in radiosensitivity among human individuals from the viewpoint of personalized radiotherapy and radioprotection in next generation. Radioresistant patients may be treated with higher dose for better control of tumors (Fig. 4). On the other hand, radiosensitive patients may be treated with lower dose to minimize adverse effects, keeping the tumor control rate. In our collaboration with clinical radiologists and oncologists, it has been shown that the activity or abundance of these molecules, which vary substantially among individuals, are associated with susceptibility to certain types of cancer and with outcome and prognosis of cancer radiotherapy. For example, DNA-PK activity in peripheral lymphocyte is associated with relapse-free survival of prostate cancer (12). Expression of XRCC4 in breast cancer tissue is associated with ipsilateral recurrence after breast-conserving radiotherapy (13). We are now investigating possible correlation between the polymorphism in DSB repair genes and clinical radiosensitivity.

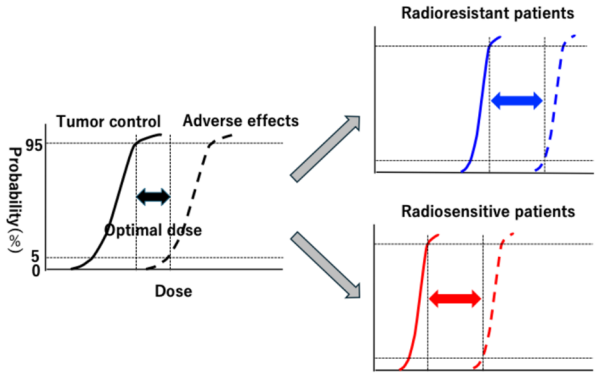

Fig. 4 Concept of personalized radiotherapy based on individual radiosensitivity.

4. Possible medical application: 2. Enhancement of Radiosensitivity Targeting DSB Repair through NHEJ

Since the discovery of the importance of DNA-PK in DSB repair through NHEJ, a great number of small molecules inhibiting DNA-PK have been developed for sensitization of cancer cells to radiotherapy and chemotherapy (14). Potent and selective inhibitors which were developed in 1990s to 2000s, such as NU7441, have been useful in functional studies of DNA-PK. Several recently developed inhibitors, including M3814 and AZD7648, are under clinical trials. Our research tools will be useful in evaluating the *in situ* activity and specificity of these inhibitors. For example, DNA-PK activity *in situ* in the presence of inhibitors can be monitored by XRCC4 phosphorylation status. The specificity of the inhibitors can be evaluated by testing whether the radiosensitivity of DNA-PKcs-deficient cell is changed or not. In addition to DNA-PKcs, an inhibitor for DNA ligase IV, SCR-7, was proven to sensitize radioresistant colorectal cancer cells (15).

4. Ongoing research and future perspectives

For the understanding of the mechanisms of the recognition and repair of DSBs more in depth, we are introducing several cutting-edge approaches. First, we are exploring the target(s) of DNA-PK employing proteomic approaches. Second, we are analyzing alterations in genomic sequence and structure through whole genome sequencing using next generation sequencer to find the footprint of NHEJ. Third, we are seeking to understand the role of the recognition and repair of DSB in the context of organogenesis through the studies using induced pluripotent stem (iPS) cells and derived organoids (16-18).

Acknowledgments

We thank laboratory members and external collaborators. Our study was supported in part by Grant-in-Aid for Scientific Research from JSPS (20H04334, 21K19842 to YM; 22K12369 to MS).

References

1. Y. Matsumoto, M.K. Sharma; Journal of Radiation and Cancer Research, Vol.11, pp.123-134 (2020).
2. Y. Matsumoto, et al.; FEBS Letters, Vol.478, pp.67-71 (2000).
3. M.K. Sharma, et al.; Journal of Radiation Research, Vol.57, pp.115-120 (2016).
4. A.R. Amiri Moghani, et al.; Journal of Radiation Research, Vol.59, pp.700-708 (2018).
5. R. Wanotayan, et al.; Biochemical and Biophysical Research Communications, Vol.457, pp.526-531 (2015).
6. K. Tsukada, et al., PLoS One, Vol.15, e0239404 (2020).
7. K. Tsukada, et al.; Mutation Research/Fundamental and Molecular Mechanisms of Mutagenesis, Vol.822, 111727 (2020).
8. K. Tsukada, et al.; eLife, Vol.14, e99217 (2025).
9. R. Imamura, et al; Journal of Radiation Research, Vol.64, pp.485-495 (2023).
10. Y. Matsumoto, et al.; Genes, Vol.12, pp.1143 (2021).
11. A.D.D.C. Asa, et al.; Journal of Radiation Research, Vol.62, pp.380-389 (2021).
12. M. Someya, et al.; Journal of Radiation Research, Vol.58, pp.225-231 (2017).
13. M. Kitagawa, et al.; Strahlentherapie und Oncologie, Vol.195, pp.648-658 (2019).
14. Y. Matsumoto; International Journal of Molecular Sciences, Vol.23, pp.4264 (2022).
15. S. Jun, et al.; Nature Communications, Vol.7, pp.10994 (2016).
16. M. Shimada, et al.; Radiation Research, Vol.202, 719-725 (2024).
17. M. Shimada, Y. Matsumoto; Radiation Research, Vol.203, 410-420 (2025).
18. M. Shimada, et al.; Journal of Biological Chemistry, Vol.301, 110328 (2025).

I-5 Development of superior CO_2 adsorbent based on 2.5-dimensional covalent organic frameworks

Yoichi Murakami

1. Introduction

Presently, atmospheric CO_2 concentration is rapidly increasing due to anthropogenic CO_2 emission, rendering it a major cause of climate change. As a counter measure, development of a large scale and low-cost CO_2 capture and separation technology is essential. However, present amine scrubbing method cannot satisfy this requirement. We have been working on the development of new generation of CO_2 adsorbent based on covalent organic frameworks (COFs). COFs are a recently emerging class of crystalline porous solids. Recently, we developed new COFs that are promising candidate for addressing the aforementioned issues.

2. Overview of outcomes

We have developed novel type of COFs described in Fig. 1. Specifically, we generated these COFs, **TK-COF-4** and **TK-COF-5**, by combining a tetrahedral monomer (**TAM**) and a triangular monomer (**TFPT/TFPB**). Unexpectedly, one out of the four amines in TAM was unreacted, resulted in the formation of unprecedented 2.5-dimensional structure; *i.e.*, microscopically 3D but macroscopically 2D (Fig. 1). Further details are presented in References 1 and 2.

Acknowledgments

This work was supported by JSPS KAKENHI Grants JP22K18286 and JP23H00165 (for Y. M.). This work was supported in part by the Cooperative Research Program of "Network Joint Research Center for Materials and Devices" from MEXT. We thank the support from the Science Tokyo GXI program from MEXT. We also thank the Open Facility Center at Institute of Science Tokyo for support provided for the measurements and Ms. Yuko Kishida for the support provided for determining the crystal face indexes.

References

1. T. Kitano, S. Goto, X. Wang, T. Kamihara, Y. Sei, Y. Kondo, T. Sannomiya, H. Uekusa, and Y. Murakami, *Nature Communications*, Vol. 16, article number 280 (10 pages), (2025).
2. News release from *EurekAlert* on February 14, 2025. URL: https://www.eurekalert.org/news-releases/1073729.

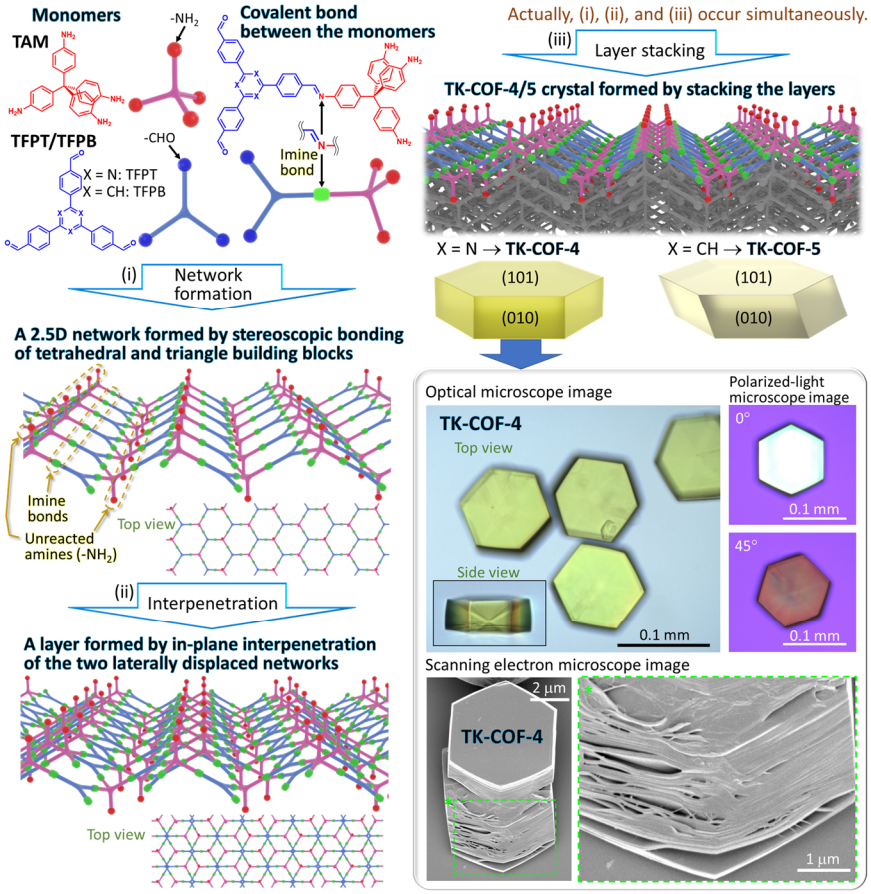

Fig. 1 Formation of 2.5D-COFs.

I-6 Design concept study for RFBB

Toru Obara

1. Introduction

Rotational Fuel-shuffling Breed-and-Burn fast reactor (RFBB) is a fast reactor which is possible to use uranium resources effectively and reduce the amount of spent fuel without reprocessing of spent fuels. In the reactor concept, it does not need to change the reactor design of conventional fast reactors. The fuel is natural uranium or depleted uranium only. The uranium is converted into fissile material in the core and is used for fissions to generate energy. In fast reactors, there are some options in fuel material and coolant material. In the study, several analyses were performed for the core using nitride fuel or metallic fuel with sodium coolant, lead coolant, or lead-bismuth eutectic coolant. Feasibility of the use of silicide fuel was investigated too.

2. Optimization of transition phase RFBB for sodium-cooled nitride fuel

The objective of this study was to clarify the feasibility of core design for sodium-cooled nitride fuel RFBB (RFBB-NS) to achieve criticality from startup. In this study, core design optimization and analysis of key parameters during the transition phase were performed for a core of 450 MW thermal power, 180 cm height, and 134 cm equivalent radius. In the analysis, a core was first designed to reach criticality in equilibrium using only natural uranium. Based on this core, a core was designed to reach criticality from startup by replacing the first loaded fuel with enriched uranium. Subsequently, a core with adjusted enrichment was designed, and changes in burnup, radiation damage, and other key indices were analyzed. In addition, scenarios such as control rod insertion and void generation were also studied. The results of the analysis showed that the effective multiplication factor was from 1.004 to 1.025, the burnup of the discharged fuel was 258 MWd/kgHM, and the maximum radiation damage of the cladding tube was 674 DPA. The core became subcritical by the complete insertion of control rods, and the void coefficient and Doppler coefficient were 2.69$ and -0.41 pcm/K, respectively. The analysis results showed that the excess reactivity could be optimized. The analysis of each major index was also performed and it was clarified that there was no safety problem for the reactor [1].

3. Feasibility of Innovative Lead-Bismuth-cooled Fast Reactor Core Design Using Metallic Fuel

The application of metallic fuel has a long history in nuclear engineering, it has the advantages such as high thermal conductivity and low heat capacity ensure the fuel can be effectively cooled and limit the amount of heat that the fuel stores. LBE was selected as the coolant in this study, it has lower melting point than lead, which contributes to the core and improves neutronic performance. The purpose of this study was to assess the feasibility of an LBE-cooled metallic fuel RFBB (RFBB-MLB). For the reference core, a 400 MWth setting with an 820-day shuffling interval was investigated. The height of the core was 220 cm, and its equivalent radius was 190 cm. The metallic U-2Zr fuel was assembled in 288 hexagonal FAs at the core's center, which was surrounded by 66 reflector assemblies and 72 borated stainless-steel shield assemblies. The FA at the center of the original design was replaced by a coolant channel, which satisfies the shuffling strategy requirement. The fresh FA moves from the most peripheral regions of the core to the inner zone, moving in a zigzag pattern, and then discharges at the middle of the core. The analysis results showed the core was able to operate under critical conditions and sustain the Breed-and-Burn (B&B) operating mode for both thermal power settings. It was clarified that the core could reach critical conditions and maintain the B&B operating mode for 400MW thermal power setting [2].

4. Burnup Characteristics of Silicide Fueled RFBB with Sodium Coolant

In recent years, research has been conducted on the use of silicide fuel in power reactors. Although silicide fuel is inferior to nitride fuel in heavy metal density and thermal conductivity, it has the advantage of not requiring isotope enrichment, which is necessary for nitride fuel. The objective of this study was to clarify the feasibility and burnup characteristics of RFBB with silicide fuel and sodium coolant (RFBB-SS). In the analysis, first, the characteristics of the equilibrium burnup core were obtained by burnup analysis with fuel shuffling in a core loaded only with natural uranium. Next, a startup core was configured based on the neutron multiplication factor of each fuel assembly in the equilibrium burnup core, and a burnup analysis was conducted while repeating fuel shuffling to load natural uranium to the fresh fuel. The fuel shuffling interval was optimized to suppress the change in the effective multiplication factor. As a result, it was clarified that this reactor is critical in the equilibrium burnup state and that the criticality is maintained from startup to equilibrium burnup state. The power distribution in the core remained almost unchanged from startup to equilibrium burnup state. The feasibility of RFBB-SS was clarified by this analysis. [3]

5. Feasibility of lead cooled nitride fuel RFBB

The purpose of this study was to demonstrate a practical core design for a lead-cooled nitride fuel RFBB (RFBB-NL). The core design is based on the Westinghouse Lead Fast Reactor and uses sodium-bonded natural uranium nitride fuel encased in ODS cladding. Numerical simulations confirmed the reactor's potential to maintain criticality in equilibrium. In addition, this study investigated the startup core design with high-assay low-enriched uranium nitride fuel. While confirming the feasibility of the startup core to

sustain the RFBB mode, the study suggests the possibility of further optimization to control excess reactivity and increase proliferation resistance. [4,5]

6. Concluding remarks

The feasibility of RFBB was investigated for the core with several fuel materials and coolant materials. Each of them has its unique feature. The study was focused on the neutronic feature and heat removal feature in steady state. Transient analyses in accidental condition will make it clear the tolerance in accidental condition of each concept. Experimental study for cladding material in high radiation dose also needed as future work.

References

1. Y Zushi, T. Obara: Proc. of 2025 annual meeting of AESJ, 2C15 (2025).
2. X. Zhao, T. Obara: Proc. of Global Symposium on Lead and Lead Alloy Cooled Nuclear Energy Science and Technology 2024 (GLANST 2024), 30 September – 2 October 2024, Brasimone, Italy (2024).
3. T. Obara, O. Sambuu: Proc. of 2024 autumn meeting of AESJ, 1G10 (2024).
4. A. Stafie, J. Nishiyama, T. Obara: Nucl. Sci. and Eng., Vol. 199, pp. 266-279 (2025)
5. A. Stafie, T. Obara: Ann. of Nucl. Energy, Vol. 218, 111379 (2025).

I-7 Innovative Nuclear Reactor Systems with Enhanced Safety Security and Non-proliferation Features – Summary of the academic year 2024 -

Hiroshi Sagara

1. Introduction

The Innovative Nuclear Reactor Systems with Enhanced Safety Security and Non-proliferation Features have been investigated in Sagara laboratory. This is the summary report on the research activity in the Japanese academic year 2024.

2. Innovative nuclear reactor with enhanced safety, security and non-proliferation

2.1. Sodium Cooled Fast Spectrum Reactors

Development of a passive safety shutdown device to prevent core damage accidents in the demonstration class MOX fuel loaded large-scale fast reactors has been performed, and the performance of the device in reactivity control and nuclear material management were evaluated from the reactor physics and non-proliferation perspectives [1].

The applicability study of the developed device to the small-scale metallic fuel loaded fast reactor was also performed, and the reactor design was proposed for long term operation without fuel exchange for more than 10 years. The effectiveness of the device was demonstrated for unprotected transient over power (UTOP) and unprotected loss of flow(ULOF) events [2].

The feasibility was evaluated on the increased ^{238}Pu production in proliferation-resistant U-10Zr fuel produced from reprocessed uranium(RepU) containing unseparated ^{237}Np in small sodium-cooled fast reactor. Using RepU with unseparated ^{237}Np can accelerate the production of ^{238}Pu at the beginning of the burnup period, up to a ^{238}Pu weight percent of 3% by only 1 MWd/kg, avoiding the production of weapon-grade-Pu entirely. Additionally, the material attractiveness of plutonium present in discharged fuel at each refueling interval can be downgraded by one level from that of standard U-10Zr fuel [3].

2.2. High Temperature Gas Cooled Reactors

In High Temparature Gas Cooled Reactors (HTGRs), a dual neutron energy spectrum core layout was proposed to implement the fuel management strategy; in addition to the original fuel zone of a reference core design (driver zone), the outer reflector blocks were replaced with fuel blocks called the “efficiency zone” for additional irradiation. The impact of neutron energy on the burnup extension in the efficiency zone has also been investigated by changing the fuel pin pitch inside the fuel block to change the moderator-to-fuel ratio. Numerical simulations showed that extended burning in the efficiency zone with the pin-pitch unchanged for 1 extra irradiation batch could increase discharge fuel burnup from 125.9 GWd/t to 140.4 GWd/t. The proliferation resistance of the discharged fuel also improved due to rise in Pu-238 ratio from 5.1 to 7.3%. Moreover, increasing the pin-pitch of the fuel blocks and 2-batch additional irradiation in the efficiency zone could potentially increase the burnup and Pu-238 ratio of the discharged fuel [4].

2.3. Small and medium PWRs with silicide fuel

Proliferation resistance of small and medium PWRs loaded with U_3Si_2 fuel was evaluated for the on-site refueling reactor system and the transportable reactor system without onsite refueling for 10 years, and safeguard issues were revealed by analyzing the misuse of the facilities and diversion pathways of nuclear materials on each system. The vulnerable diversion pathways unique to small and medium reactors were identified for irradiated fuel assembly and nuclear reactor as targets. Further, the conversion time of silicide fuel could be higher than that of the oxide fuel. Moreover, the inspection frequency could be reduced regardless of irradiation or the presence of direct-use materials, such as Pu. The addition of MA to the fuel is a technical option for initial reactivity reduction and enhances proliferation resistance [5].

2.4. Off-shore Floating Nuclear Power Plant

An offshore floating nuclear power plant (OFNP) has been proposed to drastically reduce the impacts of earthquakes and tsunamis, enhances heat removal functions based on the massive amount of surrounding sea water, and fundamentally eliminates the need for resident evacuation. It was clarified the proliferation resistance (PR) of OFNPs against host nations. As a result, there were no significant PR differences between onshore and offshore plant locations. In addition, this study suggests extending the operation period per batch during fuel transfer within the OFNP and increasing the number of fuel assemblies to be transported outside the OFNP at one time [6].

As for the security event study of OFNP, simulation study of hypervelocity jet underwater was performed for physical protection design of offshore floating nuclear power plant against light torpedo threats. The installation of underwater nets is recommended, located at least 5.0 m away from the OFNP [7].

2.5. Accelerator Driven Systems

With an accelerator-drive system (ADS cycle), the material attractiveness of plutonium was evaluated for nuclear non-proliferation by assuming the diversion of items from the facilities in the transuranium fuel cycle. The evaluation results were compared with the material attractiveness of MOX fuel assemblies for conventional boiling water reactors. All items in the ADS cycle, regardless of whether they were fresh or spent fuel, were

found to have the same attractiveness as Pu in the BWR-MOX spent fuel assembly as low level, avoiding any high or medium attractiveness level vulnerable for the proliferation risks [8].

3. Non-destructive assay technology for nuclear security and safeguards

3.1. U enrichment measurement with Photonuclear reaction induced by bremsstrahlung X-ray

To enhance the security measures socially demanded in the border control, non-destructive assay technology with photonuclear reaction induced by bremsstrahlung X-ray has been performed to identify and measure the uranium enrichment, and the measurement system requirements for photofission signal detection with coincidence neutron counting method was investigated. For the experimental simulation, the Kyoto University electron linear accelerator facility, which is known as KURNS LINAC, was modeled and simulated [9].

3.2. Special Nuclear Material Measurement in Molten Fuel Debris with Passive Neutron Measurement Method

Development of a method for the determination of spontaneous fission nuclides in irradiated fuel has been performed and its applicability to Pu quantification in fuel debris by dual time neutron measurements was investigated. Using the difference in half-life of each nuclide, Pu-240 effective mass can be quantified by two neutron measurements with long time intervals. The Pu mass can be quantified by utilizing the correlation between the mass ratio of Cm-244/ Pu-240 effective and the mass ratio of Pu/ Pu-240 effective. The results show that a long-time interval is required to reduce random errors. When the interval between the first and second measurements is 32 years, the Pu-240 effective mass and Pu mass can be quantified with uncertainties of 10-50% depending on the presence of water in the storage canister and the burnup condition of the irradiated fuel, including a mixture of several burnup compositions in fuel debris [10].

3.3. HEU detection by Active Neutron Method with Water Cherenkov Neutron Detector

Water Cherenkov neutron detector (WCND) has been developed with high efficiency, availability, and affordability for nuclear security. In the reference [11], characterization of the WCND was conducted through Monte Carlo simulations and test experiments using prototype detectors.

Compact and transportable system for detecting lead-shielded highly enriched uranium was also developed by using ^{252}Cf rotation method with a water Cherenkov neutron detector. This cost-effective NDA system was evaluated as capable of detecting 4.17 g of ^{235}U within a 12 min measurement period using a ^{252}Cf source of 3.7 MBq. Integrating this system into border control measures can enhance the prevention of HEU proliferation significantly and offer robust deterrence against nuclear terrorism [12].

3.4.Passive Neutron Emission Tomography

Development of passive neutron emission tomography (PNET) has been performed robust to its various inhibiting factors and its applicability to nuclear safeguards. PNET utilizes passive neutron measurements to obtain the projection profile of the intensity distribution of neutron sources at different detection angles. Numerical calculation were performed to validate the feasibility of PNET using a boiling water reactor (BWR) spent fuel assembly model and ideal black neutron absorber slits to discriminate the neutrons coming into the collimator. The projection profile composed of the neutrons counts at each counting zone was reconstructed using maximum likelihood-expectation maximization (ML–EM) algorithm. The reconstructed images were examined based on the original fuel rod positions under in-air and underwater measurement conditions. The result showed that the reconstructed images obtained in the in-air measurements match the original ones, although intensive noise appears in the reconstructed images and the fuel rod positions were not identified in the underwater measurements [13].

Acknowledgement

Some parts of the study were supported by Ministry of Education, Culture, Sports, Science, and Technology (MEXT) Innovative Nuclear Research and Development Program in Japan (Funder ID: 10.13039/501100001700).

References

1. H. Sagara, M. Kawashima, K. Morita *et al*., Prog. Nucl. Sci. Technol., Vol. 7, pp. 34-40, (2025).
2. H. Okazaki, M. Kawashima, H. Sagara, Prog. Nucl. Sci. Technol., Vol. 7, pp. 338-344, (2025).
3. E. M. Lisowski, H. Sagara, Nucl. Technol., Vol. 211, Issue 8, (2025).
4. H. F. Chong, H. Sagara, Prog. Nucl. Sci. Technol., Vol. 7, pp. 47-52, (2025).
5. N. Mitsuboshi, H. Sagara, Prog. Nucl. Sci. Technol., Vol. 7, pp. 318-323, 2025.
6. D. Hara, H. Sagara, Prog. Nucl. Sci. Technol., Vol. 7, pp. 324-330, (2025).
7. D. Hara , H . Sagara, J. Nucl. Sci. Technol., Vol. 62, Issue 3, p. 278-287, (2024).
8. A. Oizumi, H. Sagara, Prog. Nucl. Sci. Technol., Vol. 7, pp. 331-337, (2025).
9. K. W. Chin, H. Sagara et al., Prog. Nucl. Sci. Technol., Vol. 7, pp. 91-96, (2025).
10. T. Nagatani, H. Sagara *et al.*, Prog. Nucl. Sci. Technol., Vol. 7, pp. 41-46, (2025).
11. K. Tanabe, M. Komeda, Y. Toh, H. Sagara, Prog. Nucl. Sci. Technol., Vol. 7, pp. 67-73, 2025.
12. K. Tanabe, M. Komeda, Y. Toh, Y. Kitamura, T. Misawa, K. Tsuchiya & H. Sagara, Scientific Reports Vol. 14, Article number: 18828 (2024)
13. K. TSUCHIYA, H. SAGARA, C. Y. HAN, Prog. Nucl. Sci. Technol., Vol. 7, pp. 110-116, (2025).

I-8 Development of Surface-Enhanced Raman Spectroscopic Technique for Simple and Rapid Uranium Analysis

Takehiko Tsukahara

1. Introduction

Since an accident at the Fukushima Daiichi nuclear power station, the distribution and transport of radionuclides in the environment have become a global concern. In particular, to avoid radiological and toxic risks, determination of uranyl ions (UO_2^{2+}) in solutions is one of the most important issues for decommissioning and environmental impact assessment of nuclear-related facilities. Traditional detection methods of uranium such as fluorescence spectroscopy, radiation spectrometry, and such as inductivity-coupled-plasma mass spectrometry (ICP-MS) have superior detection performance, but have some drawbacks such as requirements of time-consuming operations, large-scale and expensive instruments, large quantities of samples, and highly skilled personnel. Therefore, the development of rapid, efficient, and economical on-site detection techniques is desirable for the detection of UO_2^{2+}.

Surface-enhanced Raman scattering (SERS) is rapidly evolving as a useful analytical method, because of its ability to acquire vibrational signatures of target molecules with high sensitivity. In particular, the greater SERS enhancement effects have been achieved by using the surface-functionalized metal nanoparticles such as gold and silver, which can bind selectively with target analytes. Therefore, in this study, we aimed to develop a novel SERS-based UO_2^{2+} sensor in aqueous and acidic media by the combination of laser Raman spectroscopy and gold nanoparticles functionalized with Amidoxime-mercaptobiphenylcarbonitrile(HS2PCN) having the coordination ability to UO_2^{2+} (see Figures 1 and 2).

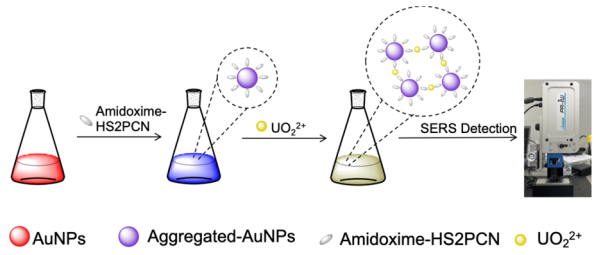

Figure 1. Concept of a novel SERS analysis process.

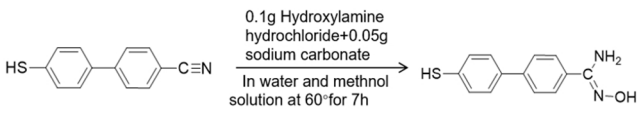

Figure 2. Schematic illustration of amidoxime-HS2PCN.

2. Experimental

2.1. Surface modification of gold nanoparticles with HS2PCN

0.1 g of hydroxylamine hydrochloride and 0.05 g of sodium carbonate were dissolved completely in 10 mL of a water/methanol solution under stirring. Subsequently, 0.05 g of 4-mercaptobiphenylcarbonitrile(HS2PCN) was added to the mixture, and the solution was stirred at 500 rpm. The reaction was carried out under reflux at 70 °C for 8 hours inside a glove box to maintain an inert atmosphere. After the reaction, the precipitate was collected, washed gently with an appropriate solvent, and dried at 40 °C.

2.2. Preparation of HS2PCN-functionalized Au nanoparticles

A 10 mM phosphate buffer solution was first prepared. Subsequently, 10 mL of a 1.83 mg/mL TWEEN20 surfactant solution (dissolved in phosphate buffer) was added to a 1 nM colloidal gold nanoparticle dispersion. The mixture was allowed to stand for at least 20 minutes. Then, 10 mL of 1 mM HS2PCN solution (dissolved in ethanol) was added under gentle stirring. The reaction was carried out at room temperature for 24 hours. After completion, the reaction mixture was centrifuged to separate the precipitate, which was washed three times with phosphate buffer to remove any unreacted materials. The recovered solid sample is determined as amidoxime-HS2PCN-modified gold nanoparticles (AuNPs).

3. Results and Discussion

1 mM UO_2^{2+} solution was prepared, and amidoxime-HS2PCN-modified AuNPs solution with different pH values (pH 5–10) were mixed with each other. The Raman measurements of the solutions were carried out, and the Raman spectra could be observed as shown in Figure 2. We found that the Raman peak intensities at around 880 cm^{-1} assigned as U=O symmetric stretching mode increased with decreasing solution pH, reaching a maximum intensity at pH = 5. The results indicate that the optimal solution pH for the detection of UO_2^{2+} is pH = 5.

Moreover, the amidoxime-HS2PCN-modified AuNPs were mixed with UO_2^{2+} solutions at different concentrations (10^{-5} to 10^{-2} M), and the Raman spectra of the samples were measured. As seen from Figure 3, the peak intensities at around 880 cm^{-1} assigned as U=O symmetric stretching mode were enhanced drastically with increasing UO_2^{2+} concentrations. Even at the same concentration of UO_2^{2+} (10^{-2} M), the peak intensity for the case of surface-modified AuNPs addition was more than 1000 times higher than that for the case of un-modified bare AuNPs. This fact means clearly that the surface-modified AuNPs gave greater SERS

enhancement effects of UO_2^{2+} in aqueous solutions compared with un-modified bare AuNPs nanoparticles.

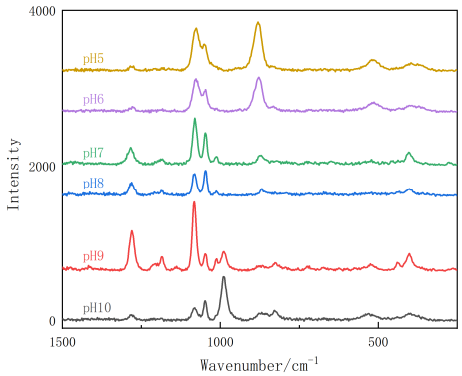

Figure 2. SERS spectra of UO_2^{2+} reacted with different pH solutions containing amidoxime-HS2PCN-modified AuNPs.

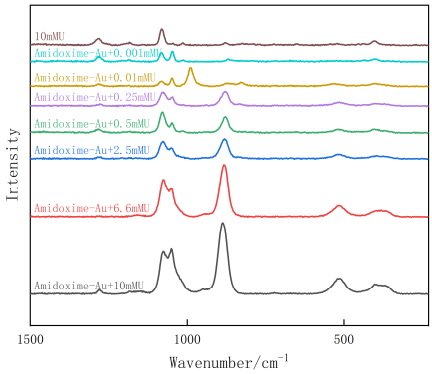

Figure 3. SERS spectra of pH = 5 solutions containing different UO_2^{2+} concentrations and amidoxime-HS2PCN-modified AuNPs.

When the peak intensities at around 880 cm^{-1} were plotted against UO_2^{2+} concentrations as shown in Figure 4, the intensities were found to be increased exponentially depending on UO_2^{2+} concentrations. Using the fitted equation, the limit of detection (LOD) for UO_2^{2+} could be determined as 2.2 μM under the present solution environments. From the relationship of LOD, laser spot area, and sample volume, the molar amount of UO_2^{2+} to be detected was calculated as 2×10^{-11}.

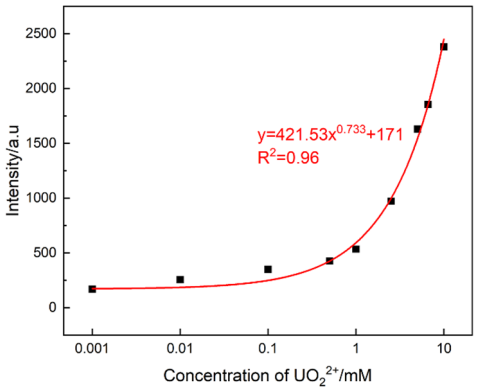

Figure 4. Plots of Raman spectral intensities at 883 cm^{-1} against UO_2^{2+} concentrations.

4. Conclusions

A novel amidoxime-AuNPs SERS substrate was developed for detecting UO_2^{2+} in aqueous solutions. The intensities of Raman peaks assigned as UO_2^{2+} was found to be proportional to UO_2^{2+} concentrations. The detection limit of 2.2 μM corresponding to 10^{-11} mol could be successfully achieved, enabling the detection of UO_2^{2+} even in acidic and contaminated aqueous solutions without any pretreatment. Compared with other methods, the SERS-based sensor has advantages invoking simple chemical operation, fast analysis, small sample volume, and low detection limit. The results demonstrate that this SERS approach has significant potential as an advanced analysis method for nuclear facility decommissioning, radioactive waste management.

Acknowledgments

The present work is partially supported by JAEA Nuclear Energy S&T and Human Resource Development Project Grant Number JPJA22F22717857, and the Secretariat of the Nuclear Regulation Authority, Japan.

References

1. Y. He, et al.; International Symposium on Green Transformation Initiative and Innovative Zero-Carbon Energy Systems (GXI-ZES), January 14-16 January, Tokyo, Japan, pp.226 (2025).

I-9 Fracture Behavior of Uni-Directional SiC_f/SiC Composites with BN Interphase Formed by Electrophoretic Deposition Method

Katsumi Yoshida

1. Introduction

Continuous silicon carbide fiber-reinforced silicon carbide matrix (SiC_f/SiC) composites have been expected to be used as next-generation heat resistant structural materials with high reliability for future nuclear and fusion applications, aerospace industries, and high-temperature gas turbines. The optimum fiber/matrix interface should be optimized and controlled to achieve high performance SiC_f/SiC composites. At present, carbon or hexagonal-boron nitride (h-BN) has been used as the interphase for SiC_f/SiC composites, and they have been coated on SiC fibers by chemical vapor deposition (CVD). Our research group has proposed the novel process to form interphases on SiC fibers for SiC_f/SiC composites based on electrophoretic deposition (EPD) method. We have already demonstrated that EPD method is effective to form the carbon interphase on amorphous and crystalline SiC fibers, and SiC_f/SiC composites with the carbon interphase showed excellent mechanical properties [1-8].

In this study, h-BN interphase, which shows better oxidation resistance than carbon, was selected as the interphase, and we tried to form dense and uniform h-BN coating on low-conductive SiC fibers by EPD method using flaked h-BN suspension. Uni-directional SiC_f/SiC composites with h-BN interphase formed by EPD method were prepared by polymer impregnation and pyrolysis (PIP) method, and their fracture behavior was evaluated.

2. Experimental procedures

2.1. Formation of BN coating on SiC fibers by EPD

Crystalline SiC fibers (Hi-Nicalon Type S, NGS Advanced Fibers Co., Ltd., Japan), which are low-conductive, were used as the reinforcement for SiC_f/SiC composites in this study. Before h-BN coating on the SiC fibers by EPD, thin conductive polymers, polypyrrole (Ppy), were coated on the SiC fibers to improve the electric conductivity of their surface according to our previous report [8]. Hexagonal-BN aqueous suspension for EPD was prepared as follows; h-BN particles (average particle size; 0.7 μm) and the nonionic surfactant were added in distilled water, and the flaked h-BN suspension was prepared by wet-jet milling. Small amount of *n*-butylamine was added to the suspension to adjust the pH to 10. BN particles were negatively charged at pH 10. The SiC fiber-preform with/without Ppy coating and graphite plates were the anode and the cathode, respectively, and the preform was placed between carbon plates in the 0.6 wt% flaked h-BN suspension. The distance between the SiC fiber preform and carbon plate was adjusted to be 10 mm. EPD was conducted at the applied voltage of 5 V for 1 h. After EPD, the preforms were dried, and then heat-treated at 1000°C for 2 h in Ar atmosphere. To demonstrate the effectiveness of Ppy coating on the SiC fibers for BN coating by EPD, BN coating was formed by EPD (EPD voltage; 8 V, EPD time; 1 h) on the SiC fibers without Ppy coating.

2.2. Fabrication of uni-directional SiC_f/SiC composites

Uni-directional SiC_f/SiC composites were fabricated by polymer impregnation and pyrolysis (PIP) process using allylhydridopolycarbosilane (AHPCS) and β-SiC powder. The weight ratio of AHPCS to SiC was 7:3. Three kinds of SiC fibers; (1) without coating, (2) with h-BN coating after Ppy coating, and (3) with h-BN coating without Ppy coating, were prepared as the reinforcement for SiC_f/SiC composites. Eight of the preforms impregnated with AHPCS-based suspension were stacked in a mold, and then uniaxially pressed at 0.4 MPa. The stacked preforms were dried at 200°C for 1 h, and then heat-treated at 1200°C for 1 h in Ar atmosphere. The heat-treated compacts were dipped into the AHPCS suspension prepared above, and the suspension was impregnated into the compacts under vacuum for 5 min. The compacts were dried at 200°C, and then heat-treated at 1200°C for 1 h in Ar atmosphere. This process was repeated five times to increase the density of the compacts, and the unidirectional SiC_f/SiC composites were fabricated.

2.3. Mechanical properties of SiC_f/SiC composites

The uni-directional SiC_f/SiC composites were cut into rectangular bars along the fiber direction. Their bulk density and open porosity were measured by Archimedes' method. Bending strength of the SiC_f/SiC composites was measured by three-point bending test at room temperature. Fracture energy was roughly calculated from the area of load-crosshead displacement curve in three-point bending test divided by twice the fracture surface area. Microstructure and fracture surface of the specimens after three-point bending test were observed with a field-emission scanning electron microscope (FE-SEM).

3. Results and discussion

Their bulk density and open porosity were 2.00-2.08 g/cm^3 and 21-24 %, respectively. The fiber volume fraction of the SiC_f/SiC composites ranged from 15.4 to 18.7 %.

The typical stress-crosshead displacement curves of the SiC_f/SiC composites in three-point bending test at room temperature are shown in Fig. 1. Figure 2 shows SEM micrographs of the fracture surface of the SiC_f/SiC composites after three-point bending test at room temperature. The SiC_f/SiC composites with uncoated SiC fibers showed the average bending strength of 102 ± 16MPa and the average fracture energy of 1014 ± 307 J/m^2. The stress-crosshead displacement curve of the SiC_f/SiC

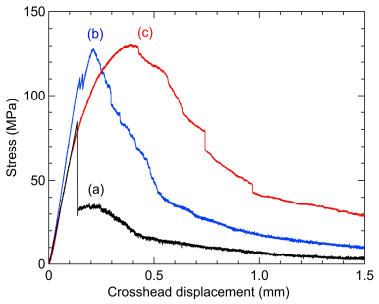

Fig. 1 The typical stress-crosshead displacement curves of SiC_f/SiC composites in three-point bending test at room temperature. (a) Uncoated SiC fibers, (b) h-BN-coated SiC fibers by EPD without Ppy coating, (c) h-BN-coated SiC fibers by EPD with Ppy coating.

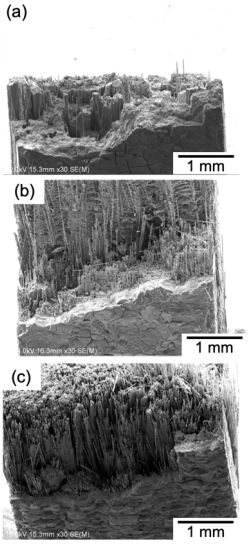

Fig. 2 SEM micrographs of the fracture surface of the SiC_f/SiC composites after three-point bending test at room temperature. (a) Uncoated SiC fibers, (b) h-BN-coated SiC fibers by EPD without Ppy coating, (c) h-BN-coated SiC fibers by EPD with Ppy coating.

composites with uncoated SiC fibers showed the sudden reduction of the stress after reaching the maximum stress, followed by the gradual decrease of the stress with the increase in the crosshead displacement, i.e., almost brittle fracture behavior. From the SEM observation of their fracture surface, SiC matrix was porous and large voids were observed. In addition, small amount of fiber pullout was observed, but the length of the fiber pullout was very short and interfacial debonding was very little because the interphase was not formed on the SiC fibers and the fibers and the matrix were bonded tightly. As a result, the SiC_f/SiC composites with uncoated SiC fibers showed almost brittle fracture behavior. When h-BN-coated SiC fibers by EPD without Ppy coating were used as the reinforcement for SiC_f/SiC composites, their stress-crosshead displacement curve showed pseudo-ductile fracture behavior, and their average bending strength and fracture energy were 141 ± 17 MPa and 1462 ± 376 J/m^2, respectively. These values were higher than those of the SiC_f/SiC composites with uncoated SiC fibers, and large amount of fiber pullout was observed by SEM. The SiC_f/SiC composites using the h-BN-coated SiC fibers by EPD with Ppy coating also exhibited pseudo-ductile fracture behavior similar to the SiC_f/SiC composites using the h-BN-coated SiC fibers by EPD without Ppy coating. Their average bending strength was almost the same as that of the SiC_f/SiC composites using the h-BN-coated SiC fibers by EPD without Ppy coating, and the value was 131 ± 6 MPa. On the other hand, the fracture energy of the SiC_f/SiC composites using the h-BN-coated SiC fibers by EPD with Ppy coating was 3835 ± 103 J/m^2, and the value was extremely higher than that of the SiC_f/SiC composites using the h-BN-coated SiC fibers by EPD without Ppy coating. This result can be explained from the viewpoint of the h-BN coating on the SiC fibers by EPD; as described above, whereas h-BN particles were partially and slightly deposited on the SiC fibers by EPD without Ppy coating, Ppy-coated SiC fibers was wholly coated with flaked h-BN particles by EPD. The thickness of h-BN interphase on the SiC fibers without Ppy coating was around 100 nm. On the other hand, the SiC fibers with Ppy had the h-BN interphase with the thickness of 200-600 nm, and the h-BN coating was sufficiently formed on the SiC fibers by EPD.

4. Conclusion

Hexagonal-BN interphase, which shows better oxidation resistance than carbon, was selected, and h-BN coating was formed on low-conductive SiC fibers by EPD method using flaked h-BN suspension prepared. Uni-directional SiC_f/SiC composites with h-BN interphase formed by EPD method were prepared by PIP method, and their fracture behavior at room temperature was evaluated. Whereas the SiC_f/SiC composites with uncoated SiC fibers showed almost brittle fracture behavior, the SiC_f/SiC composites using the h-BN-coated SiC fibers by EPD with Ppy coating exhibited pseudo-ductile fracture behavior with the large amount of fiber pullout, and their bending strength and fracture energy were higher than the SiC_f/SiC composites with uncoated SiC fibers. From these results, it is concluded that the SiC_f/SiC composites with h-BN interphase formed by EPD showed pseudo-ductile fracture behavior with higher fracture energy.

Acknowledgments

This work was partially supported by KAKENHI (26420677), Hosokawa Powder Technology Foundation, Advanced Institute of Materials Science, and A-STEP from JST Japan Grant Number JPMJTR202M.

References

1. K. Yoshida et al.; Key Eng. Mat., **352**, 77-80 (2007).
2. K. Yoshida et al.; J. Nucl. Mat., **386-388**, 643-646 (2009).
3. K. Yoshida et al.; Mat. Sci. Eng. B-Adv., **161**, 181-192 (2009).
4. K. Yoshida; J. Ceram. Soc. Jpn., **118**[2], 82-90 (2010).
5. K. Yoshida et al.; Compos. Sci. and Technol., **72**, 1665-1670 (2012).
6. K. Yoshida et al.; Key Eng. Mat., **617**, 213-216 (2014).
7. K. Yoshida et al.; Prog. Nucl. Energ., **82**, 148-152 (2015).
8. K. Yoshida et al.; J. Ceram. Soc. Jpn., **131**[9], 542-548 (2023).

I-10 Electron Temperature and Density Diagnosis in Argon Dual-Frequency ICP by Tomographic Optical Emission Spectroscopy

Hiroshi Akatsuka, Atsushi Nezu

1.Introduction

Low-pressure discharge plasmas are widely applied in the semiconductor industry for etching and deposition processes. Controlling plasma parameters such as electron temperature (T_e) and electron density (N_e) is essential for optimizing these processes. Furthermore, in inductively coupled plasma (ICP) systems, the addition of a capacitive bias system allows for independent control of plasma density and ion energy. A fundamental understanding of plasma physics is essential for optimizing etching processes. Our previous work has focused on diagnosing basic plasma parameters in argon (Ar), nitrogen (N_2), carbon tetrafluoride (CF_4), and oxygen (O_2) ICPs [1–3].

This study focuses on the 2D horizontal distribution of Te and Ne in an argon ICP obtained using optical emission spectroscopy (OES) and a spectral tomography algorithm, as well as Langmuir probe measurements with bias power applied at a different frequency than the ICP discharge.

2. Experiment

Figure 1 shows a schematic diagram of the dual-frequency ICP experimental chamber equipped with a probe measurement system and an optical emission spectroscopy measurement system. The antenna coil of the upper electrode is connected to a 13.56 MHz radio frequency (RF) source, and the lower electrode is connected to a 12.5 MHz RF power source. The OES system measures the optical emission intensity through synthetic quartz windows from both the x and y directions of the chamber. The plasma optical emission is collected using 34 optical fibers connected to 17 lenses in each direction. The measurement range of the OES system is 350 to 940 nm.

3. Results and discussion

Figure 2 shows a comparison of the electron temperature and density results under two conditions: no bias power (P_{bias} = 0W) and with bias power (P_{bias} = 100W), while maintaining a pressure of 1 Pa, a gas flow rate of 10 sccm,

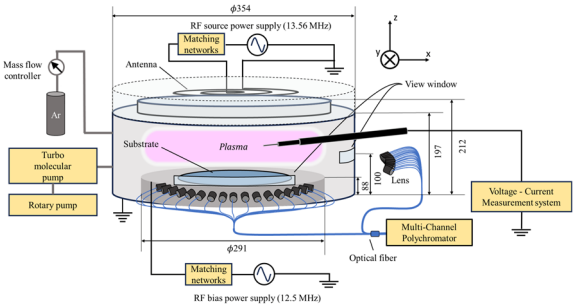

Fig. 1 Schematic diagram of the ICP experimental setup for spectroscopic and probe measurements [1,2].

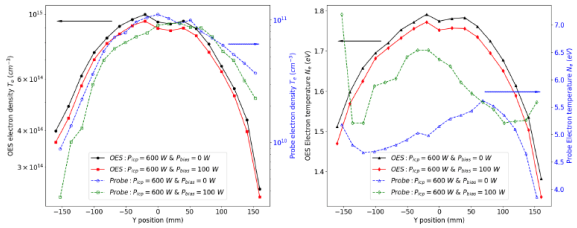

Fig. 2 Schematic diagram of the ICP experimental setup for spectroscopic and probe measurements [1].

and an RF source power of P_{source} = 600W. When bias power is applied, there is a slight decrease even near the chamber wall. However, the electron temperature shows contrasting results: the electron temperature increases in the measurement from the probe with bias power applied, while the OES results show a slight decrease.

The determination of T_e and N_e by OES measurement was carried out by minimizing the error as the objective function, Eq. (1). The analysis incorporated the gas temperature, diffusion radius, and population density of argon ground states to estimate T_e and N_e. These parameters were determined by fitting rate equations derived from argon collisional-radiative model (CRM) [1]. The comparison between experimental and calculated level densities was performed using an objective function, which is given by:

$$f = \frac{1}{N}\sum_{I}\left(\log N_{\mathrm{exp},i} - \log N_{\mathrm{crm},i}\right)^2 \qquad (1)$$

Figure 3 shows the distribution of local minima within the dense band of the T_e- N_e parameter space. The emergence of distinct solution regions has been shown, which indicates multiple solutions to optimization problems. It is necessary to avoid the local optimized solution, whose countermeasure is now being discussed.

References

1. Y. Ye, et al.: ISPlasma2025/IC-PLANTS2025, 05P-24 (2025).
2. Y. Yamashita, et al.: ESCAMPIG XXVI, p2-P29 (2024).
3. H. Akatsuka, et al.: 45th Dry Process Symp. P-24 (2024).

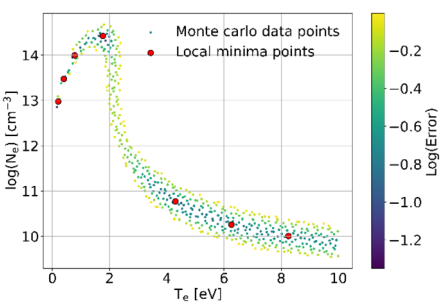

Fig. 3 Distribution of local minima in T_e and N_e. [1]

I-11 Spectroscopic Measurement of Atomospheric-pressure Non-equiribrium Ar Plasma Based on Continuum and Line spectra with Weighted Analysis

Hiroshi Akatsuka, Atsushi Nezu

1. Introduction

Non-equilibrium atmospheric-pressure plasmas are being actively used in a variety of process applications. However, a simple, non-invasive experimental method for determining the electron temperature T_e, electron density n_e, or electron energy distribution function (EEDF) has not yet been established. Assuming two temperature distributions in the generalized EEDF, information obtained from continuum can be used to restrict the possible range of the EEDF, and a more detailed EEDF can be estimated by fitting a line spectrum [1]. However, this analysis is impossible if the search range cannot be obtained from the continuous spectrum. Therefore, we propose a more general method for estimating the generalized EEDF parameters T_e, [eV], n_e [cm^{-3}], and parameter γ by minimizing the sum of the errors between the continuous spectrum and the line spectrum estimates and the experimental values [2,3]. The goal is to determine the weight w such that the dependence of T_e and n_e on the discharge voltage V_{in} appears smoothly.

2.Numerical methodology

The objective function to be minimized consists of two different mean square logarithmic errors (MSLEs): one is the error between the experimental value and the theoretical value MSLEC calculated from bremsstrahlung, and the other is the error between the experimental value of the excited state number density obtained from the line spectrum and the theoretical value MSLEL calculated from CRM. The objective function to be minimized is then set to the MSLE (Eq. (1)), which is the weighted sum of the two values, weighted by a coefficient w.

$$\mathrm{MSLE}(w,T_e,n_e,\gamma) = w\cdot\mathrm{MSLEL}(T_e,n_e,\gamma) + (1-w)\cdot\mathrm{MSLEC}(T_e,n_e,\gamma). \quad (1)$$

The analysis was performed for each applied voltage V_{in} in of $w = 10^{-6}$–1. To globally minimize Eq. (1), local optimization was performed using the grid search method and the multi-point start method using the GPU Nvidia RTX 2070Ti and the Python library CuPy.

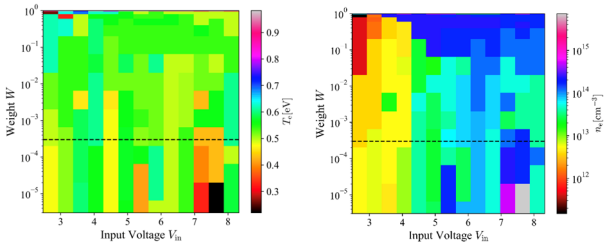

(a) (b)

Fig. 1 Result for (a) T_e and for (b) n_e. Their x-axes and y-axes represent V_{in} and w, respectively. The black dashed lines indicated the smoothest V_{in} dependency of both T_e and n_e [3].

3.Experiments

The experiment was conducted using the same dielectric barrier discharge nonequilibrium atmospheric pressure Ar plasma device used in the experiment by Onishi et al. [2]. This device has a double glass tube structure, with an electrode filled with distilled water inside the inner tube. The gap between the electrodes is 1 mm. Ar gas, which acts as a discharge source, flows through the outer tube at a rate of 4 L/min. The line of sight is located in the center of the gap between the electrodes, and the window above the line of sight is made of quartz glass. In this experiment, the spectral emissivity was measured by varying V_{in} from 2.7 to 8.1 kV.

4. Results and discussion

Figure 1 shows the analysis results for T_e and n_e. In the range $w = 10^{-4}$–10^{-3}, n_e increases monotonically with increasing V_{in}, while T_e tends to remain constant. For $w < 10^{-5}$, T_e is sometimes less than 0.3 eV and n_e exceeds 10^{15} cm^{-3}, which are spurious results. Furthermore, when $w > 10^{-1}$, n_e dependence on V_{in} becomes less smooth and inconsistent. Figure 2 shows the average MSLE for each V_{in}. For $10^{-5} < w < 3\times10^{-4}$, the MSLE decreases by a factor of 1.4 along w. Furthermore, the MSLEC increases significantly for $w > 3\times10^{-2}$. These results imply that the optimal weight w lies in the range $3\times10^{-4} < w < 3\times10^{-2}$. Since the MSLE monotonically increases with w, simple minimization of MSLE with respect to w will not yield optimal results. In conclusion, optimizing these functions alone is not sufficient to complete the diagnosis, and verification by other analyses, such as plasma simulations, is required.

Reference

1. W. Kikuchi, et al: J. Phys. D: Appl. Phys. **57**, 335202 (2024).
2. W. Kikuchi, et al: 50th EPS Conf. Plasma Phys. P1-009 (2024).
3. W. Kikuchi, et al: 5th Int. Conf. Data-Driven Plasma Sci. (ICDDPS-5) 2B (2024).

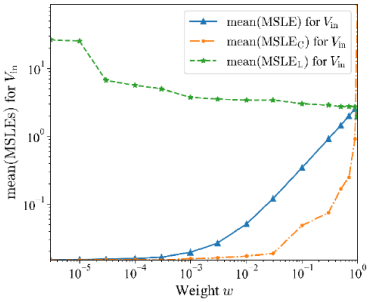

Fig. 2 Mean MSLEs for V_{in}. The blue line represents for MSLE(Eq.(1)), the yellow for continuum spectrum MSLE, and the green for line spectrum MSLE [3].

I-12 Numerical Demonstration of DC Induction Acceleration

Jun Hasegawa

1. Introduction

An induction accelerator accelerates charged particles using the electric field induced by the magnetic flux swing in ferromagnetic cores. It is regarded as a 1:1 transformer, in which a beam is accelerated on the secondary side of the transformer by a power supply on the primary side. In the induction synchrotron, beam confinement and acceleration can be controlled simultaneously by controlling the acceleration voltage. This feature enables charged particle groups, which in RF synchrotrons exist as multiple beam bunches on the circulating orbit (Fig. 1a), to exist as a single "super bunch" spread over the circulating orbit (Fig. 1b). However, repeated use of the ferromagnetic core for induction acceleration requires a so-called "reset" operation, where the core is magnetized in the opposite direction for the succeeding beam acceleration. During this reset operation, a decelerating electric field is induced in the acceleration gap, so the length of the super bunch in the induction synchrotron is limited to about half of the circulating orbit.

To overcome this limitation, a concept of direct current (DC) induction acceleration was recently proposed by KEK. In this concept, charged particles are distributed throughout the orbit and a DC beam is continuously accelerated in a circular accelerator (Fig. 1c). To demonstrate the DC induction acceleration, we performed 3D electromagnetic field analysis.

2. Principle of DC Induction Acceleration

In the DC induction acceleration, charged particles are accelerated by an electric field $\boldsymbol{E} = -\partial \boldsymbol{A}/\partial t$. Here, $\boldsymbol{A}$ is the vector potential. The acceleration voltage over the entire obit is given by

$$V_{\mathrm{acc}} = \oint_C \boldsymbol{E}_{\mathrm{ind}} \cdot d\boldsymbol{l} = -\frac{\partial}{\partial t}\iint_S \boldsymbol{B} \cdot d\boldsymbol{S} = -\frac{\partial \Phi}{\partial t}.$$

Here, S is the closed surface defined by the circular orbit C, and Φ is the total magnetic flux penetrating S. Almost all the magnetic flux density $\boldsymbol{B}$ exists within the ferromagnetic core, so Φ is equal to the magnetic flux within the core. To continuously accelerate charged particles, the magnetic flux must keep increasing linearly. However, the magnetic flux will eventually saturate, so the core must be magnetized in the opposite direction (reset) before that happens. So, it is essential to repeatedly magnetize the core for beam acceleration and reset it in preparation.

The basic idea of DC induction acceleration is to use two induction acceleration cells at the same time, and while one cell is accelerating the beam, the other cell is reset. This is repeated alternately to continue the beam acceleration. To prevent the beam from being decelerated while resetting the core in one of the cells, it is necessary to force an induced current along the beam orbit so that the magnetic flux change due to the resetting the core can be cancelled. To control the direction of the induced current in the beam duct, the DC induction accelerator uses high-voltage diodes. In addition to the acceleration gap, a reset gap is also provided on the outer conductor of the DC induction cell, and the diodes are placed on both. The duct current induced during the acceleration by each of the cells is impeded by these diodes, while that during the reset operation flows freely through the diodes. With this mechanism, only acceleration fields are induced on the orbit, and the beam is continuously accelerated by two DC induction cells.

3. Electromagnetic Field Analysis

The temporal evolution of the vector potential field in a DC induction accelerator model was calculated under a quasi-steady approximation using the finite element method (Fig. 2). Two DC induction acceleration cells were aligned along a racetrack-shaped copper beam duct. The size and internal structure were based on the induction cell developed at KEK. Each cell contains six toroidal ferromagnetic cores with a diameter of 500 mm and a thickness of 15 mm. A large ferrite core (hereafter, "external inductor") was also placed along the beam duct. The magnetic flux induced by

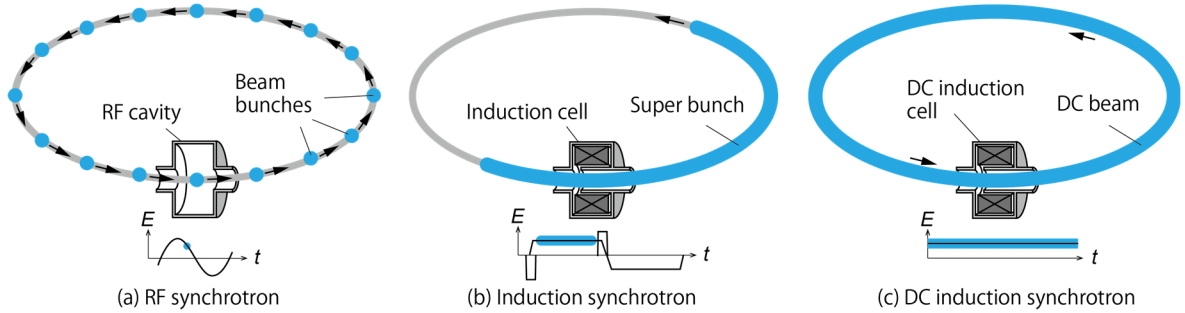

(a) RF synchrotron (b) Induction synchrotron (c) DC induction synchrotron

Fig. 1. Schematic diagrams of beam acceleration by various synchrotrons.

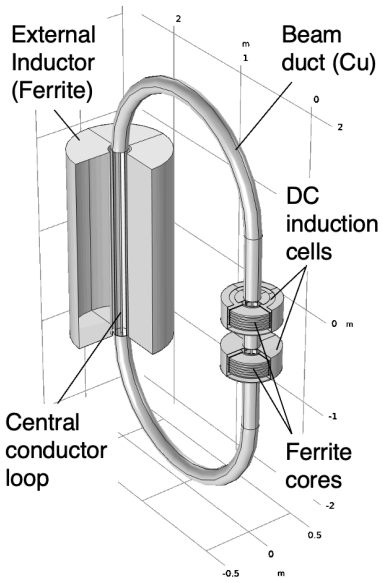

Fig. 2. A calculation model used in the 3D electromagnetic field simulation.

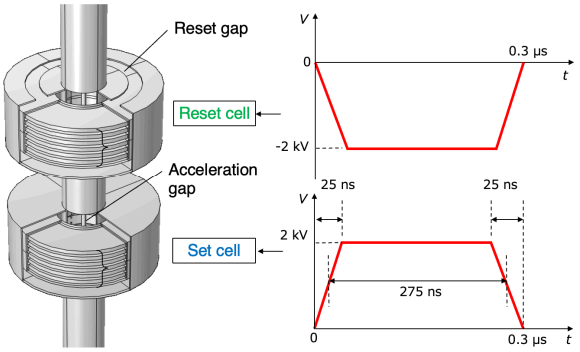

Fig. 3. A calculation model to simulate set and reset operations.

the duct current is stored in this core during the operation. A copper conductor was placed along the beam orbit, which worked as a virtual one-turn coil and was used to evaluate the total acceleration energy of a charged particle travelling one revolution along the orbit.

Figure 3 shows the configuration of the induction cell models. To simplify the calculation, the upper induction cell simulated only the reset operation (reset cell), and the lower simulated only the acceleration (set cell). The actions of the forward currents flowing through the diodes placed in the acceleration gap were simulated by placing four conductor rods placed symmetrically in the acceleration gap in the reset cell. Square waves with reversed polarity and an amplitude of 2 kV and a pulse width of 275 ns were applied to these cells at the same time.

A typical electric field distribution calculated by the set-reset model is shown in Fig. 4. A strong electric field is generated in the acceleration gap of the set cell, while the strong electric field is concentrated in the reset gap of the reset cell and the electric field around the acceleration gap of the reset cell is well suppressed. The voltage waveforms induced in the central conductor loop are shown in Fig. 5. The acceleration voltage felt by charged particles is equal to

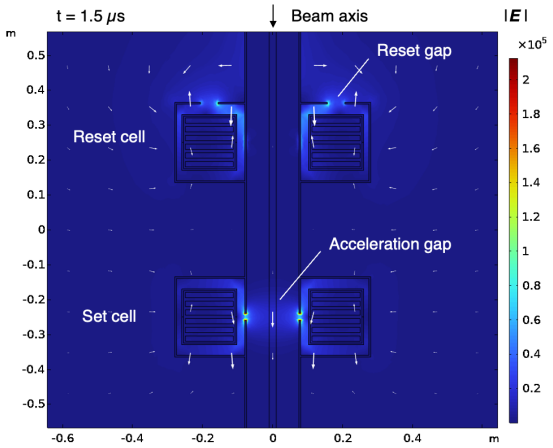

Fig. 4. A typical electric field distribution around induction cells (set-reset model).

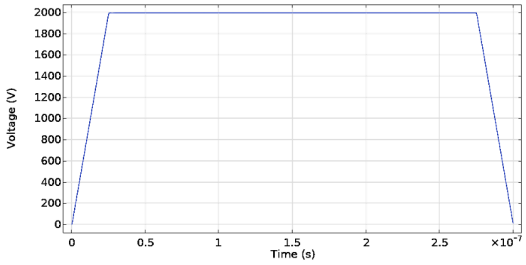

Fig. 5. Voltage waveforms induced over the circular beam orbit of the DC induction accelerator model.

the voltage applied to the set cell, indicating that the voltage applied to the reset cell has almost no net effect on the beam. This result proves that the DC induction acceleration cell works properly according to the principle.

4. Conclusion

The fundamental principle of the DC induction accelerator was numerically confirmed by three-dimensional electromagnetic field analyses. While the induced duct current during the core reset operations plays an essential role in the beam acceleration using the DC induction cell, it is also a factor limiting the continuous operation time. When designing a circular accelerator using DC induction acceleration, it is necessary to determine the beam acceleration system and power supply specifications, considering not only the induction acceleration cell itself but also the inductance and its saturation limit due to magnetic materials (electromagnets, etc.) on the beam line.

Acknowledgments

This study is supported by JSPS KAKENHI Grant Number 24K03200.

I-13 Theoretical nuclear studies for better society

Chikako Ishizuka

1. Nuclear Data

Nuclear energy systems are increasingly regarded as essential components of a sustainable global energy infrastructure. They emit no greenhouse gases and can provide the high-power density required to support the rapid growth of artificial intelligence technologies, data centers, and advanced industrial processes. In Japan, following the Fukushima accident, significant efforts have been devoted to developing new reactor concepts and fuel designs that place the highest priority on safety and reliability. These developments represent a new stage in the evolution of nuclear energy, emphasizing both technological innovation and public trust.

Nearly a century has passed since the discovery of nuclear fission, and more than half a century since nuclear reactors were first put into operation. Over this long period, extensive experience has been accumulated with conventional uranium-fueled reactors, and the fundamental mechanisms of uranium fission are now well understood. However, the safe and economical realization of next-generation nuclear energy systems, such as fast reactors, accelerator-driven systems, and fusion–fission hybrids, requires detailed and reliable information on a wide range of nuclear reactions that extend far beyond uranium fission. Such information is indispensable for the accurate prediction of fuel behavior, transmutation processes, and material performance under irradiation.

This need for high-quality nuclear information has given rise to the field of nuclear data research, which aims to compile, evaluate, and provide reliable data on nuclear reactions based on both experimental measurements and theoretical modeling. Nuclear data form the foundation of almost every quantitative analysis in reactor physics, radiation transport, and nuclear engineering. They determine reaction probabilities, secondary particle emissions, and energy distributions, which directly affect reactor core design, neutron economy, and safety margins.

Our research group focuses on developing new methodologies for next-generation nuclear data libraries, with special attention to uncertainty quantification. In modern reactor simulations, uncertainty in nuclear data can significantly influence macroscopic quantities such as reactivity coefficients, neutron spectra, fuel burnup, and fission product yields. Therefore, evaluating not only the central values of reaction cross sections but also their covariance information and uncertainty propagation is essential for predictive reactor design and reliable safety assessment. We study how these uncertainties propagate through large-scale reactor physics calculations, including deterministic and Monte Carlo transport methods, to quantify their impact on integral parameters.

To improve predictive capability, our work combines theoretical nuclear models and machine learning approaches. We employ microscopic reaction models derived from nuclear many-body theory to describe processes such as fission, scattering, and particle emission. At the same time, we apply data-driven techniques including Bayesian neural networks and deep learning frameworks to optimize model parameters, capture correlations among observables, and estimate posterior uncertainties. These hybrid approaches allow us to integrate physical insight with statistical inference, thereby refining nuclear data evaluations and enhancing their consistency with experimental results.

The evaluated data we produce are directly utilized in the development of the Japanese Evaluated Nuclear Data Library (JENDL) led by the Japan Atomic Energy Agency (JAEA). Our recent results have been incorporated into JENDL-5, contributing to the national and international community's efforts to provide standardized, high-fidelity nuclear data for energy and non-energy applications alike.

Beyond the field of nuclear power, precise and uncertainty-qualified nuclear data play a vital role in medicine, industry, and environmental research. They are used to optimize radiation therapy, improve diagnostic imaging, design medical isotopes, and assess radiation shielding for space missions. The same data that describe how neutrons and protons interact with atomic nuclei underpin technologies that directly benefit human health and safety.

Through these studies, our long-term goal is to establish a next-generation framework for nuclear data science that connects nuclear theory, artificial intelligence, and reactor physics into a coherent predictive system. By advancing both the accuracy and the uncertainty quantification of nuclear data, we aim to make reactor simulations more reliable, to support the design of innovative and inherently safe nuclear systems, and ultimately to contribute to a sustainable, carbon-neutral, and human-centered society.

2. Highlight of Our Research

Our group conducts a wide range of research activities, including fundamental studies on the mechanism of nuclear fission, the development of advanced technologies for cancer treatment, and the application of machine learning to investigate the energy dependence of fission product yields in actinide nuclei. In this section, we introduce one of our research highlights from FY 2024, focusing on recent progress in the study of molten salt reactors.

In recent years, molten salt reactors (MSRs) have attracted

growing interest as advanced nuclear systems that might offer improved safety, flexibility, and sustainability compared to conventional water-cooled reactors. According to the International Atomic Energy Agency (IAEA), MSRs are reactors in which the nuclear fuel or the coolant, or both, consists of a molten salt.

Among the many MSR concepts under development, one particularly promising variant is based on chloride salts and is designed to operate in a fast neutron spectrum.

Why focus on chloride salts instead of the more common fluoride salts used in many MSR designs? The main reason is that chloride salts allow the reactor to operate with fast neutrons, meaning neutrons that have higher kinetic energy, rather than slow (thermal) neutrons. A fast-spectrum reactor offers significant advantages for nuclear waste management and fuel efficiency. It can more effectively transmute long-lived transuranic (TRU) elements found in spent fuel, thereby reducing the volume and radiotoxicity of nuclear waste. In contrast, most fluoride-salt MSRs operate in a thermal spectrum and cannot achieve the same level of transmutation performance.

Our research group has focused on a conceptual 700 MWt molten chloride salt fast reactor (MCSFR) and has examined its neutronic behavior using a continuous-energy Monte Carlo simulation code. We compared results obtained with different evaluated nuclear data libraries and found that a key parameter, the effective multiplication factor ($k_e$ff), which represents how many new neutrons are generated on average from each fission event, varied by approximately two percent depending on the library used. Although a two percent difference may appear small, in reactor design such a variation can have meaningful implications for safety margins, reactor performance, and long-term operation.

By performing sensitivity studies, we found that the largest source of this variation was related to the cross-section data for the reaction of chlorine-35 with neutrons producing protons, denoted as ^{35}Cl(n,p)^{35}S, in the energy range of about 1 to 10 MeV. Because chlorine is a major component of the molten salt fuel and coolant, this reaction strongly influences how neutrons are absorbed or converted, thereby affecting the neutron economy, fuel burnup, and the reactor's capability to reduce nuclear waste through transmutation.

The results convey two important messages. First, they demonstrate that the choice of nuclear data library can have a significant impact on reactor physics calculations, particularly for advanced systems such as fast reactors employing nontraditional fuels or coolants. Second, they show that uncertainty in critical nuclear data can become a limiting factor in the reliable design and deployment of next-generation reactors. To improve the reliability of such systems, we recommend new experimental measurements and more precise evaluations of key reactions such as ^{35}Cl(n,p), together with covariance and uncertainty data.
In summary, this research contributes to establishing a roadmap for molten chloride salt fast reactor development by linking advanced reactor design concepts, fuel cycle optimization, and nuclear data improvement. It highlights that achieving high-performance, safe, and sustainable nuclear energy systems requires not only innovative engineering and reactor physics but also a robust foundation of accurate nuclear data and well-quantified uncertainties.

Acknowledgments

A part of this study has been carried out as a project conducted by the consortium led by the Beyond Energy R&D Association (BERD), which was funded by the Ministry of Economy, Trade and Industry (METI) and commissioned by the Japan Atomic Energy Agency (JAEA). We express sincere thanks to METI for their financial support.

References

1. O. Iwamoto et al.: Japanese evaluated nuclear data library version 5: JENDL-5; Journal of Nuclear Science and Technology Vol.60, No.1, 1-60 (2023).
2. Y. Tahara et al.: Request for ^{35}Cl(n,p) reaction cross-section measurements and re-evaluations from the standpoint of molten chloride salt fast reactor design; Journal of Nuclear Science and Technology Vol. 61, No. 2, 277-284 (2024).

I-14 Progress of Experimental Studies on Nuclear Data at Science Tokyo

Tatsuya Katabuchi

1. Neutron capture cross section measurement of ^{99}Tc at J-PARC

The nuclear industry faces challenges in disposing of long-lived fission products (LLFPs) within nuclear waste due to their extended half-lives. Nuclear transmutation of LLFPs into stable or short-lived nuclides is a potential solution, necessitating accurate neutron-induced nuclear reaction data. While transmutation studies on minor actinides (MAs) are extensive, LLFP transmutation has received less attention, impacting both LLFP and MA transmutation system designs. This study focuses on reducing uncertainties in the neutron capture cross section of ^{99}Tc, vital for transmutation system performance.

Experiments at the Japan Proton Accelerator Research Complex (J-PARC) used the Accurate Neutron-Nucleus Reaction Measurement Instrument (ANNRI) to measure the neutron capture cross section of ^{99}Tc. A pulsed neutron beam from a spallation neutron source of the Materials and Life Science Facility, monitored by a neutron detector, was employed. The ^{99}Tc metal pellet, enclosed in aluminum, was used in measurement.

The neutron capture yield of ^{99}Tc was derived using the pulse height weighting technique. Backgrounds were estimated and removed. Data analysis to finalize the cross section data is still ongoing.

2. Development of a detection technique for nuclear fuel materials using photonuclear reactions

Nuclear security at nuclear reactor facilities is a significant concern, particularly with regards to the theft and smuggling of nuclear material, as well as sabotage of the facilities. One crucial task to prevent these security incidents is the development of non-destructive detection techniques for identifying nuclear material. Although numerous techniques have been proposed, further study is still needed to meet the necessary requirements.

Previous research has proposed employing a photon beam from the inverse Compton scattering using a large accelerator[1]. However, this approach requires a large accelerator facility.

In comparison to previous research, the present research aims to develop a new system using a small accelerator. This research uses the nuclear reaction ^{7}Li(p,γ)^{8}Be that has never been focused upon in nuclear security fields. A non-destructive detection system using this high-energy γ-ray source is under development. When a high-energy photon interacts with nuclear material, such as uranium or plutonium, it induces nuclear fission and emits fast neutrons. In this way, the existence of nuclear materials can be identified by measuring neutrons . Neutrons possess a high power of penetrability, enabling the detection of nuclear material even if it is concealed within a container made of high-Z materials[1]. As the first step, a neutron detection technique employing ^{7}Li(p,γ)^{8}Be photon source is being studied. A gold sample is used for a test experiment and neutrons from the photonuclear reaction ^{197}Au(γ,n)^{196}Au are detected. When ^{197}Au is irradiated with γ -rays, it produces both neutrons and γ -rays. To separate neutrons and γ -rays, the pulse shape discrimination technique was employed. Time-of-flight (TOF) can also be used for reducing background.

3. Development of neutron activation method using UV curable resin scintillator

The reliable determination of neutron capture cross-sections is crucial for validating models of s-process nucleosynthesis. As an N=50 magic-number nucleus, ^{88}Sr acts as a bottleneck in the stellar reaction network due to its small (n,γ) cross-section. However, existing measurements show significant conflict[2], with the Maxwellian-averaged cross-section at 30 keV differing between 6.13±0.18 mb from the activation method and 5.46±0.45 mb from a time-of-flight method. This discrepancy highlights the critical need for an improved experimental approach, especially in neutron activation analysis. The core of the present study lies in improving the detector efficiency for neutron activation analysis by developing a novel plastic scintillator based on UV-curable resin. Traditional activation methods often count γ-rays, but the product isotope, ^{89}Sr ($T_{1/2}$ = 50.5 days), decays solely via β-ray emission. Previous attempts to detect these low-energy β-rays using semiconductor detectors may have suffered from low signal-to-background ratios and low counting rates, potentially leading to an overestimation of the cross-section. Our innovation leverages the unique properties of UV-curable resins to fabricate a scintillator with superior geometry and enhanced light collection. By utilizing this resin, we can easily mold the plastic scintillator to completely encapsulate the irradiated sample, significantly increasing the solid angle and overall detection efficiency for the low-energy β-rays from the ^{89}Sr decay. This higher efficiency is essential for overcoming the low count rates and improving the signal-to-background ratio.

Reference

1. R. Kimura, *et al*., *J. Nucl. Sci. Technol*. **53**, 1978 (2016).
2. T. Katabuchi et al., Phys. Rev. C. 108. 10.1103 (2023).

I-15 Study on Photoacoustic Ultrasonic Reception using Laser Deflection

Hiroshige Kikura and Weichen Zhang

1. Introduction

Fuel debris was produced because of a serious accident that occurred at the Fukushima Daiichi Nuclear Power Plant as a result of the Great East Japan Earthquake and tsunami that occurred in 2011. The environment of murky water and intense radiation necessitates the development of novel characterization approaches, which are necessary because retrieval technology has not yet been widely developed. However, the effective imaging depth of ultrasonic sensing is less than 100 millimeters, which is a limitation that limits its potential. In order to circumvent this constraint, Shoji and his colleagues at the Muroran Institute of Technology came up with a novel ultrasonic signal reception technique that they called the Photoacoustic Probes System (Fig.1). Through the utilization of the interaction between laser light and ultrasonic vibrations, this method is utilized. Through the use of laser deflection, the Photoacoustic Probes System is able to detect ultrasonic signals. This allows it to circumvent limits in terms of reception angle and aperture width, while simultaneously receiving reflections uniformly across a wide frequency bandwidth. Additionally, it is anticipated that this concept will be able to accomplish side-lobe suppression when the technique of pulse compression is utilized for attenuation correction. Within the scope of this study, the constructed Photoacoustic Probe System is shown, and its ultrasonic wave reception performance is evaluated throughout.

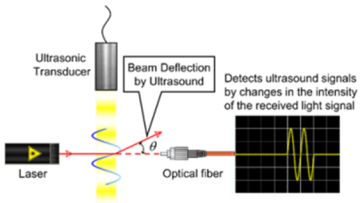

Fig. 1 Principle of the Photoacoustic Probe System

2. Photoacoustic Probe System

As seen in Figure 2, the Photoacoustic Probe System is comprised of an optical fiber semiconductor laser with an optical wavelength of 635 nm and an optical power ranging from 0 to 2.7 mW. This laser is responsible for the transmission of probe light, and it is accompanied by a collimating lens that is responsible for collimating the light that is transmitted from the optical fiber. The light receiving system is made up of an optical fiber that is responsible for receiving the laser light that has been deflected by ultrasonic waves. This light is then converted into a change in the intensity of the incident light by using a micro light-receiving surface. Finally, the light is directed to a photodiode (APD410A2/M, Thorlabs Inc.). To gather ultrasonic waveform data that has traveled over the optical route, the signal that has been photoelectrically converted is sent to an oscilloscope (Keysigt Infini Vision DSOX2004A).

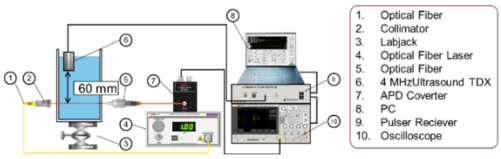

Fig. 2 The develped 3-D vector UVP system

3. Experiment

The distance between the laser beam and the ultrasonic transducer was set to 60mm. To confirm the receivable bandwidth of the Photoacoustic Probe System, ultrasonic pulses with center frequencies of 1 MHz, 2 MHz, 4 MHz, and 8 MHz were transmitted toward the laser beam. The reception results for each pulse pattern are shown in Fig. 3. In conventional ultrasonic probes, the receivable frequency bandwidth is limited by the resonance frequency of the ultrasonic element. In contrast, the Photoacoustic Probe System does not use a physical transducer for ultrasonic reception. It was demonstrated that a single probe can receive ultrasonic pulses over a wide frequency band. This wideband reception characteristic suggests that effective side-lobe suppression can be expected when applying the pulse compression method used to compensate for distance-dependent attenuation, which is a key challenge in ultrasonic sensing technology.

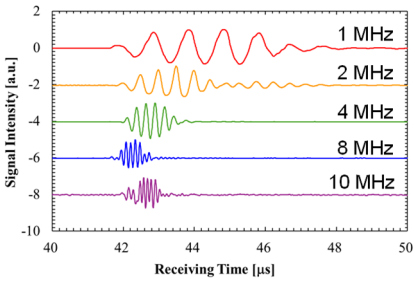

Fig. 3 Results of detected ultrasonic

4. Conclusion

A Photoacoustic Probe System utilizing light deflection was developed for non-contact reception of ultrasonic pulses in water. The system was shown to receive wideband ultrasonic waves. This feature is expected to allow for effective side-lobe suppression when pulse compression is applied for distance attenuation correction. The system will be developed into an ultrasonic reception sensor. This sensor will be applied to measure the shape of fuel debris.

Reference

1. S. Oshima, N. Shoji, H. Kikura, H. Takahashi: Basic Research on Ultrasonic Signal Reception System using Laser Beam; 14th Pacific Symposium on Flow Visualization and Image Processing, November 27-29, 2024, The University of Canterbury in Christchurch, New Zealand, ID-5.

I-16 Performance of All-Solid-State Batteries under Radiation

Hiroshige Kikura and Weichen Zhang

1. Introduction

The Fukushima Daiichi accident and the Great East Japan Earthquake in 2011 showed how important it is to have devices that can withstand radiation to help with nuclear decommissioning. Decommissioning robots need reliable power sources in areas with a lot of radiation; thus batteries that can handle a lot of radiation are necessary for safe and continuous operation. This study concentrates on all-solid-state batteries (ASSBs) as a viable power source for nuclear decommissioning robots. The study examines the electrical performance of ASSBs, focusing on current and voltage characteristics, in conditions of high radiation exposure to assess their applicability. Experimental results show how radiation affects battery performance, which helps us understand how stable and long-lasting they are under extreme conditions.

2. Measurement System

The radiation measurement system is shown in Fig.1. This measurement system includes a charger (Skyrc D200neo) and a discharger (Hitec AD350). The charging and discharging are controlled using Skyrc's dedicated software, Charge Master V1.19. The All-Solid-State AMP-Battery models used in this experiment are AMP7197247 (rated capacity 15,000mAh, operating voltage 3.85V, rated current 4.4A). The battery temperature is maintained at 25°C, and the discharge current is kept constant during measurements. The photo of experiment set up is shown in Fig.2. The anode and cathode of the all-solid-state lithium battery are connected to the charger Skyrc D200neo, which is then connected to the discharger Hitec AD350 to discharge the All-Solid-State AMP-Battery. The charger Skyrc D200neo is connected to a computer via USB, and the software Charge Master is used to record the changes in voltage, current overtime, and capacity during the discharge process of the All-Solid-State AMP-Battery. To prepare for the discharge experiment, the All-Solid-State AMP-Battery is fully charged. After the All-Solid-State AMP-Battery is fully charged, the discharge experiment is conducted in a radiation environment. The discharge process continues from 100% charge until the charger automatically stops when it can no longer discharge. The changes in voltage, current overtime, and capacity data are recorded through the software Charge Master.

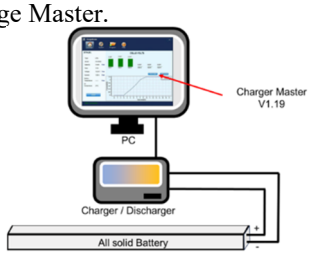

Fig.1 Experiment setup for ultrasonic measurement

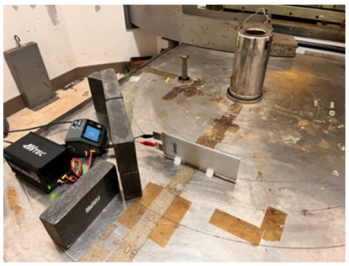

Fig.2 Photo of battery in irradiation chamber

3. Result and Discussion

The current and voltage result for All-Solid-State AMP-Battery AMP7197247 is shown as Fig.3 which the source distance is 0.2m (260Gy/h) and Fig.4 which source distance 0.5m (44Gy/h). The blue curve represents the voltage; red curve represents the current and the number under graph shows the capacity. From the result, even the distance of the battery to the radiation source changes from 0.2m to 0.5m, the trend of current and voltage seems similar, and the capacity of the battery for discharging is similar too. This result indicates that the effect on current, voltage from the radiation is little, the battery keeps stable in electrical.

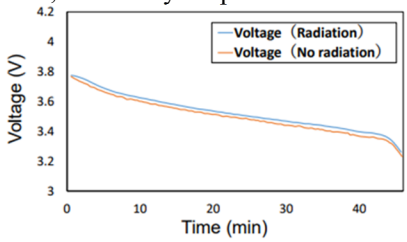

Fig.3 Voltage curve of battery under radiation or not

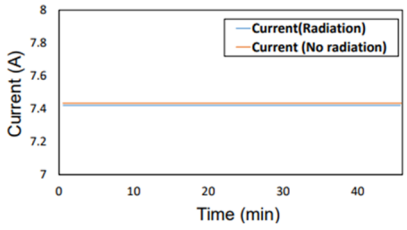

Fig.4 Current curve of battery under radiation or not

4.Conclusions

This study evaluated the electrical performance of all-solid-state batteries under high-radiation conditions. The results show that voltage, current, remained largely unchanged even at radiation levels up to 260 Gy/h. These findings indicate that batteries maintain stable performance during irradiation.

Reference

1.Weichen Zhang, Hiroshige Kikura, Yutaka Tamaura, Tadashi Kawamoto: Investigation of Radiation Effects on All-Solid-State Battery Performance; AESJ The 23rd Young Researchers' Presentation, Tokyo, 2024 11.8

I-17 Liquid metal technology for seawater desalination

Masatoshi Kondo

1. Introduction

Water scarcity is an important issue to be addressed for the achievement of sustainable society of the world. Seawater desalination can satisfy the huge demand for freshwater. However, seawater desalination plants based on reverse osmosis (RO) and multi stage flash distillation (MSF) discharge huge amounts of brine as waste, which has a higher concentration of metallic elements than seawater

Groundwater is the largest and most reliable source of freshwater in some countries, although it is polluted by arsenic (As). The purification of As-polluted groundwater can satisfy the huge demand for freshwater. However, conventional methods such as absorption and electrocoagulation processes require large energy consumption and treatment of contaminated sludges.

The collection and recovery of metallic elements from these feed solutions from the seawater desalination brine and polluted groundwater is the common issue. The collection of metal resources from seawater and desalination brine can contributes both to securing resources and reducing wastes. However, conventional methods have some issues. An electrodialysis (ED) process consumes large amounts of electricity. A carbonation process discharges hazardous wastes produced by using absorbent agents.

Liquid metal fluids are considered as a coolant of energy power plant and the technologies have been studied so far. The strong chemical affinity of liquid metal fluids can be applied for the collection of metal resources from the seawater, desalination brine and polluted ground water. The purpose of the present study is to establish novel desalination method based on the liquid technology which can recover the metal elements without the emission of huge wastes.

2. Desalination of seawater with liquid metal Sn[1]

Liquid metal tin (Sn: melting point 505 K) works as coolant of the desalination system in the present study. Seawater is directly sprayed to the free surface of liquid Sn to produce fresh water according to the distillation reaction. Valuable metal elements contained in seawater are then dissolved into liquid Sn. The elements dissolved are precipitated and recovered by decreasing the temperature according to the temperature dependences of the metal solubilities in liquid Sn. Therefore, the concentrated brine is not discharged in this concept.

The desalination plant was conceptually designed in 2024 and 2025, and the major specifications was determined. The liquid metal inventory is approximately 6.3×10^2 L. If this plant is operated in Egypt where water scarcity is serious problem and solar radiation is abundant, the amount of fresh water produced and valuable resources recovered were estimated as 3.6×10^2 ton/y and 1.1 ton/y, respectively.

The chemical interaction between liquid Sn and seawater was investigated by means of the liquid Sn and seawater direct contact experiments. Artificial seawater at room temperature was dripped on the free surface of liquid Sn at 573 K at the dripping ratio of 5 mL/50 min or 20 mL/200 min. The composition of the water produced in the test at 573 K was chemically analyzed with ICP-MS. The concentration of Na and Mg in the water produced by the were 432 mg/L and 46.3 mg/L, which satisfy the drinking water quality standards set by World Health Organization. The surface condition of Sn after the test was metallurgically analyzed with SEM/EDX. The precipitations of Na chloride (NaCl), Mg compound and Sn oxide (SnO) were recognized.

2. Collection of metal elements from desalination brine and polluted ground water with liquid metal Sn[2]

Liquid metal Sn pool is used for the collection of metal elements from the brine and the polluted groundwater, which does not release the wastes. The brine of 0.2 mL/min was sprayed onto the surface of liquid Sn at 573 K. Metal and non-metal elements (e.g., Na and Cl) were dissolved into liquid Sn and collected as precipitates in the cooling process at 505 K for 600 min. The enrichment and precipitation of mineral elements such as Na, Mg, K and Ca contained in brine were demonstrated by means of the cold-trapping experiments with liquid Sn pool. Na, Mg, K and Ca contained in brine were dissolved and accumulated in liquid Sn during the direct contact reaction process. The metallic elements were precipitated from liquid Sn cooled at lower cooling rate. The metallic elements of Na, Mg, K and Ca were separately precipitated in liquid Sn pool.

The water containing As of 5 mL was dropped on the surface of liquid Sn at 573 K for 50 min. As3+ ion dissolved into liquid Sn as an atomic state. The distillation of As-polluted water was demonstrated by means of the direct contact reaction experiments with liquid Sn. The distillation process at higher temperature induced the advection of As according to the evaporation. However, the evaporation of As was suppressed when As contained in water was captured by liquid Sn.

Reference

1. T. Horikawa, M. Kondo, et al.; Water Reuse, Vol.15, No.1, 109 (2025).
2. T. Horikawa, M. Kondo: Progress in Nuclear Science and Technology, Vol. 7, pp. 250-256 109 (2025).

I-18 Design and development of an informatics framework for actinide extractant discovery leveraging the IDEaL Database

Masahiko Nakase, Tomohiro Okamura, Takahiro Nishihara

1. Introduction

Separating minor actinides (MAs) such as americium (Am) and curium (Cm), helps reduce the size of the final repository area. However, separating trivalent MAs from similar lanthanides (Lns), which are more abundant in spent nuclear fuels and have large neutron-capture cross-sections, is difficult under strong acid conditions. The chemicals used to extract MAs typically contain an N-donor group, which gives them low solubility and causes third-phase formation. To overcome this problem, fluorinated solvents, such as hydrofluorocarbons (HFCs) and hydrofluoroolefin (HFOs), were studied as diluents. Some fluorinated compounds are safe, hard to catch fire, non-toxic, and don't have the potential for ozone layer depletion. These types of solvents have already been shown to work in extraction processes. Their chemical properties can be adjusted by altering their structure, with many possible options. Traditional research methods require careful planning and repeated testing; however, preparing and synthesizing many chemicals is costly, and experiments with radioactive materials generate waste, which slows development. To solve these problems, a machine learning (ML) tool named AACE was developed in 2024. This year, to improve ML's capabilities, we developed an interface to integrate with the International Database for Extractant Ligands (IDEaL), an extractant database managed by OECD/NEA.

2. Methodology

The outline of the informatics approach, combining several databases for ML, is illustrated. To combine a variety of databases that contain usable information for ML, the database (DB) should be able to handle unstructured data. Hence, we created the integration based on MongoDB, one of the most famous schema-less DBs, combined with the existing AACE program, and tested some regression to explore the candidate sidechain structure of the extractant for MA separation from Lns.

3. Results and Discussion

The preliminary attempt to create a regression model to predict Am extractability with DGA-type extractants, using the reported data from IDEaL, was carried out. Firstly, the chemical structural data in IDEaL are transformed into mol (2D), mol2 (3, and SMILES (an alphabetic way to represent molecular structures). Then, molecular fingerprints are generated using Coulomb matrices and the Morgan fingerprint. Based on these fingerprints, a clustering technique was implemented to increase the training data from the IDEaL rationally, and regression attempts were carried out. As a result, the optimized sidechain structure of the DGA molecules, which is suitable for a fluorinated diluent, was preliminarily obtained for the first time.

4. Conclusions and Future Work

The first attempt was successful, and a parametric survey for many exploration studies of molecular structures will be implemented extensively.

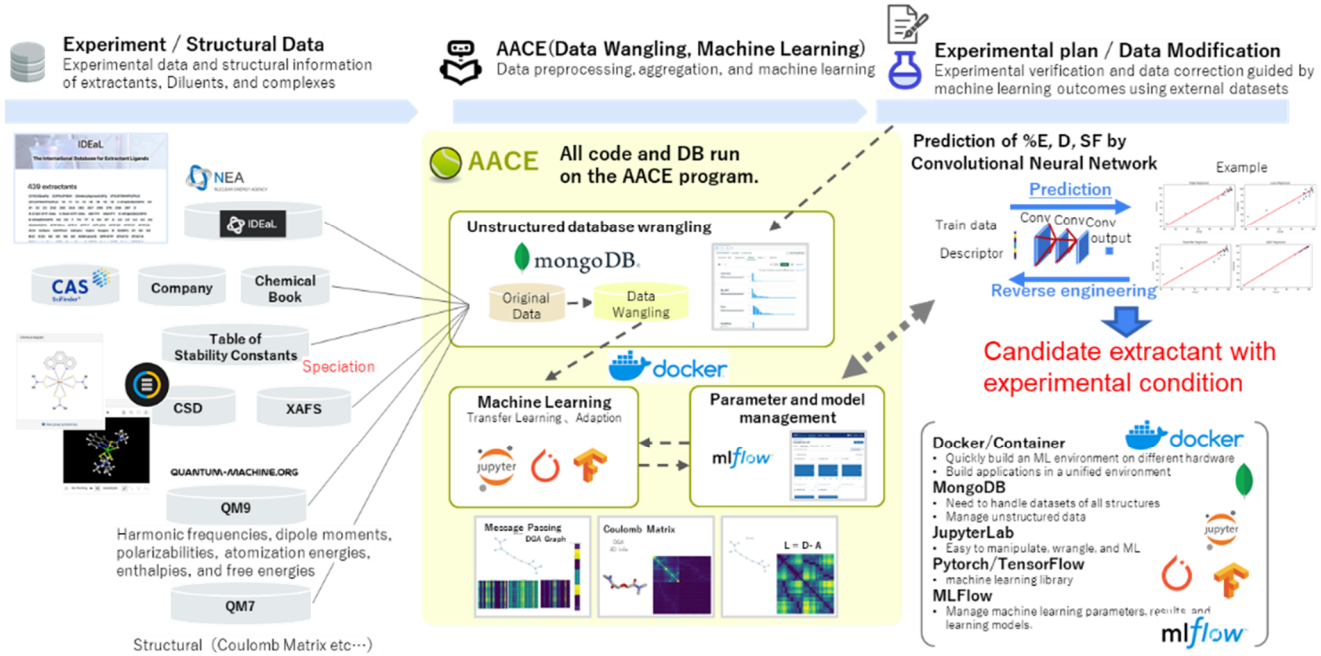

Fig1. Outline of the informatics approach combining several databases for ML.

I-19 Securing Reversibility of $U^{V}O_2^{+}/U^{VI}O_2^{2+}$ Redox Equilibrium in [emim]Tf_2N-Based Liquid Electrolytes towards Uranium Redox-Flow Battery

Koichiro Takao

1. Introduction

Nuclear power is one of promising, realistic, and well-demonstrated solutions to maintain the energy-demanding modern society. However, we also have to seriously think various cumbersome issues arising from nuclear wastes.[1] While back-end stream after nuclear power production such as spent nuclear fuels and high-level radioactive wastes is frequently focused, one has to be aware that depleted uranium (DU) is also afforded as another nuclear waste after enrichment of a fissile U isotope, ^{235}U, to prepare fresh nuclear fuels for the light water reactors.[2] Despite the cost and labor dedicated for mining and refining natural U as well as the following ^{235}U isotope enrichment, few applications of DU are available except for fertiles to breed Pu and some military uses such as penetrating projectiles. As a result, approx. 10^6 tons of DU without any efficient utility is accumulated today.[3]

In general, isotope effects are negligibly small in chemistry, because chemistry of each element is governed by nature and behavior of its electrons. This tendency is more remarkable in heavier elements, most typically in U, the naturally occurring heaviest element. Therefore, we can anticipate to find effective and peaceful use of DU in chemical directions. It is well-known that U shows rich redox behavior from U(III) to U(VI) and unique coordination chemistry associated with each oxidation state.[4] While U^{3+} and U^{4+} are present as spherical metallic ions, U(V) and U(VI) commonly form *trans*-dioxocations, UO_2^{n+} (n = 1, 2), so-called *uranyl(V)* and *-(VI)*, respectively. Both redox couples of U^{3+}/U^{4+} and $U^{V}O_2^{+}/U^{VI}O_2^{2+}$ are chemically reversible and kinetically rapid in principle, because these reactions do not involve any structure rearrangements. This is strikingly different from redox chemistry of vanadium employed in redox flow battery (RFB).[5] While V^{2+}/V^{3+} is chemically reversible actually, $V^{IV}O^{2+}/V^{V}O_2^{+}$ is rather irreversible due to attachment/detachment of O^{2-} through the redox process. To resolve this issue, utilization of DU as alternative electrode active materials in RFB has been proposed.[6]

The largest issue herein is design and optimization of actual redox systems in which all oxidation states from U(III) to U(VI) must be well stabilized to make U^{3+}/U^{4+} and $U^{V}O_2^{+}/U^{VI}O_2^{2+}$ redox equilibria reversible and repeatable. However, U^{3+} is highly sensitive to reduce H^+ to H_2 and to react with various organic molecules including solvents and ligands designed for its stabilization. $U^{V}O_2^{+}$ exhibits strong tendency towards disproportionation to afford U(IV) (U^{4+} or $U^{IV}O_2$) and $U^{VI}O_2^{2+}$. Despite significant efforts dedicated to molecular design of organic ligands, the above problems are not fully resolved even today.[1]

In contrast, stabilization of U species at any valence states is not always difficult in molten salts and their eutectics, although a highly volatile species like UX_6 (X = F, Cl) may be formed and tends to escape from such a high temperature system. Therefore, we can learn something and get helpful hints from such pyrochemical processes. Due to extremely high temperature, any well-designed organic molecules are no longer applicable, while an anionic constituent of a molten salt employed, most typically Cl^-, indeed works well as a ligand to stabilize any valences of U.[7] To transfer these insights to the ordinary solution chemistry, ionic liquids (ILs, Fig. 1) were frequently employed as liquid electrolytes accessible even at room temperature. As a result, $U^{V}O_2^{+}$ was successfully stabilized as a tetrachloro complex, $[U^{V}O_2Cl_4]^{3-}$, in a [emim]BF_4/Cl liquid electrolyte to show a reversible $[U^{V}O_2Cl_4]^{3-}/[U^{VI}O_2Cl_4]^{2-}$ redox reaction.[8] More recently, we have also observed a quasi-reversible U(III/IV) redox equilibrium in a [emim]Tf_2N-DMF mixture dissolving [emim]Cl,[9] where hexachloro complexes $[U^{III}Cl_6]^{3-}/[U^{IV}Cl_6]^{2-}$ seems to be formed.

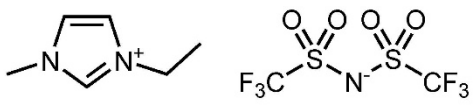

Fig. 1. Schematic structures of ionic liquid components used in this work. [emim]$^+$: 1-ethyl-3-methylimidazolium, Tf_2N^-: bis(trifluoromethyl)sulfonylamide.

Although all U oxidation states from III to VI would be stabilized by chloro complexation in IL-based liquid electrolytes thanks to implications obtained from the former molten salt systems, the media employed in the previous works are still not well unified. In this work, we aim to revisit the $U^{V}O_2^{+}/U^{VI}O_2^{2+}$ redox chemistry in the [emim]Tf_2N-based liquid electrolyte common to our recent work for U(III/IV).[9] Electrochemical reduction of $[U^{VI}O_2Cl_4]^{2-}$ in [emim]Tf_2N was studied to explore fundamentals of $U^{VI}O_2^{2+}$ electrochemistry in this IL.

2. Results and Discussion

Figure 2 shows cyclic voltammograms of $U^{VI}O_2^{2+}$ (3.82 mM) in [emim]Tf_2N liquid electrolyte containing 1.32 M [emim]Cl. In use of a glassy carbon working electrode (GC WE, Fig. 2(a)), a couple of cathodic and anodic peaks appeared at -1.06 ± 0.01 V (E_{pc}) and -0.97 ± 0.02 V (E_{pa}) *vs.* Fc/Fc$^+$, respectively, at any potential sweep rates (v) from 10 mV·s^{-1} to 500 mV·s^{-1}. Although it is hard to precisely determine the peak current of the anodic wave (i_{pa}), the

observed redox process seems to be chemically reversible. Indeed, the semiempirical relationship derived by Nicholson[10] resulted in the ratio of i_{pa} compared with the cathodic peak current (i_{pc}) close to unity. Furthermore, the cyclic voltammogram traces were well reproduced in multiple CV scans. A peak potential separation ($\Delta E_p = E_{pa} - E_{pc}$) at v = 10 mV·s^{-1} was 65 mV, and increased with an increase in v up to 123 mV at v = 500 mV·s^{-1}. This is a typical trend of an electrochemically quasi-reversible system. The formal potential ($E^{\circ\prime} = (E_{pc} + E_{pa})/2$) is almost constant at −1.014 ± 0.002 V *vs.* Fc/Fc$^+$ with regardless of v. Previously, we have reported a quasi-reversible redox couple of $[U^{V}O_2Cl_4]^{3-}$/$[U^{VI}O_2Cl_4]^{2-}$ in the [emim]BF$_4$/Cl (50:50 mol%) system in a similar potential region at $E^{\circ\prime}$ = −0.989 ± 0.002 V *vs.* Fc/Fc$^+$,[8] indicating that the same U(V/VI) redox equilibrium (Eq. (1)) has been observed in the current [emim]Tf$_2$N solution of Fig. 2(a).

$$[U^{VI}O_2Cl_4]^{2-} + e^- = [U^{V}O_2Cl_4]^{3-} \quad (1)$$

From the relationship between i_{pc} and a square root of v, a diffusion coefficient (D_O) of $[U^{VI}O_2Cl_4]^{2-}$ in this system was estimated to be 1.7 × 10^{-7} cm^2·s^{-1}, which is in the same order of magnitude with self-diffusion coefficients of both components of this ionic liquid ([emim]$^+$: 4.8 × 10^{-7} cm^2·s^{-1}; Tf$_2$N$^-$: 2.9 × 10^{-7} cm^2·s^{-1}).[11]

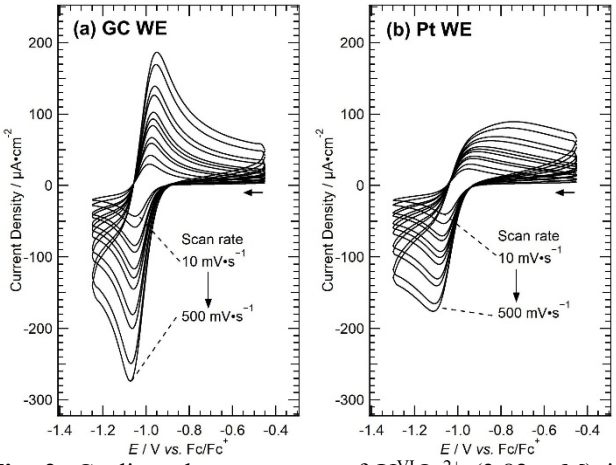

Fig. 2. Cyclic voltammograms of $U^{VI}O_2^{2+}$ (3.82 mM) in [emim]Tf$_2$N dissolving 1.32 M [emim]Cl at steady state after repeating potential sweep cycles 3 times at 298 K. WE: GC (a), Pt (b); RE: Ag/AgCl (3 M NaCl) connected to sample solution through [emim]Tf$_2$N liquid junction; CE: Pt wire. Scan rate: 10-500 mV·s^{-1}.

As shown in Fig. 2(b), it is noteworthy that reversibility of the redox reaction of $[U^{VI}O_2Cl_4]^{2-}$ has become remarkably worse, when Pt WE was employed instead of GC WE. Note that a cathodic wave still appeared at around −1.07 V *vs.* Fc/Fc$^+$ in a similar manner to that in use of GC WE (Fig. 2(a)), implying that $[U^{VI}O_2Cl_4]^{2-}$ initially present in the test solution is once reduced to $[U^{V}O_2Cl_4]^{3-}$. However, the cathodic current density is smaller than that observed on GC WE (Fig. 2(a)). While the anodic response at v = 50 mV·s^{-1} clearly appeared, the electrochemical reversibility of this redox equilibrium is getting worse and worse with an increase in v up to 500 mV·s^{-1} (Fig. 2(b)). Note that the chemical reversibility of this system was confirmed in the multi-scanned cyclic voltammograms on Pt WE at any v tested. Although it is hard at this moment to further know what actually happens in this system, a set of these results with Pt WE suggests that both forward and backward electrode reactions of Eq. (1) proceed more slowly on Pt WE compared with those on GC WE. As an electrode material in RFB, GC is more suitable to secure the reversibility and rapid electron transfer of the redox reaction between $[U^{VI}O_2Cl_4]^{2-}$ and $[U^{V}O_2Cl_4]^{3-}$ in the current system.

3. Conclusion

In this work, we have studied how to secure the $U^{V}O_2^+$/$U^{VI}O_2^{2+}$ redox reversibility in [emim]Tf$_2$N-based liquid electrolyte, where loading Cl$^-$ is mandatory to stabilize the reductant, $U^{V}O_2^+$. One of large hudrles to adopt DU in RFB application is electromotive force (*emf*), which can be expected only ~0.4 V.[9] This is much smaller than that of the V-based RFBs (1.26 V) already implemented.[5] To overcome this issue, cell-stacking would be efficient, or it is still necessary to explore better systems in terms of both liquid electrolytes and ligands stabilizing all U oxidation sates from III to VI.

Acknowledgments

This work was supported by Grants-in-Aid for Scientific Research (No. 20H02663).

References

1. K. Takao, *Dalton Trans.* **2023**, *52*, 9866-9881.
2. M. Benedict, T. H. Pigford, H. W. Levi, *Nuclear Chemical Engineering*, 2nd ed., McGraw-Hill, United States, **1981**.
3. *Uranium 2022: Resource, Production and Demand*, OECD-NEA, IAEA, Boulogne-Billancourt, France, **2022**.
4. *The Chemistry of the Actinide and Transactinide Elements*, Springer, Netherlands, **2010**.
5. Y. Wu, R. Holze, *Batteries* **2018**, *4*, 47
6. Y. Shiokawa, T. Yamamura, K. Shirasaki, *J. Phys. Soc. Jpn.* **2006**, *75*, 137-142.
7. T. Nagai, A. Uehara, T. Fujii, O. Shirai, N. Sato, H. Yamana, *Electrochem.* **2009**, *77*, 614-616.
8. T. Ogura, K. Takao, K. Sasaki, T. Arai, Y. Ikeda, *Inorg. Chem.* **2011**, *50*, 10525-10527.
9. K. Ouchi, A. Komatsu, K. Takao, Y. Kitatsuji, M. Watanabe, *Chem. Lett.* **2021**, *50*, 1169-1172.
10. R. S. Nicholson, *Anal. Chem.* **1966**, *38*, 1406.
11. T. Umecky, Y. Saito, H. Matsumoto, *J. Phys. Chem. B,* **2009**, *113*, 8466-8468.

I-20 Development Progress of Metal-Supported Solid Oxide Electrolysis Cells Using Thermal Spray Method

Hiroki Takasu

1. Introduction

With the increasing disposal of surplus energy due to the expansion of renewable energy, it has become an effective option to store and reuse this wasted energy across time and space. Our laboratory is focusing on the electrolysis of carbon dioxide (CO_2) as a promising technology candidate for the future. In carbon neutrality, the goal is to achieve a virtual zero emission of greenhouse gases such as CO_2. Negative emission technologies are currently being considered as a solution for industries and transportation sectors where it is not practically feasible to eliminate carbon use entirely. On the other hand, carbon is utilized not only as an energy source but also in various materials used in everyday life, and its use is expected to continue in the future. Therefore, it is necessary to consider both the emission and supply of carbon. CO_2 electrolysis, capable of equalizing the amount of carbon supplied and emitted, is exactly the technology needed. In most cases, carbon is ultimately emitted as CO_2. To reuse carbon, it is necessary to chemically convert this stable CO_2 into a substance with higher energy status by applying some form of energy input. For example, by converting CO_2 into high-value-added substances such as carbon monoxide or formic acid, it can be reused as a clean raw material for chemical products and fossil fuels. Although various CO_2 conversion technologies are conceivable, CO_2 electrolysis utilizing high-quality electrical energy, which can be easily controlled in terms of voltage and current, can be considered a promising technology that can meet the demands of large-scale CO_2 conversion required by industrial and social sectors.

Our laboratory is currently working on the development of solid oxide electrolysis cells (SOECs) with a view toward larger scale production (Figure 1).

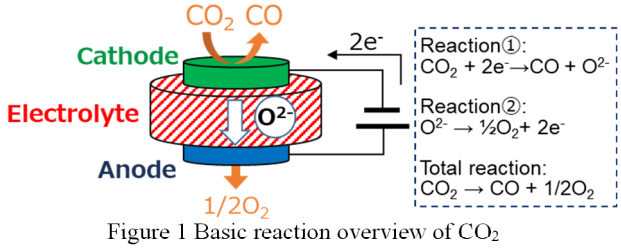

Figure 1 Basic reaction overview of CO_2 electrolysis using SOEC

Specifically, we are developing metal-supported SOECs (MS-SOEC) as shown in Figure 2 with a unique structure that utilizes a metal wire mesh as a support and introduces a reaction layer through thermal spraying[1]. Using metal as a support enables us to address challenges such as large-area (high-capacity) cell production and cost reduction in existing cells, while also expecting improvements in startup speed during operation. In fact, we prepared coin-type cells with a diameter of 2 cm and reported the principle demonstration of CO_2 high-temperature electrolysis[2].

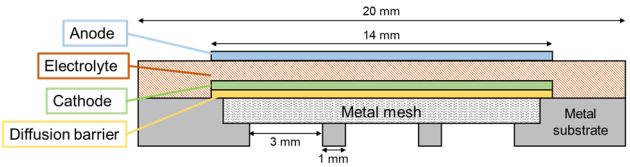

Figure 2 Basic cross-section structure diagram of MS-SOEC

2. Evaluation of MS-SOEC

As an example of the experiments, Figure 3 shows the results of direct CO_2 electrolysis tests conducted at around 800°C using the developed MS-SOEC. Apparent increases in current associated with CO_2 electrolysis were observed starting around 1 V in both the 750-850°C temperature ranges. Furthermore, differences in oxygen ion conductivity within the electrolyte at varying temperatures revealed that the increase in ohmic resistance was more apparent at lower temperatures. Therefore, improving electrolyte performance or operating at higher temperatures are potential avenues for enhancing cell performance.

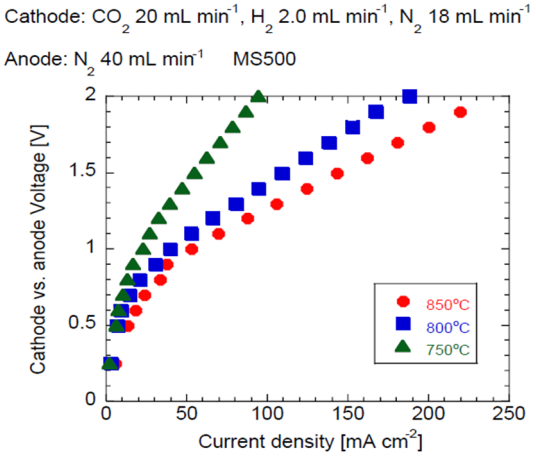

Figure 3 I-V characteristics of CO_2 electrolysis under high-temperature conditions using the developed MS-SOEC

Additionally, we are working on densifying the electrolyte, an important factor in the development of MS-SOEC using thermal spray method. Specifically, to achieve this improvement, the spray particle size of the electrolyte was reduced from 29 to 18 μm, and the spray conditions were adjusted[3]. As a result, cross-sectional observations confirm that the porosity has been successfully reduced by approximately half. Furthermore, cells with the densified electrolyte demonstrated a reduction in the total resistance during CO_2 electrolysis at 800°C. This is thought to be due to the formation of favorable oxygen ion conduction pathways resulting from the densification process.

To date, we conducted various efforts including cell manufacturing studies for MS-SOEC, proof-of-concept demonstrations for CO_2 electrolysis, and investigations into

improving the electrolyte layer. Currently, we are working through the National Project to further enhance the cell performance, strengthen the durability, and increase the cell capacity of this MS-SOEC.

2. Conclusion

Our laboratory is currently developing SOECs with an eye toward larger-scale production, specifically focusing on the development of MS-SOECs. The MS-SOEC employs a unique structure utilizing a metal wire mesh as the support substrate, with the reaction layer introduced via thermal spraying method. In addition to considering the basic structure of MS-SOEC, we conducted a proof-of-concept demonstration of direct CO_2 electrolysis at 800°C under coin-cell scale. We also conducted densification studies on the electrolyte, a key component layer of MS-SOEC. By reducing the particle size of the thermal spray, we successfully reduced the layer's porosity by half. For future development, we will pursue efforts to further enhance the cell performance of this MS-SOEC, strengthen its durability, and increase its cell capacity.

Acknowledgments

Part of this report is based on results obtained from a project, JPNP16002, commissioned by the New Energy and Industrial Technology Development Organization (NEDO).

References

1. Y. Numata, K. Nakajima, H. Takasu, Y. Kato, Carbon Dioxide Reduction on a Metal-Supported Solid Oxide Electrolysis Cell, ISIJ International, 59, 4, 628-633, 2019
2. H. Takasu, Y. Maruyama, Y. Kato, Development of Metal Supported SOEC for Carbon Recycling Iron Making System, ISIJ International, 60, 12, 2870-2875, 2020
3. K. Umeda, Y. Maruyama, S. Kuzukami, S. Tominaga, Y. Kato, H. Takasu, “Effect of electrolyte particle size on CO_2 electrolysis performance of metal-supported solid oxide electrolysis cells prepared by atmospheric plasma spraying method”, Progress in Nuclear Science and Technology, 7, 273-278, 2025

I-21 Estimation of Plasma Vertical Position by Long-Short Term Memory Network with Time2Vec in a Small Tokamak Device PHiX

Sejung JANG, Hiroaki TSUTSUI

1. Introduction

Although tokamak is one of the leading a candidate for a fusion power reactor, there remain many problems to be solved for commercial application. Since tokamak plasma with an elongated cross-section have demonstrated high performance [1, 2], many tokamak devices use elongated plasma. The vulnerability of elongated plasmas to vertical instability emphasizes the importance of estimation to minimize and analyze the occurrence of vertical displacement events (VDEs) [3]. Estimating plasma vertical position using operational data is crucial for safely controlling elongated plasma and mitigating disruptions linked to VDEs, which lead to the influx of impurities and wall damage due to plasma interactions with the wall. In order to solve this problem, we utilized machine learning techniques to develop models which can estimate plasma vertical position. So, we create a data-driven model for multivariable regression of VDEs by utilizing the neural network [4]. Plasma discharge experimental data are obtained as time series data such as densities, temperature and magnetic field, etc. These data are important resources for solving the many problems, but there are limitations as humans cannot analyze the enormous time series data. However, the neural network can easily deal with the enormous amount of data.

Conversely, we developed a deep learning-based regression model using noisy data and used this model to predict the vertical position of the plasma in real time. The recurrent neural network (RNN)-based models [7] such as long short-term memory (LSTM) [8] have been conventionally used to estimate plasma disruptions [9–11] using time-series data. In contrast to standard feedforward neural networks, RNNs have an internal loop, a kind of memory function, which allows them to retain and apply information through a series of data points. The results of these RNN-based models suggest that data-driven models for plasma disruption can be utilized to mitigate and prevent such disruptions. Despite the advancements, they face limitations such as frequent false alarms, compounded by the challenge of interpreting LSTM networks due to their complexity and non-linearity. Therefore, LSTM alone falls short in delivering sufficient performance. Hence, there's a necessity for an approach to supplement the LSTM and improve its efficacy.

In this study, we apply the LSTM, which is an advanced version of the RNN model, and the Time2Vec [12] is a novel approach that incorporates time-related features for multivariate regression to estimate VDEs using plasma discharge experimental data from PHiX [13] at Tokyo Institute of Technology.

2. LSTM with Time2Vec

Original LSTM models do not treat time itself as a feature assuming that inputs are synchronous. When time is known to be a relevant feature, it is fed in another input dimension. Time2Vec [12] is a learnable vector representation which is embedded instead of the time τ. The advantages of using Time2Vec include capturing temporal patterns and handling irregular time intervals. It helps the neural network understand time-related data by providing vectors with learnable parameters.

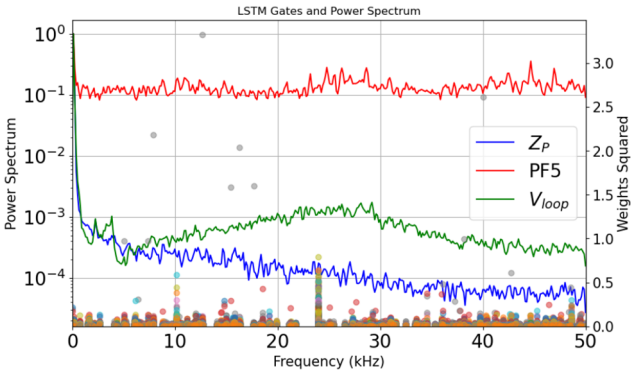

Fig. 1 A comparison of the power spectra of the experimental data and the learned parameters in Time2Vec. The solid lines represent the average power spectra, which are normalized to have a value of unity at frequency =0, of the plasma vertical position, PF5 currents, and loop voltage in the training data. The dots are squared weights of the trained model.

3. Application to Small Tokamak

In order to check the efficiency of Time2Vec, we compared the distribution of W^2 and the power spectra of plasma vertical positions, PF5 currents, and loop voltage in the training data are depicted in Fig. 1. It shows significant weight changes at 10 kHz and 24 kHz. When comparing the power spectra of multiple inputs and output, no special frequencies were found. Regarding the reasons for this phenomenon, it is currently under investigation and remains unknown. The original paper on Time2Vec [12] demonstrates the extraction of characteristic frequencies. However, the experimental data used in this study do not have inherent characteristic frequencies according to the power spectra.

4. Conclusions

This study aims to analyze plasma VDEs by estimating the plasma vertical displacement. This data-driven model with accumulated data from a specific tokamak demonstrates the capability to estimate plasma movements thereby enabling us to design a operational scenario. We observed that the model employing Time2Vec yielded better performance in terms of test loss compared to LSTM without Time2Vec. Additionally, we attempted to confirm how Time2Vec affects the model's predictions by extracting weight parameters from Time2Vec, and two special frequencies are identified. However, the experimental data used in this study do not have corresponding frequency components. Further research is, therefore, needed regarding the significant changes in weight at specific frequencies.

Acknowledgments

This work was supported by JSPS KAKENHI Grant Number 21H01061.

References

[1] F. Troyon, R. Gruber, H. Saurenmann, S. Semenzato and S. Succi, Plasma Phys. Control. Fusion 26(1)A, 209 (1984).
[2] R.J. Goldston, Plasma Phys. Control. Fusion 26(1)A, 87 (1984).
[3] Y. Nakamura, R. Yoshino, N. Pomphrey and S.C. Jardin, J. Nucl. Sci. Technol. 33(8), 609 (1996).
[4] S.Weidman, Deep Learning from Scratch (O'Reilly Media, Sebastopol, CA, 2019), Chap. 2.
[5] T. Yokoyama, H. Yamada, S. Masuzaki, B.J. Peterson, R. Sakamoto, M. Goto et al., Plasma Fusion Res. 17, 2402042 (2022).
[6] S. Inoue, Y. Miyata, H. Urano and T. Suzuki, Nucl. Fusion 62(8), 086007 (2022).
[7] D.E. Rumelhart, G.E. Hinton and R.J. Williams, Nature 323(6088), 533 (1986).
[8] S. Hochreiter and J. Schmidhuber, Neural Comput. 9(8), 1735 (1997).
[9] J. Kates-Harbeck, A. Svyatkovskiy and W. Tang, Nature 568, 526 (2019).
[10] A. Pau, A. Fanni, S. Carcangiu, B. Cannas, G. Sias, A. Murari and F. Rimini, Nucl. Fusion 59, 106017 (2019).
[11] A. Agarwal, A. Mishra, P. Sharma, S. Jain, S. Ranjan and R. Manchanda, Plasma Phys. Control. Fusion 63(11), 115004 (2021).
[12] S.M. Kazemi, R. Goel, S. Eghbali, J. Ramanan, J. Sahota, S. Thakur et al., arXiv preprint arXiv:1907.05321 (2019).
[13] S. Naito, M. Murayama, S. Hatakeyama, D. Kuwahara, Y. Suzuki, H. Tsutsui and S. Tsuji-Iio, Nucl. Fusion **61**(11), 116035 (2021).

I-22 Research on Quantum Entanglement of Gamma Photons

Mizuki Uenomachi

1. Introduction

"Quantum Entanglement", which is the phenomenon that correlated properties are maintained even between spatially separated particles, was experimentally demonstrated around 1982 by Alan Aspect et al. They verified its existence through polarization measurements of visible photon pairs generated via cascade transitions, thereby demonstrating the violation of Bell's inequality. Since then, this phenomena has been applied to advanced technologies such as quantum computing, quantum communication, quantum cryptography, and so on.

In the 1940s, theoretical and experimental studies were also conducted on the entanglement of annihilation gamma photons generated by electron-positron annihilation. However, due to the difficulty of measuring the polarization of high-energy photons with optical polarizers, the experiments were not suitable to verify the violation of Bell's inequality. In recent years, with advances in theory and measurement technology, research on quantum entanglement of gamma photons has once again attracted considerable attention. In particular, as positrons are used in positron emission tomography (PET), studying the quantum entanglement of annihilation photons may contribute to improving PET imaging.

In this study, we performed Monte Carlo simulations using the Geant4 toolkit to evaluate polarization measurements with our originally developed gamma-ray pixel detectors, aiming at future applications to PET and other high-energy entangled photon measurements.

2. Monte Carlo simulations of quantum entanglement of annihilation gamma photons

The annihilation gamma photons in a quantum-entangled state have mutually orthogonal polarization states. The Klein–Nishina formula shows that in Compton scattering, the angular distribution of scattered photons depends on the polarization of the incident gamma rays. Since gamma rays tend to scatter perpendicular to their polarization, the polarization correlation between two annihilation photons can be evaluated by measuring Compton scattering events.

In a simulation, an 8×8 array of $Gd_3(Al,Ga)_5O_{12}(Ce)$ pixel scintillator detectors (pixel size: 2.5 mm × 2.5 mm ×9 mm, pitch size: 3.2 mm × 3.2 mm) identical to those in our developed detectors were arranged in a ring geometry around a ^{22}Na point source (Fig. 1). The simulation was conducted to measure the polarization correlation of quantum-entangled annihilation gamma photons emitted from positrons produced by the ^{22}Na source. Using Geant4 (v11.3.2), which enables simulations of quantum-entangled annihilation photons, we evaluated their polarization correlation measurement.

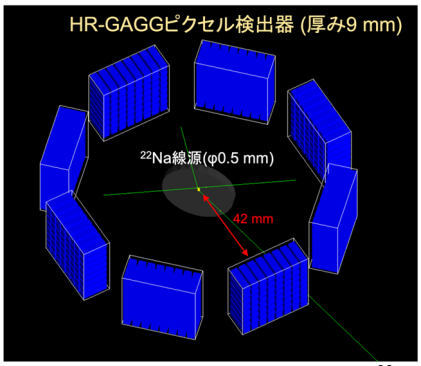

Fig. 1 Setup of GAGG pixel detectors and ^{22}Na source

3. Simulation results of the polarization correlation

The polarization correlation between the two annihilation gamma rays was calculated as a function of the relative azimuthal scattering angle, defined as $\Delta\phi = \phi_1 - \phi_2$, where ϕ_1 and ϕ_2 are the scattering directions of each photon. Coincidence events were selected in which the total energy detected in two pixels was 511 keV $\pm$ 10%, and the calculated Compton scattering angle satisfied $72° \leq \theta_{sca} \leq 92°$. The result of polarization correlation is shown in Fig. 2. The enhancement ratio between the maximum ($\Delta\phi = \pm 90°$) and minimum ($\Delta\phi = 0°$) scattering probabilities R was approximately 1.60, which is close to the classical limit of $R = 1.63$. In previous studies, R values exceeding 1.8 have been reported; therefore, we are reviewing and refining our analysis method and simulation setup.

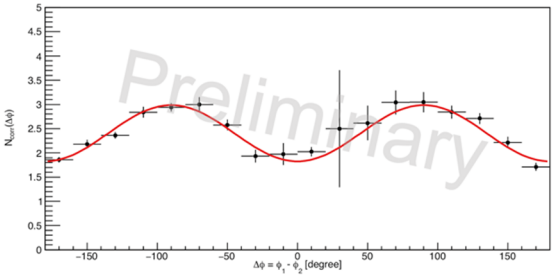

Fig. 2 Preliminary result of simulated polarization correlation between annihilation of gamma rays

4. Summary

We performed Monte Carlo simulations to evaluate polarization measurements with our GAGG pixel detectors. The obtained enhancement ration $R = 1.60$ was close to the classical limit of $R = 1.63$. We are currently reviewing and refining our analysis method and simulation setup. In addition, we are going to perform actual measurements and compare the results with the simulation.

Acknowledgments

This work was supported by JST PREST, Japan, Grant Number JPMJPR23F1.

I-23 Investigation of wurtzite-type ferroelectrics

Shintaro Yasui, Sou Yasuhara

1. Wurtzire-type ferroelectrics

The definition of ferroelectric can be a compound with a polar phase produced by a structural transition from a nonpolar high-symmetry paraelectric state, with an electric polarization that can be switched between two or more symmetry-related variants by application of an electric field. A wurtzite structure (S.G.: *P*63*mc*) is a polar crystal due to non-centrosymmetric crystal structure. It has been thought to be a non-ferroelectric crystal because of firmly formed tetrahedron by strong covalent bonding, its electric polarization cannot be switched by electric field. In this reason, wurtzite structure is categorized non-ferroelectric polar crystal. However, if we consider relative displacement of cation against anion along c-axis, we can find centro-symmetric paraelectric state (S.G.: *P*63/*mmc*) in between two polar states (*P*63*mc*). If the potential barrier of this displacement is low enough, through this paraelectric state (*P*63/*mmc*), electric polarization can be switched between two equivalent polar states (*P*63*mc*). In this case, wurtzite structure should be a candidate for new class of ferroelectric materials. Former theoretical calculations for polarization and piezoelectric in wurtzite structure, all of these reports, they only considered atomic displacement within the tetrahedron. They did not mention the possibility of ferroelectricity of this wurtzite structure. Experimentally, Onodera *et al.* reported dielectric anomaly at 330 K and *D-E* hysteresis loop of Li doped ZnO with quite small polarization of 0.044 uC/cm^2 at room temperature. Joseph *et al.* also reported dielectric anomaly at 340 K. For wurtzite structure BeO, Sawada *et al.* reported *D-E* hysteresis loop with relatively large polarization of 0.061 C/m^2 at 805 ºC. Detailed mechanism of the observed ferroelectric like behavior is still unclear.

2. Ferroelectricity of $LiGaO_2$ family

We focus on β-$LiGaO_2$, which exhibits a distorted wurtzitetype structure. The crystal structure of β-$LiGaO_2$ falls within the orthorhombic system with a space group of $Pna2_1$, and spontaneous polarization takes place along the c-axis. A single crystal growth of β-$LiGaO_2$ was reported to serve as a substrate on which to deposit GaN thin films. Due to the difference in ionic radii between Li^+ and Ga^{3+}, the tetrahedra are distorted compared to those in the wurtzite-type structure. Moreover, the selectivity in doping elements is improved because of the presence of monovalent and trivalent cations in the structure. $NaGaO_2$, $AgGaO_2$, and $CuGaO_2$ are reported to possess the same structure as β-$LiGaO_2$. However, it is difficult to treat $NaGaO_2$ in air due to its high deliquescence. Besides, the synthesis of $AgGaO_2$ and $CuGaO_2$ requires $NaGaO_2$ as a starting material. Therefore, we decided to investigate the ferroelectricity in β-$LiGaO_2$. In this study, we carried out first-principles calculation and thin film preparation to evaluate a polarization switching of $LiGaO_2$ system.

We investigated ferroelectricity in $LiGaO_2$ by using calculation and preparation/evaluation of epitaxial thin films. We carried out first-principles calculations by using the VASP code for $LiGaO_2$ and Sc-doped $LiGaO_2$. The calculated results suggested that Sc doping reduces the barrier height energy of polarization switching in Sc-doped $LiGaO_2$. Then, we have started to prepare $LiGaO_2$ epitaxial thin film, and revealed that $LiGaO_2$ was epitaxially grown on a (111)$SrTiO_3$ substrate by a pulsed laser deposition method. The growth relationships between $LiGaO_2$ ($Pna2_1$) and the $SrTiO_3$ substrate are follows: (001)$LiGaO_2$//(111)$SrTiO_3$ and (010)$LiGaO_2$//(10-1)$SrTiO_3$. Here, the pure $LiGaO_2$ does not show any ferroelectric behavior by using *P–E* measurements and PFM. We then prepared Sc-doped $LiGaO_2$ epitaxial thin films. We successfully observed ferroelectric behavior via PFM measurement for $LiGa_{0.8}Sc_{0.2}O_2/SrRuO_3$/(111)$SrTiO_3$ substrates.

References

1. H. Moriwake, et al.; Applied Physics Letters, Vol.104, p. 242909 (2014).
2. S. Yasuhara, et al.; RSC Advanses, Vol. 14, pp. 13900-13904 (2024).

I-24 Materials Interaction Mechanism of Core Degradation during Severe Accident in Fukushima Daiichi Nuclear Power Station

Ayumi Itoh

1. Introduction

Understanding the formation and evolution of fuel debris is crucial for the safe decommissioning of the Fukushima Daiichi Nuclear Power Station (FDNPS). Following the severe accidents at Units 1–3, extensive forward simulations and backward analyses have been conducted to reconstruct the accident progression. Recent metallographic and thermodynamic studies have shed light on two critical aspects of debris behavior. The first concerns the formation of metallic Fe–Zr debris, which may have contributed to reactor pressure vessel (RPV) failure by creating a metallic pool with lower melting points than UO_2–ZrO_2 debris. Experimental investigations under non-isothermal conditions revealed the formation of intermetallic phases such as $(Fe,Cr,Ni)_{23}Zr_6$ and MZr_2, and demonstrated that Zr-rich melts aggressively degraded stainless steel, especially when oxide layers were penetrated. The second aspect involves the degradation of stainless steel–boron carbide (SS–B_4C) control-rod alloys. Steam oxidation tests clarified that boron is volatilized as oxides (e.g., H_3BO_3) through Fe–B–O layers, with kinetics strongly dependent on temperature and steam availability. These findings provide a mechanistic understanding of both metallic and control-rod-derived debris formation and oxidation. Together, they enhance accident analysis models and contribute essential data for evaluating the chemical state, re-criticality potential, and retrievability of debris in Unit 2.

2. Formation mechanism of Fe-Zr metallic debris

The interaction of Fe–Zr melts with stainless steel (SS) was studied to clarify metallic debris formation[1]. Zr-rich melts exhibited strong wettability and formed thick intermetallic layers, including $(Fe,Cr,Ni)_{23}Zr_6$, $(Fe,Cr,Ni)_2Zr$, and $(Fe,Cr,Ni)Zr_2$, whereas Fe-rich melts produced thinner layers dominated by $(Fe,Cr,Ni)_{23}Zr_6$. The onset of reaction occurred at lower temperatures for Zr-rich alloys (≈1210 K) compared with Fe-rich alloys (≈1630 K), reflecting eutectic effects. When SS was pre-oxidized, the $FeCr_2O_4$ layer initially delayed corrosion; however, once penetrated by Zr, catastrophic degradation followed, especially above 1723 K. Severe reactions involved Zr–Ni interactions, generating convective flow and rapid material loss. Thermodynamic modeling reproduced diffusion-controlled growth of reaction layers, validating experimental results. Importantly, liquidus temperatures of the products were below 2000 K, suggesting that such metallic debris could have re-melted and accumulated as pools in the RPV lower head, contributing to structural failure observed in Fukushima Unit 2.

2. Oxidation of SS-B_4C control-rods derived debris

SS–B_4C alloys, representing degraded control rods, were oxidized under steam-starved conditions at 1288–1573 K. The samples developed layered structures comprising Fe–Ni–Cr, Fe–Cr–O, and Fe–B–O phases. Boron volatilization occurred mainly as H_3BO_3 and HBO_2, confirmed by mass spectrometry. Evaporation followed an Arrhenius law with two regimes: below 1423 K (Ea ≈ 44 kJ/mol) and above 1423 K (Ea ≈ 80 kJ/mol). Lower oxygen partial pressure suppressed Fe–O formation, enhancing outward boron diffusion and increasing evaporation. The mechanism was not limited by bulk diffusion but controlled by surface reactions at Fe–B–O precipitates. The obtained kinetics were comparable to B_4C oxidation, implying that once formed, SS–B_4C debris releases boron at similar rates. This behavior directly impacts neutron absorption capacity and re-criticality risk in Unit 2. By providing quantitative evaporation rates and structural evidence, the study improves accident models and supports more reliable evaluation of boron retention during decommissioning operations.

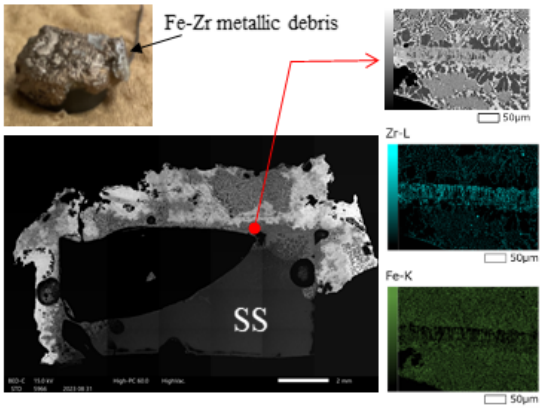

Fig. 1 Fe-Zr metallic debris on SS

Acknowledgments

The work of section 2 was supported by the JAEA Nuclear Energy S&T and Human Resource Development Project Grant Number JPJA21F21461577.

References

1. A. Itoh, et al.; Annals of Nuclear Energy 217 (2025)111333.
2. K.Inoue, A. Itoh, et al.; Journal of Nuclear Materials, Vol.603(2024)155456.

I-25 In-situ Synchrotron XAFS-XRD Observations of High-Temperature Fuel Reactions: From Feasibility Tests to UO_2-ZrO_2 Reaction

Ayumi Itoh

1. Introduction

Understanding high-temperature interactions of nuclear fuel and cladding is crucial for predicting fuel melting and debris formation in severe accidents. Previous studies relied mainly on post-mortem analyses of quenched samples, subject to uncertainties introduced during heating and cooling. Thus, intrinsic conditions for reactions such as UO_2 dissolution into Zr or Zr oxidation have remained unclear. To overcome this limitation, in-situ synchrotron techniques provide direct access to dynamic structural and chemical changes at extreme temperatures. X-ray absorption fine structure (XAFS) reveals local structure, while X-ray diffraction (XRD) tracks crystallographic transformations; their simultaneous application yields a comprehensive view of reaction pathways. Recently, we developed a high-temperature in-situ XAFS–XRD system at SPring-8 BL22XU, enabling simultaneous observation above 2000 K. Using Zr–Y_2O_3 as a model, the technique captured Zr oxidation, phase transitions, and solid-solution onset, validating its applicability. Building on this, we applied the system to UO_2–ZrO_2 under accident-relevant conditions, directly monitoring U/Zr mutual solubility and metastable phases, linking experimental findings with Fukushima-derived debris.

2. Feasibility of measurement technique with Zr-Y_2O_3 test

The feasibility of the developed in-situ XAFS–XRD system was first verified using Zr–Y_2O_3 mixtures, which undergo reactions similar to those in nuclear fuels[1]. Measurements were performed up to ~2500 K, capturing Zr oxidation to Zr(O) and ZrO_2, followed by the ZrO_2–Y_2O_3 solid-state reaction. XRD profiles revealed phase transitions from hexagonal Zr to tetragonal/cubic ZrO_2, while EXAFS spectra showed corresponding chemical shifts at the Zr K-edge. At ~1950 K, the onset of Y_2O_3–ZrO_2 solid-solution formation was observed, consistent with literature reports. Local structural analysis confirmed interatomic distance variations and anharmonic effects at high temperature. Importantly, temperature calibration was achieved by monitoring Y_2O_3 lattice parameters, ensuring accuracy beyond the pyrometer range. These results demonstrated that the system provides both crystallographic and local structural information under extreme conditions, validating its reliability. The Zr–Y_2O_3 experiment thus established a robust methodological basis for extending measurements to UO_2–ZrO_2 fuel materials.

3. In-situ experiment with UO_2-ZrO_2

The UO_2–ZrO_2 mixture was studied in-situ under Ar atmosphere up to ~2300 K[2]. Upon heating, monoclinic ZrO_2 transformed to tetragonal at 1343–1505 K, consistent with the phase diagram. Between 1803 and 1879 K, mutual dissolution of U and Zr was detected: UO_2 peaks in XRD weakened and eventually vanished above 2100 K, indicating complete dissolution into ZrO_2. Simultaneously, EXAFS revealed contraction of U–O distances toward Zr–O values, confirming U substitution into the ZrO_2 lattice. Notably, the reaction onset occurred about 200 K higher than predicted by equilibrium phase diagrams, reflecting kinetic effects. During quenching (~20 K/s), monoclinic ZrO_2 reappeared at ~1890 K, ~300 K above equilibrium, evidencing metastable phase behavior. SEM/EDS confirmed uniform U distribution within ZrO_2 grains. These results highlight that accident-relevant heating/cooling rates induce departures from equilibrium, enabling formation of phases consistent with Fukushima-derived U-bearing particles, and providing new insights into debris evolution mechanisms.

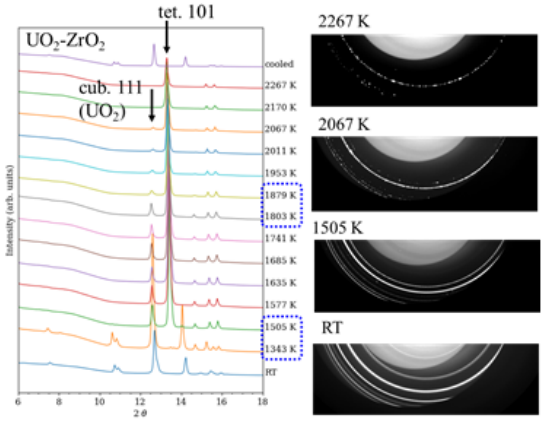

Fig. 1 XRD patterns of UO_2-ZrO_2 during heating

Acknowledgments

The synchrotron radiation experiments were performed at BL22XU of Spring-8 with the approval of the Japan Synchrotron Radiation Research Institute (JASRI) (Proposal No. 2024A3740). This work was supported by the Innovative Nuclear Research and Development Program by Ministry of Education, Culture, Sports, Science and Technology (MEXT) in Japan (JPMXD0223813709).

References

1. A. Itoh et al.; Synchrotron Radiation, Vol.31, No.4, pp.810-820 (2024).
2. A. Itoh et al.; The 38th Annual Meeting of the Japan Synchrotron Radiation Society & Joint Symposium on Synchrotron Radiation Science, January 10-12 (2025), Tsukuba, Ibaraki.

I-26 Thermochemical energy storage based on calcium hydroxide and silicon carbide-based foam support

Shigehiko Funayama and Yukitaka Kato

1. Introduction

Thermochemical energy storage (TCES), which employes reversible gas–solid reactions, can offer long-term storage of thermal energy. For the TCES material, calcium hydroxide ($Ca(OH)_2$) has attracted researchers' interest because of its availability, low cost, and high reactivity of its dehydration to form calcium oxide (CaO) and the reverse rehydration as shown in the following equation:

$$Ca(OH)_2(s) \rightleftharpoons CaO(s) + H_2O(g);\ \Delta H_r = 104\ kJ\ mol^{-1} \quad (1)$$

Despite its outstanding advantages, thermal conductivity of pure $Ca(OH)_2$/CaO powder is low (0.1–0.5 W m^{-1} K^{-1}). Thus, composite materials that have high thermal conductivities are required to be developed. In this context, we previously developed a composite that combined $Ca(OH)_2$ with silicon-infiltrated silicon carbide (Si–SiC) foam support [1–3]. It was revealed that the composite exhibited a higher thermal charge/discharge power density compared with a reference pure $Ca(OH)_2$ powder. However, the optimal volume fraction of Si–SiC was yet unknown so that we aimed to explore the optimal volume fraction of Si–SiC in composite that can maximize the thermal discharge power density during CaO hydration using numerical analysis.

2. Materials and methods

2.1. Materials

Calcium hydroxide slurry was prepared to load onto the porous foam support. Si–SiC foam support had a porosity of 92%, i.e., 8 vol% of Si–SiC, and a pore diameter of approximately 0.4 mm. The slurry was introduced into the Si–SiC foam support, and then the samples were dried at 120 °C for more than 12 h. Schematic and a photograph of the composite is shown in Fig. 1. The sample had a diameter of 44 mm and a heigh of 48 mm [1]

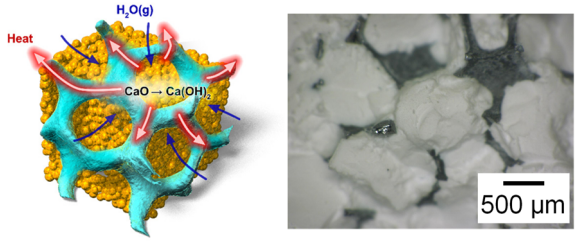

Fig. 1 Composite material using $Ca(OH)_2$ and Si–SiC foam support: (a) schematic; (b) photograph [1].

2.2. Experimental setup and procedure

To assess the performance of the composite, a packed-bed reactor was employed. The reactor had an inner diameter of 48 mm and height of approximately 50 mm. The cylindrical samples were loaded on the reactor. The initial temperature was set 350 °C. The water vapor at 83–85 kPa was introduced into the reactor from the top of the bed to initiate hydration.

2.2. Numerical methods

A numerical model of the composite during CaO hydration was developed based on the finite element method [4,5]. The main assumptions are as follows: (1) the composite is uniform and isotropic; (2) the bed volume is constant; (3) solid and gas phases are in local thermal equilibrium; (4) thermal radiation is negligible.

The governing equations of the mass, momentum, and energy balance though porous media were used. The mass sink term and heat source term were included in the mass and energy equations, respectively. The source terms are proportional to the hydration rate. Thus, the kinetic equations of the hydration were derived through a thermogravimetric analysis.

The boundaries of the reaction bed were imposed with experimental data and a constant temperature of 350 °C for the model validation and parameter analysis, respectively. The pressure on the top of the bed was maintained within 83–85 kPa. The model was implemented and computed using COMSOL Multiphysics®.

We conducted the parameter analysis to investigate the effects of the Si–SiC fraction on the thermal discharge power density of the composite. The range of Si–SiC fraction was set to 0–20 vol%. The effective thermal conductivity of the composite highly depends on the Si–SiC fraction. The effective thermal conductivity measured by the laser flash analysis were employed for the parameter analysis. The thermal discharge power of the composite was calculated by integrating the heat flux over the boundary surface.

3. Results and discussion

Fig. 2 compares the numerical results with the experimental data of the composite with a Si–SiC fraction of 8 vol%. The center temperature of the reaction bed increased rapidly up to the equilibrium temperature of 500 °C. The conversion reached more than 90%. Both of computed temperature and conversion agree well with the measurements, indicating that the numerical model has been successfully been validated. With this validated numerical model, we conducted the parameter analysis to investigate the effects of the Si–SiC fraction on the thermal discharge power density of the resulting composites.

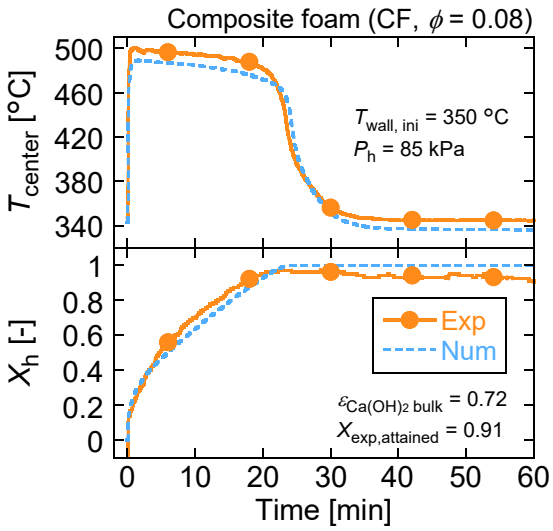

Fig. 2 Model validation

Fig 3 illustrates the calculated center temperature, conversion, thermal discharge power density at different Si–SiC fractions in the range of 0–20 vol%.

The temperature plateau, in which the temperature is maintained over 450 °C, is markedly reduced from 55 min to within 5 min when the fraction increases from 0 to 20 vol%. This is because the heat transfer through the reaction bed is improved by increasing the Si–SiC fraction. The conversion rate is also enhanced with increasing fraction, which can be attributed to an increase in the effective thermal conductivity and decrease in the amount of $Ca(OH)_2$ in the composite. Consequently, the power density is also enhanced as the fraction increases.

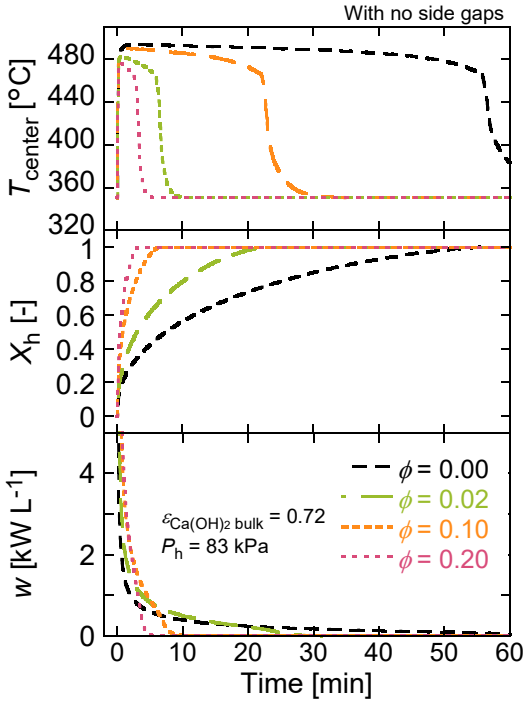

Fig. 3 Temperature, conversion, and power density at various fractions of Si–SiC

The effects of the Si–SiC fraction on the thermal discharge power density at 5 min is shown in Fig. 4. The power density increases as the fraction elevated until 6 vol%. However, the power density decreases with increasing fraction at a fraction over 6 vol%. This is because there is a tradeoff relationship between the effective thermal conductivity and the amount of $Ca(OH)_2$ in composite, both of which have a great impact on the power density. The maximum power density at a Si–SiC fraction of 6 vol% is 0.97 kW L_{bed}^{-1}, which is 1.6 times higher than that of the pure CaO powder bed.

The developed model can a helpful tool for optimizing the composite not only for the composite with $Ca(OH)_2$ and Si–SiC foam but also for other heat transfer-enhanced composites for thermochemical energy storage applications.

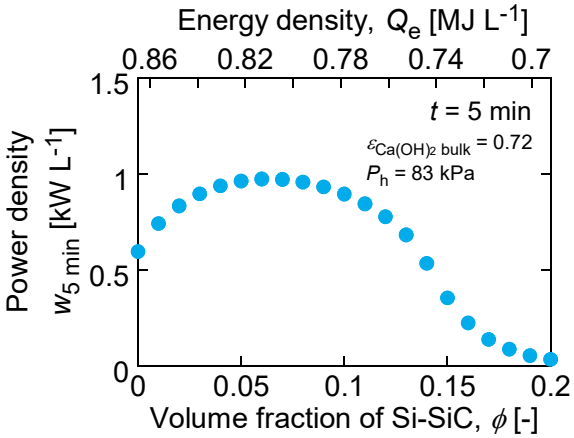

Fig. 4 Volume fraction of SiSiC vs. power and energy density of the composite foam

4. Conclusions

In this study, we have developed a numerical model of the composite material using $Ca(OH)_2$ and Si–SiC foam support to explore the optimal fraction of Si–SiC in the composite. The parameter analysis showed that the composite exhibited a maximum thermal discharge power density at 5 min of 0.97 kW L_{bed}^{-1} when the fraction was 6 vol%. The proposed numerical model can be a powerful tool for optimizing the design of heat transfer-enhanced composites for thermochemical energy storage applications.

Acknowledgments

This study was supported by the JST-Mirai Program Grant Number JPMJMI21E4, Japan. We also would like to thank the group of Thermochemical Systems at the German Aerospace Center for fruitful discussion on this research.

References

1. S. Funayama, *et al.*; *Applied Thermal Engineering*, Vol. **220**, 119675 (2023).
2. S. Funayama, *et al.*; *Applied Thermal Engineering*, Vol. **238**, 121947 (2024).
3. K. Mochizuki, *et al.*: *Prog. Nucl. Sci. Technol.*, Vol. **7**, 286–292 (2025).
4. S. Funayama, *et al.*; *Applied Thermal Engineering*, Vol. **274**, 126575 (2025).
5. S. Funayama *et al.*; *The 61st National Heat Transfer Symbosium*, May 30th, 2024, Kobe

I-27 Development of Photonic Crystal Films Functionalized by Silyl Phosphate Derivatives for Uranyl Ion Sensing

Naokazu Idota, Takehiko Tsukahara

1. Introduction

Rapid and easy analysis of uranyl ion (UO_2^{2+}) in solutions is one of the most important issues for decommissioning and environmental impact assessment of nuclear-related facilities. Based on the permissible limit of uranium in wastewater discharged from the nuclear-related facilities, on-site monitoring devices of trace uranium concentration at micro-molar (10^{-6} M) level is expected to be developed. We here developed a novel on-chip UO_2^{2+} sensing film with photonic crystals (PCs) consisting of 100 nm-sized periodic array structures embedded in polydimethylsiloxane (PDMS). The film can reflect certain wavelengths according to the inter-particle distances of PCs, originating a structural color. The wavelength of structural color can be changed by the swelling behavior of the polymer embedded with PCs, and facile colorimetric analysis would be allowed by controlling the swelling [1, 2]. In this study, tris(trimethylsilyl) phosphate (TMSPa) having an affinity functional group, P=O, to UO_2^{2+} were immobilized on surfaces of the PDMS for swelling control in response to UO_2^{2+}.

2. Experimental Methods

Aqueous dispersion containing polystyrene nanoparticles (particle size: 180 nm) was dropped onto a glass substrate, and the surface of the dispersion was covered with silicone oil. As the dispersion medium evaporates slowly through silicone oil, polystyrene PCs could be formed by self-assembling. Next, PDMS prepolymers containing curing agents diluted with hexamethyldisiloxane was introduced into the void among prepared PCs. The PDMS mixture was cured at room temperature for 12 hours, followed by heating at 80℃ for 2 hours. Such operations were repeated a few times to increase the inter-particle distances of PCs. Next, TMSPa in hexamethyldisiloxane was added into PDMS framework of the PC films. After drying hexamethyldisiloxane, TMSPa were adsorbed on PDMS through the hydrophobic interactions, thus the surfaces of the film can be modified with P=O groups.

In order to evaluate UO_2^{2+} sensing abilities of the film, the film was put into 1 mL of UO_2^{2+} solution with different concentrations. After 1 minute of reaction at room temperature, the changes of colors and reflection spectra were measured by microscope and fiber-optic reflectance spectrometer, respectively.

3. Results and Discussion

AFM observation of the PDMS-based PC films showed the close-packed structure of polystyrene nanoparticles and increases in their inter-particle distances by additional PDMS filling and curing. According to the inter-particle distance, the structural color of PCs films was changed from blue to bluish-green (**Figure 1**).

The color insight and diffraction spectrum of the surface-modified PDMS-based PC film were examined by microscope and fiber-optic reflectance spectrometer. The reflection peak of the bluish-green PCs film was found to be observed as a maximum peak at 508.5 nm. The reflection peak positions of the structural color changed to ca. 550 nm when the film was contacted with nitric acid solutions (pH = 1), and shifted to longer wavelength in solution containing UO_2^{2+} (**Figure 2**). In addition, the red-shifts of the reflection peak were increased with increasing UO_2^{2+} concentrations from 10^{-8} to 10^{-5} M. From ICP-MS of the UO_2^{2+} solutions and contact angle measurements of the film surfaces, the structural color change of PC films could be caused by hydrolysis of TMSPa depending on the coordination of UO_2^{2+} with P=O group of TMSPa. Interestingly, the shifts of reflection peak positions in the PC films were found to be hardly occurred regardless of the presence of other metal ions (Cs^+, Sr^{2+}, La^{3+}) and their concentration. In conclusion, we demonstrated that the surface-modified PDMS-based PC film with TMSPa is useful as a colorimetric on-chip device that can analyze 10^{-6} M level UO_2^{2+}.

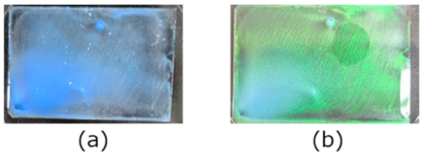

Figure 1. Photos of PDMS-based PC films. Number of additional PDMS filling and curing; (a) one, (b) two.

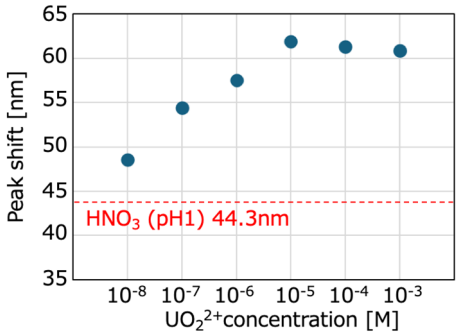

Figure 2. Dependence of UO_2^{2+} concentration on reflection peak shift of structural color for PDMS-based PC film.

References

1. T. Tsukahara, et al.; *J. Phys. Chem. B*, **123**(13), 2948-2955 (2019).
2. T. Tsukahara, et al.; *Langmuir*, **36**(1), 159-160 (2020).

I-28 Electromagnetic simulation of a TE_{211} mode single hybrid cavity linac

Shota Ikeda, Noriyosu Hayashizaki

1. Introduction

The Single-Hybrid-Cavity (SHC) linac is a linear accelerator that integrates a radio-frequency quadrupole (RFQ) and an Interdigital-H-mode drift tube linac (IH-DTL) into a single cavity resonator, enabling efficient acceleration of ion beams in the low-energy region up to 2–3 MeV/u. Conventional SHC linacs, composed of either IH- or four-rod-type RFQs coupled with an IH-DTL, operate in the TE_{111} fundamental mode. This constrains the resonance frequency to below ~100 MHz, which is favorable for heavy-ion acceleration but unsuitable for proton acceleration, where higher frequencies are desirable. We propose a TE211-mode SHC linac designed for operation in the 200–500 MHz range, suitable for proton acceleration, and are currently developing a proof-of-principle prototype. The TE211 SHC employs a single cavity structure comprising an RFQ section, a drift tube section, and a matching cell. The RFQ section is equivalent to a conventional four-vane RFQ, while the drift tube section adopts a double IH-DTL configuration with alternately mounted drift tubes. This configuration allows the entire accelerator to be driven by a single RF system, resulting in a compact and simplified design with improved efficiency for high-current proton acceleration.

2. Simulation model of TE211-mode SHC linac

In the development of a prototype of the TE_{211}-mode SHC linac, the electromagnetic field characteristics of the accelerating cavity were analyzed using three-dimensional electromagnetic field simulation software. Based on the cell parameters designed with a particle trajectory calculation code, a three-dimensional model was constructed. The total cavity length is approximately 1.7 m, and the design allows for the acceleration of a 50 mA proton beam up to 2.5 MeV. The RFQ section has a total length of 1170 mm, while the matching cell and DT section together have a length of 570 mm

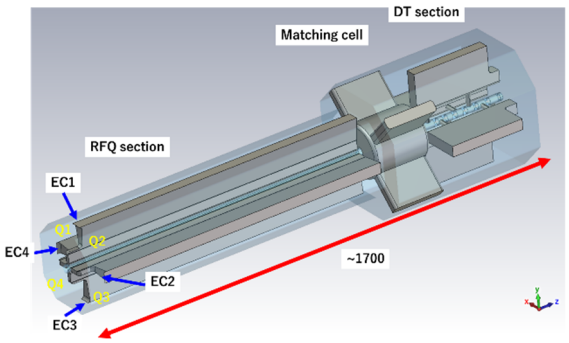

Fig. 1 Schematic of TE_{211}-mode SHC linac

3. Electromagnetic simulation

Using the three-dimensional model shown in Fig. 1, electromagnetic field simulations were carried out, and it was confirmed that the TE_{211} mode is excited around 200 MHz. When the depth of the “end cut” at the edge of the RFQ section was varied, the electric field distribution changed: the field strength and the ratio among the quadrants in the RFQ section were altered (Fig. 2), and the corresponding drift tubes in the DT section exhibited variations in their field strength (Fig. 3). These results indicate that adjusting the end-cut depth provides a means to control the electric field distribution in the cavity.

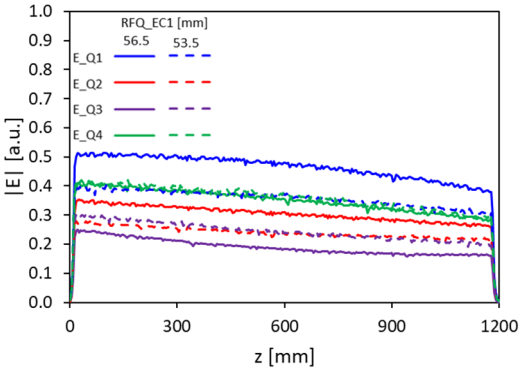

Fig. 2 Electric field distributions of the RFQ section

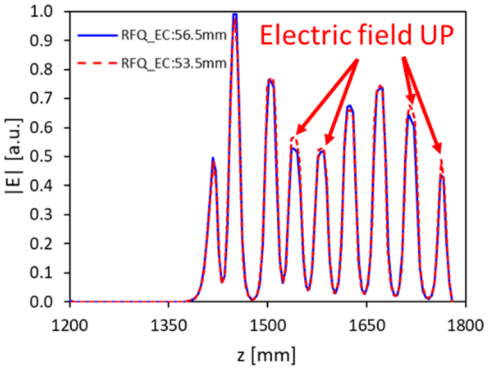

Fig. 3 Electric field distributions of the DT section

4. Summary

To evaluate the RF property of the TE_{211}-mode SHC linac, we performed three-dimensional electromagnetic field simulations of the accelerating cavity, and found that the electric field distribution is affected by the cavity geometry, such as the end cuts.

Acknowledgment

This work has been supported by Grant in Aid for JSPS Fellows Grant No. JP23H03668.

I-29 TASKI: AI Based Nuclear Knowledge Management System

Tomohiro Okamura, Takahiro Nishihara, Masahiko Nakase

1. Introduction

In recent years, following the emergence of Large Language Models (LLMs) centered on OpenAI's ChatGPT, the enhancement of computational resources and the accelerated development of API infrastructures have led to the rapid development of applications centered on Generative AI. LLMs, which possess parameters on the scale of hundreds of billions, not only exhibit advanced language understanding and generation capabilities by learning from vast amounts of data on the internet but also, remarkably, generate sophisticated code generation abilities. The latest Generative AI can automatically generate high quality code based on requirement specifications given in natural language, and can even propose refactoring and unit tests. This new software development methodology of " Requirements Description → Generation → Human Verification & Decision-Making " is prompting fundamental transformations across all industries.

Generative AI has various functional aspects, serving as a tool for innovation not only in business improvement but also in diverse fields such as the rationalization of manufacturing processes, new materials discovery through materials informatics, and even the social sciences, with applied research being conducted in these areas.

2. Applicability to the Nuclear Field

The nuclear field is no exception; the application of Generative AI is being explored in a wide range of areas, including the operation and maintenance of nuclear power plants, design, radiation management, education and training, regulatory compliance, and decommissioning. It has been reported that the US NRC has initiated trials utilizing Generative AI for knowledge retrieval from large-scale data by its staff.

Furthermore, the development of LLMs specialized for the nuclear sector is progressing. The US ORNL is collaborating with the startup Atomic Canyon to develop "Neutron Enterprise," a Generative AI system specialized for the nuclear field. This system is characterized by its ability to perform high-speed document retrieval and generation using Retrieval-Augmented Generation (RAG) technology, coupled with an LLM trained on billions of pages of technical documents and regulatory materials. In fact, the system is scheduled for full-scale implementation at PG&E's Diablo Canyon Nuclear Power Plant in the U.S. by the end of 2024, where it has achieved positive results in searching procedures and records.

Additionally, in September 2024, the NRC, in collaboration with the Canada CNSC and the UK ONR, published "Considerations for Developing Artificial Intelligence Systems in Nuclear Applications". Regulatory organizations are advancing discussions on the specific uses and challenges of Generative AI in the nuclear industry, and it is anticipated that operators will follow suit with system introductions.

3. TASKI: AI-based Nuclear Knowledge Management

Our research group, in collaboration with NEUChain Technologies Inc., is developing TASKI, an AI-based Knowledge Management system for the nuclear sector. Amidst the global trend of re-evaluating nuclear power generation, efficient human resource development and the succession of knowledge and technology are urgent tasks. TASKI is an AI-based knowledge management platform aimed at solving these challenges.

The knowledge environment in the nuclear field faces approximately the following three structural challenges:

1. Knowledge Dispersion and Personalization: While literature, reports, and design data are vast, their interconnection is insufficient, making access to necessary information difficult.
2. Language Barriers: Much of the international literature is published in English, which poses a readability challenge for Japanese engineers. Conversely, knowledge accumulated in Japanese is difficult to leverage for its international value.
3. Information Asymmetry with Society: Although information is publicly available, it is often esoteric, and external communication in an easy-to-understand format is lacking.

TASKI is not limited to simple RAG-based document retrieval and generation; it is being designed and implemented as an AI agent that integrates functions such as numerical analysis and data visualization to substitute for advanced operational tasks. This paper focuses on the functionality of the knowledge retrieval RAG, which is its core technology.

4. Conclusion

Institute of Science Tokyo and NEUChain Technologies Inc. are jointly advancing development toward the practical application of TASKI, an AI-centric nuclear knowledge management system. Due to space limitations, details have been omitted in this paper; however, collaborative projects with domestic and international research institutions, regulatory authorities, and industry have now been initiated, and it is anticipated that the utilization of Generative AI will expand rapidly throughout the nuclear sector.

I-30 Investigation of phase equilibrium of TiO_2–CeO_2 system for prediction of precipitated phase during solidification of radioactive waste into SYNROC

Ryota Nakazawa, Masahiko Nakase

1. Introduction

Synroc has been proposed as a durable waste form for immobilizing radioactive wastes containing actinides (An), owing to its excellent long-term chemical and structural stability. Synroc consists of multiple crystalline phases capable of incorporating various waste elements, enabling it to accommodate a wide range of waste compositions. However, the crystalline phases and their compositions vary significantly depending on the initial composition and sintering temperature, making it essential to develop predictive approaches for phase assemblages during fabrication. To predict the crystalline phases precipitated during the sintering of An-bearing Synroc, the authors have been focusing on constructing thermodynamic phase diagrams based on experimental phase-equilibrium data and CALPHAD modeling. In this study, attention was directed to the chemically stable rutile phase (TiO_2) in Synroc, and its phase changes upon the addition of actinide oxides were investigated experimentally using CeO_2 as a surrogate for AnO_2. The high-temperature phase equilibria of the TiO_2–CeO_2 system were examined.

2. Experimental Procedure

Powders of TiO_2 and CeO_2 were weighed according to the compositions listed in Table 1 and mixed in an agate mortar. The mixed powders were pressed into pellets (ϕ15 mm) and sintered in an electric furnace at 1673 K for 6 h in air. After heat treatment, part of each pellet was pulverized for phase identification using X-ray diffraction (XRD). The remaining portion of each pellet was embedded in resin, polished, gold-coated, and examined using scanning electron microscopy with energy-dispersive spectroscopy (SEM–EDS) for microstructural observation and compositional analysis.

Table 1. Weighed composition of TiO_2 and CeO_2 mixed powder

Mole fraction	Comp. 1	Comp. 2	Comp. 3	Comp. 4
TiO_2	0.8	0.6	0.4	0.2
CeO_2	0.2	0.4	0.6	0.8

3. Results and Discussion

Figure 1 shows the backscattered electron image of the sample with TiO_2:CeO_2 = 0.8:0.2 after heat treatment. Two major contrast regions, phase (1) (dark) and phase (2) (gray), and a minor phase (3) (white) were observed. EDS point analyses revealed the following compositions (in at%):
Phase (1): Ti 33.67 ± 0.86, Ce 0.03 ± 0.05, O 66.31 ± 3.61
Phase (2): Ti 25.09 ± 0.90, Ce 12.66 ± 0.53, O 62.24 ± 2.97
Phase (3): Ti 2.43 ± 0.35, Ce 39.13 ± 1.10, O 58.44 ± 2.28

Figure 2 presents the XRD pattern of the same sample, in which peaks of rutile (TiO_2), brannerite ($CeTi_2O_6$), and fluorite (CeO_2) were identified. These phases correspond to the compositions of phases (1), (2), and (3) in the EDS results, respectively. Therefore, the sample consists mainly of rutile and brannerite phases, with a small amount of unreacted fluorite phase. From these results, the equilibrium phases at 1673 K for the TiO_2:CeO_2 = 0.8:0.2 composition were determined to be rutile and brannerite, while the fluorite phase was attributed to unreacted CeO_2. Furthermore, the Ce solubility in the rutile phase was found to be below 0.1 at%, indicating a very limited Ce incorporation. This suggests that in actinide-bearing systems such as TiO_2–UO_2, similar low solubility of U in rutile and comparable rutile–brannerite phase equilibria may occur. The equilibrium phase for other compositions were brannerite-fluorite or brannerite-rutile.

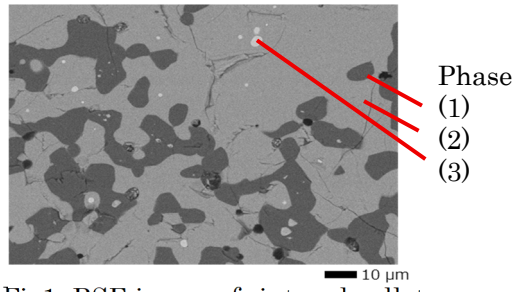

Fig1. BSE image of sintered pellet (TiO_2:CeO_2=0.8:0.2)

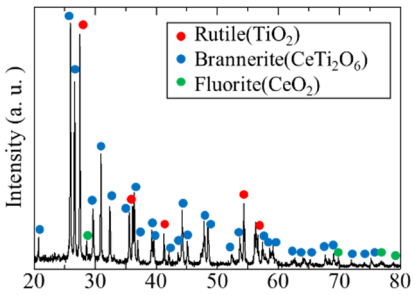

Fig2. XRD pattern of pulverized sintered (TiO_2:CeO_2=0.8:0.2)

4. Conclusions and Future works

To predict the crystalline phases precipitated during the sintering of An-bearing Synroc, the high-temperature phase equilibria in the TiO_2–CeO_2 system were investigated using CeO_2 as a surrogate for actinide oxides. The results revealed

a brannerite-fluorite or brannerite-rutile two-phase equilibrium and a very low Ce solubility (< 0.1 at%) in rutile. These findings suggest that similar behavior may occur in TiO_2–UO_2 and other actinide-containing systems. Future work will include experiments using uranium and the development of calculated phase diagrams based on the CALPHAD approach.

II. Co-operative Researches

II. Collaborative Researches

II.1 Collaborative researches with the partner inside university

(1) Effect of Nitrogen Admixture to Underwater Argon Arc Discharge Plasma for Nuclear Decommissioning, Prof. Shinsuke Mori, Major in Chemical Science and Engineering, School of Materials and Chemical Technology.
(2) Spatially Resolved Measurements of Reduced-Pressure Oxygen ICP by Tomographic Eemission Spectroscopy, Prof. Shun-ichiro Ohmi, Dr. Kazuhiro Naiki, Major in Electrical and Electronic Engineering, School of Engineering
(3) Study on nuclear forensics with Hitoshi Sagara and Tatsuya Katabuchi
(4) Study on nuclear security, Hiroshi Sagara.
(5) Toward personalized radiotherapy based on individual difference in DNA damage response, Ryoichi Yoshimura.
(6) Effects of ionizing radiation on cardiomyocytes, Tetsuro Sasano, Keisuke Ihara, Giichi Nitta.
(7) Proteomic analysis of DNA damage response, Nobuhiro Hayashi.
(8) Li-ion batteries, Prof. Yosuke Shiratori, Prof. Sou Yasuhara, Prof. Takuya Hoshina, Prof. Mitsuru Itoh
(9) Ferroelectrics, piezoelectrics and Multiferroics, Prof. Hiroshi Funakubo, Prof. Mitsuru Itoh, Prof. Taro Kuwano, Prof. Hiroko Yokota, Prof. Sou Yasuhara, Prof. Takuya Hoshina
(10) Conventional Ceramics Button, Prof. Toshihiro Isobe

II.2 Collaborative researches with the partner outside university

(1) Plasma Diagnostics Technology for Production Equipment with AI Technology, ULVAC, Inc. via "ULVAC Advanced Technology Collaborative Research Cluster", Dr. Kenta Doi, Mr. Tetsuji Kiyota, ULVAC, Inc.
(2) OES Diagnostics of Atmospheric Pressure Argon Plasma: Electron Temperature and Density Assessment through Visible Bremsstrahlung Inversion Method and Collisional-Radiative Model, Professor Motoshi Goto, Professor Shinji Yoshimura, Dr. Keren Lin, National Institute for Fusion Science
(3) Comparison of Electron Densities and Temperatures in Helium and Argon Nonthermal Atmospheric-Pressure Plasmas by Continuum Spectral Analysis, Professor Kiyoyuki Yambe, Niigata University.
(4) Reconsideration of Temperatures for Non-Equilibrium Plasmas with Low-Ionization Degree Based on Various Entropy Theory, JSPS Grant-in-Aid Scientific Research (C), 22K03566, 2022-2025.
(5) Development of DC Induction Accelerator, High Energy Accelerator Research Organization (KEK).
(6) Development of Laser Ion Sources Using Liquid Metal Targets, Nagaoka University of Technology
(7) Development of inorganic-organic hybrid nanomaterials, Prof. Yoshiyuki Sugahara, Waseda University.
(8) Study on fluorocarbon-free rubbers and fluororubber recycling, Mitsubishi Materials Corporation.
(9) Study of a TE211 mode single hybrid cavity linac for high efficiency high intensity proton beam acceleration, Grants-in-Aid for Scientific Research, Grant-in-Aid for Scientific Research (B), Japan Society for the Promotion of Science
(10) Human Resource Development through Fuel Debris Research and the Establishment of SEEM, JAEA Nuclear Energy S&T and Human Resource Development Project, Yutaka Watanabe
(11) Study on prompt-neutron emission mechanism of nuclear fission based on a statistical model, with Kazuki Fujio (LANL, USA)
(12) Study on prompt-neutron emission mechanism of nuclear fission based on a statistical model, with Anabella Tudora (University of Bucharest, Romania)
(13) Development of quantitative evaluation method for charge polarization using Density functional study, with Shinichiro Ebata (Saitama Univ.)
(14) Study of nuclear reactions using AMD, with Akira Ono (Tohoku Univ.)
(15) Fission study, Fedir Ivanyuk (Institute for Nuclear Research, Kiev, Ukraine), Mark Usang (Malaysian Nuclear Agency), Satoshi Chiba (NAT)
(16) Study on Molten Salt Reactor, with Yoshihisa Tahara (NICE)
(17) Research on the Formation Mechanisms of Metallic Fuel Debris at Fukushima Daiichi Nuclear Power Station, Tokyo Electric Co., Ltd.
(18) Development of an In-situ Observation Technique for Nuclear Fuels at Ultra-High Temperatures,

Fukui university, Tohoku university, Japan Atomic Energy Agency

(19) In situ high-temperature XRD/XAFS study of phase equilibria for hypo-stoichiometric region in U-Zr-O system, Fukui university, Tohoku university

(20) Development of nuclear data evaluation framework for innovative reactors, MEXT Innovative Nuclear Research and Development Program.

(21) Study on neutron capture cross section of carbon-13. Research Collaboration between the South West Nuclear Hub, University of Bristol and Institute of Innovative Research, Tokyo Institute of Technology and The Institute for Integrated Radiation and Nuclear Science, Kyoto University

(22) Development of Ultrasonic Measurement Technology for Three-Phase Flow Fields in Pipelines, AIST

(23) Development of a Laser Deflection-Type Ultrasonic Wideband 3D Imaging System for In-Vessel Visualization in High-Radiation and Non-Visible Environments, Japan Atomic Energy Agency

(24) Research on Advancing the Radioactive Material Migration Evaluation Model for Sodium-Cooled Fast Reactors, Japan Atomic Energy Agency

(25) Preliminary Testing of Emergency Condensers During Pool Surface Fluctuations and Identification of Issues, Central Research Institute of Electric Power Industry

(26) Research on Incorporating the Latest Technological Trends in Nuclear Fuel Material Transportation, Nuclear Fuel Transport Company, Ltd.

(27) Research on Performance Evaluation of Storage Batteries under Radiation Environments, Tamaura Labo. LLC.

(28) Fundamental Study on Mechanism of Blasting Decontamination Device for Small Diameter Pipe (Part 6), Fuji Electric Engineering & Construction Co. Ltd.

(29) Fundamental Research for the Advancement of Ultrasonic Sensing Technology Part V , Tokyo Electric Power Company Holdings, Inc.

(30) Advanced Research of Water Level Measurement Technology Using Ultrasound, Tokyo Electric Power Company Holdings, Inc.

(31) Research on Enhancing Analytical Accuracy, Safety Assessment, and Margin Evaluation in BWR Thermal-Hydraulic Simulation and Human Resource Development, Tohoku Electric Power Co., Inc.

(32) Fundamental Research on Flow Measurement in Heat Exchangers Part3, TOKYO RADIATOR MFG. Co. Ltd.

(33) Development of Thermodynamics of Advanced Fuels - International Database (TAF-ID), Phase 3, OECD/NEA, with international organization from Canada, France, Netherlands, Sweden, United Kingdom, United States, and European Commission.

(34) Development of database for debris property based on the elucidation of debris formation mechanism and verification of accident progression analysis results by synthesis of sim-debris on the basis of analytical results of materials surrounding fuel debris, Fukui Univ, Tohoku Univ, and Osaka Univ.

(35) Modification of Al_2O_3 inclusion by Ca in molten steel, Nippon Steel Corporation.

(36) Advanced Research on Liquid Metal Devices toward the Realization of Commercial Laser Fusion Reactors, EX-Fusion Liquid Metal Collaborative Research Cluster, EX-Fusion CO., LTD.

(37) Paradigm shift in mutation research brought by next generation sequencing: from specific locus test to whole genome analysis, Grant-in-Aid for Challenging Research, JSPS.

(38) Development of ultrasensitive and high throughput single cell element analyzing system and creation of single cell metallomics, Grant-in-Aid for Scientific Research S, JSPS, Akitoshi Okino (Science Tokyo).

(39) Rapid and sensitive analysis of the effects of low dose rate and long term radiation exposure, Grant-in-Aid for Scientific Research A, JSPS, Yoichi Gondo (Osaka University).

(40) Study on the effects of low dose rate radiation on genome through continuous irradiation experiment and cutting-edge analysis based on the prediction by dose-rate responsive mathematical modeling. Research Project on the Health Effects of Radiation, Ministry of Environment, Yuichi Tsunoyama (Kyoto University).

(41) Investigation on Fuel Cycle based on Actinide Management Towards Sustainable Use of Nuclear Energy, Nuclear Energy Systems Research and Development Project, Kyoto University, 2024.

(42) Study on rationalization of geological disposal facility design in diversified fuel cycle conditions, Center for Promotion of Nuclear Energy Environment and Funds Management, Agency for Natural Resources and Energy, Re-commissioned Research, Nuclear Environment Improvement Promotion and Fund Management Center, 2024.

(43) Assessment of Impact by reprocessing and nuclide separation technologies for PGM management, Voluntary research and study project by the Nuclear Environment Promotion and Funds Management Center, Nuclear Environment Improvement Promotion and Fund Management Center, 2024.

(44) Study on fabrication of simulated waste bodies by spark plasma sintering, FY2024 Technology Development Project on Geological Disposal of High-Level Radioactive Waste, Kobe Steel, Ltd., 2024.

(45) Research on Safety Technology Development for the Development of Common Fundamental Technologies for Molten Salt Reactors, Development of Common Fundamental Technologies for Innovative Nuclear Technologies, BERD, 2024.

(46) Research on Decommissioning-Related Technologies of the Fukushima Daiichi Nuclear Power Plant, TEPCO Decommissioning Frontier Technology Creation Collaborative Research Center, TEPCO Holdings, 2020.

(47) Simulation study and in-line analytical study to construct MA recovery flowsheet by extraction chromatography, Japan Atomic Energy Agency, 2024.

(48) Study on effective separation of critical metals by nobel diamide extractants, JSPS Invitational Fellowships for Research in Japan, JSPS, 2024.

(49) Conceptual Study of Innovative Nuclear Systems Using Ships Equipped with Fast Molten Salt Reactors, Science Tokyo Zero Carbon Energy Institute GXI Startup Research Funding, Science Tokyo, 2024.

(50) Improvement to critical safety technology for Fukushima-Daiichi NPS decommissioning, Tokyo City University, Nagaoka University of Technology, Nuclear Damage Compensation and Decommissioning Facilitation Cooperation

(51) Study on Off-shore Floating Nuclear Power Plant, Japan Atomic Energy Agency.

(52) The evaluation of core characteristics of next generation innovative reactors and their material balance evaluation, Radioactive Waste Management Funding and Research Center.

(53) Nuclear Forensics of reprocessed Pu and its important signature nuclides, Japan Atomic Energy Agency

(54) Frontier Exploration of Redox Behavior of Transuranic Elements for Reinforcing Nuclear Chemistry Foundations, Helmholtz-Zentrum Dresden-Rossendorf

(55) Japan-Germany Research Network on Actinide Chemistry for Development of Nuclear Fuel Materials Precipitation Method, Helmholtz-Zentrum Dresden-Rossendorf

(56) Control of Divertor Configuration by Induced Current Drive and Prediction of Position, Hasegawa Makoto, Masuzaki Suguru, Nakamura Kazuo, Mitarai Osamu, Idei Hiroshi, Hanada Kazuaki

(57) Plasma Equilibrium Reconstruction Using Gaussian Process, Watanabe Kiyomasa, Suzuki Yasuhiro

(58) “Medical imaging by optical-electrical hybrid transparent semiconductor”, Kenji Shimazoe (The University of Tokyo), Ayaki Takeda (University of Miyazaki), Hidenori Toyokawa (Konan University), Keitaro Hitomi (Tohoku University)

(59) “Development of Multi-Channel Integrated Circuits Employing Time-Domain Signal Processing for Applications in Particle Physics, Astrophysics, and Medical Imaging”, Tadashi Orita (The University of Tokyo)

(60) Li-ion batteries, Prof. Takashi Teranishi, Prof. Ken Watanabe, Prof. Kingo Ariyoshi, Dr. Yosuke Suzuki, Prof. Ken-ichi Kaminaga, Prof. Kamala Bharathi, Prof. Alex Rettie

(61) Ferroelectrics, piezoelectrics and Multiferroics, Prof. Yoshitaka Ehara, Prof. Yosuke Hamasaki, Dr. Hiroki Moriwake, Prof. Ayaka Yamamoto, Prof. Tsukasa Katayama, Prof. Takenori Kiguchi, Dr. Jianging Yu, Prof. Nobuo Nakajima, Prof. Jun Kano, Prof. Hiroki Taniguchi, Prof. Shingo Maruyama, Prof. Hiroshi Naganuma

(62) Study on Neutron-Irradiation Resistance of Orientation-Controlled Ceramics: National Institute for Materials Science (NIMS)

(63) Research and development of mechanical properties evaluation of ceramic-based composites

with novel oxidation-resistant microstructures: Japan Aerospace Exploration Agency (JAXA)

(64) Research on Formation and Characterization of Oxide Nanopowder : Vinca Institute, University of Belgrade, Serbia.

(65) 3D Printing of Hierarchical Porous Silicon Carbide Ceramics : The University of Melbourne, Australia

III. List of Publications

V. List of publications

Journals

(1) Yosuke Shimada, Hiroshi Akatsuka: Evaluating Plasma Fluctuation by Collisional-Radiative Model Using Malliavin Derivative; *Japanese Journal of Applied Physics*, Vol. **63**, Issue 5, 05SP02 (2024).

(2) Hiroshi Akatsuka: Quantitative Analysis of Optical Emission Spectroscopy for Plasma Process Monitoring; *Japanese Journal of Applied Physics*, Vol. **63**, Issue 5, 050102 (2024). [Invited review]

(3) Wataru Kikuchi, Yuya Yamashita, Atsushi Nezu, Hiroshi Akatsuka: Spectroscopic Measurement of Atmospheric-pressure Non-equilibrium Ar Plasma Using Continuum and Line Spectra; *Journal Physics D: Applied Physics*, Vol. **57**, Issue 33, 335202 (2024).

(4) Keren Lin, Thijs van der Gaag, Wataru Kikuchi, Hiroshi Akatsuka, Motoshi Goto: OES Diagnostics of Atmospheric Pressure Argon Plasma: Electron Temperature and Density Assessment through Visible Bremsstrahlung Inversion Method and Collisional-Radiative Model; *Applied Physics Letters*, Vol. **124**, Issue 23, 234103 (2024).

(5) Yosuke Shimada, Hiroshi Akatsuka: Sensitivity Analysis of Excited-State Population in Plasma Based on Relative Entropy; *Entropy*, Vol. **26**, No. 9, 782 (2024).

(6) Hiroshi Akatsuka, Ryo Nakanishi, Atsushi Nezu, Shinsuke Mori: Effect of Nitrogen Admixture to Underwater Argon Arc Discharge Plasma for Nuclear Decommissioning; *Progress in Nuclear Science and Technology*, Vol. **7**, pp. 182-188 (2025).

(7) Y. Inoue, J. Hasegawa, N. Matsubara, K. Takahashi, J. Tamura, K. Horioka, K. Takayama: Development of a Long-Life Laser Ion Source Using a Cryogenic Solidified Gas Target; *Progress in Nuclear Science and Technology*, **7**, 371-376 (2025).

(8) K. Matsuda, J. Hasegawa: Investigation of High Energy Particle Dynamics in a Linear Inertial Electrostatic Confinement Fusion Device by Particle-In-Cell Monte Carlo Collision Method; *Progress in Nuclear Science and Technology*, **7**, 364-370 (2025).

(9) J. Hasegawa, Y. Inoue, N. Matsubara, J. Tamura, K. Takahashi, K. Horioka, K. Takayama: A Long-life Laser Ion Source Using a Reproducible Solidified Gas Target; *Journal of Physics: Conference Series*, **2743**, 012018-012018 (2024).

(10) K. Ishikuro, K. Takahashi, T. Sasaki, T. Kikuchi, J. Hasegawa, J. Tamura, K. Horioka, K. Takayama: Effect of Solenoidal Magnetic Field on Ion Charge State Distribution in Laser Ion Source; *Journal of Physics: Conference Series*, **2743**, 012061-012061 (2024).

(11) Daisuke Nagae, Aki Suzuki, Shota Ikeda, Sosuke Kikuchi, Ryoichi Yoshimura, Yoichi Ma, Daigo Narita, Noriyosu Hayashizaki: Conceptional design of a He beam accelerator system for ^{211}At production; *Progress in Nuclear Science and Technology*, Vol. **7**, pp. 357-363 (2025).

(12) Shota Ikeda, Tomohiro Kobayashi, Yoshie Otake, Noriyosu Hayashizaki: Development status of the accelerator system for transportable compact neutron source RANS-Ⅲ; *Progress in Nuclear Science and Technology*, Vol. **7**, pp. 388-394 (2025).

(13) Y. Takai, K.C. Park, N. Idota, N. Sasaki, T. Tsukahara: Synthesis and characterization of boron-containing biocompatible polymer-coated Gd_2O_3 nanoparticles for neutron capture therapy-based theranostics; *Colloid and Surface A: Physicochemical and Engineering Aspects*, Vol.**711**, 136328 (2025).

(14) J. Chen, Y. Mukobara, C. Ishizuka, T. Katabuchi, S. Chiba: Bayesian approach to energy dependence of fission product yields of ^{235}U by data augmentation; *Journal of Nuclear Science and Technology,* Vol.61, pp. 1509-1520 (2024).

(15) Y. Mukobara, T. Sanami, A. Ono, T. Inakura, T. Katabuchi, S. Chiba, C. Ishizuka: Mean-field dependence of fragment-production cross sections in heavy-ion induced reactions; *Journal of Nuclear Science and Technology*, Vol.61, pp. 206-217 (2024).

(16) A. Tudora, K. Fujio, C. Ishizuka, S. Chiba: Prompt emission calculations for ^{239}Pu(n_{th},f) with the DSE model code and a pre-neutron fragment distribution Y(A,TKE); *European Physical Journal A*, Vol.60, 25 (2024).

(17) F. A. Ivanyuk, C. Ishizuka, S. Chiba: Five-dimensional Langevin approach to fission of atomic nuclei; *Physical Review C*, Vol.109**,**

034602 (2024).

(18) Itoh A., Hagiwara R., Yasui S., Kobayashi Y., Sakamto K., Mizokami M., Hirai M. and Ito K.: Microstructure evolution formed during early liquefaction stage between pre-oxidized Zircaloy 4 with SUS316 stainless steel at 1573 K, *Journal of Nuclear Science and Technology*, Vo.**61**, No.4, pp.530-540 (2024).

(19) Itoh A., Inoue K., Kobayashi Y., Sakamoto K., Endo Y., Nozaki K., Suehiro S., Honda T., Owada K., Mizokami M., Hirai M., Ito K. and Mizokami S.: Early-phase core degradation interpretation by interaction between fuel cladding and fuel components in Fukushima Daiichi nuclear power plant Unit 2, *Journal of Nuclear Science and Technology*, Vo.**61**, No.11, pp.1453-1469 (2024).

(20) Yamada M., Nakazawa R., Itoh A., Yasui S., Kobayashi Y. and Abe T.: Oxygen Solubility in Molten Sm--La--O Alloys and Equilibrated Oxide Phases., *Journal of the Japan Institute of Metals & Materials / Nippon Kinzoku Gakkaishi*, Vo.**88**, Issue 10, pp.245 (2024).

(21) Itoh A., Matsuo S., Yoshida K., Konashi K., Ikuta R., Niino K., Arita Y., Kobata M., Fukuda T., Kobayashi T., Tanida H. and Yaita T.: In situ XAFS–XRD study of the Zr–Y_2O_3 interaction at extra-high temperatures, *Synchrotron Radiation*, Vol.**31**, No.4, pp.810-820 (2024).

(22) Inoue K., Itoh A., Mizokami M. and Hirai M.: Evaluation of boron evaporation kinetics from stainless-steel–B4C alloy during steam oxidation at high temperatures, *Journal of Nuclear Materials*, Vol. **603**, p.15546 (2024).

(23) Kanno T., Iwama T., Sato T., Itoh A., Nagae Y., Inoue R. and Ueda S.: Reaction behavior of molten 316L stainless steel with B4C at 1450C during a core melt accident of BWR, *Journal of Nuclear Materials*, Vol. **607**, p.155705 (2025).

(24) Itoh A., Kanno T., Iwama T., Ueda S., Sato T., Nagae Y.: Experimental investigation of nonisothermal interaction between Fe-Zr melt and stainless steel forming “metallic debris” in Fukushima Daiichi Nuclear Power Station, *Annals of Nuclear Energy*, Vo. **217**, p.111333 (2025).

(25) Gerard Rovira, Atsushi Kimura, Shoji Nakamura, Shunsuke Endo, Osamu Iwamoto, Nobuyuki Iwamoto Yosuke Toh, Mariko Segawa, Tatsuya Katabuchi: Neutron Capture Cross Section of 129I and 127I using the NaI(Tl) spectrometer of the ANNRI beamline at J-PARC; *European Physical Journal A,* Vol. **60**, Article Number 120 (2024).

(26) Jingde Chen, Yuta Mukobara, Chikako Ishizuka, Tatsuya Katabuchi, Satoshi Chiba: Bayesian approach to energy dependence of fission product yields of ^{235}U by data augmentation; *Journal of Nuclear Science and Technology*, **61**, pp. 1509-1520 (2024).

(27) V. Alcayne et al. (Katabuchi, 59th in 129 Authors): Measurement and analysis of the ^{246}Cm and ^{248}Cm neutron capture cross-sections at the EAR2 of the n_TOF facility at CERN; EPJA Vol. **60** (2024).

(28) F. García-Infantes et al. (Katabuchi, 59th in 129 Authors), Measurement of the ^{176}Yb cross section at the n_TOF facility at CERN, *Physical Review C* **110**, (2024)

(29) T. Y. Saito, M. Niikura, T. Matsuzaki, H. Sakurai, M. Igashira, H. Imao, K. Ishida, T. Katabuchi, Y. Kawashima, M. K. Kubo, Y. Miyake, Y. Mori, K. Ninomiya, A. Sato, K. Shimomura, P. Strasser, A. Taniguchi, D. Tomono, Y. Watanabe: Muonic x-ray measurement for the nuclear charge distribution: The case of stable palladium isotopes; *Physical Review C*, **111**, 034313 (2025).

(30) Katsumi Yoshida, Ryosuke Maki, Jelena Maletaskic, Anna Gubarevich, Tatsuya Katabuchi, Tohru S. Suzuki, Tetsuo Uchikoshi: Helium gas release behavior of highly microstructure-controlled B4C-based ceramics irradiated with helium ion beam; *Progress in Nuclear Science and Technology*, 7, pp. 207-213 (2025).

(31) T. Bauer, M. Prenzel, S. Funayama, Y. Kato: Potential of thermal energy storage for endothermic reconversion of hydrogen carriers, *Energy Convers. Manag.* **342** (2025).

(32) S. Funayama, M. Zamengo, K. Risthaus, K. Mochizuki, T. Furuya, A. Hanke, A. Wimmer, I. Bürger, M. Linder, M. Schmidt, H. Takasu, Y. Kato: Maximization of thermal discharge power density of composite foam for thermochemical energy storage using calcium hydroxide and silicon-impregnated silicon carbide, *Appl. Therm. Eng*., **274**, 126575(2025).

(33) Y. Shinoda, K. Harada, R. Hamamura, H. Takasu, Y. Kato: Fabrication of palladium-copper alloy membrane for hydrogen purification using a reverse build-up method, *Prog. Nucl. Sci. Technol.*,

7, 261-266 (2025).

(34) K. Umeda, Y. Maruyama, S. Kuzukami, S. Tominaga, Y. Kato, H. Takasu: Effect of electrolyte particle size on CO_2 electrolysis performance of metal-supported solid oxide electrolysis cells prepared by atmospheric plasma spraying method, *Prog. Nucl. Sci. Technol*., **7**, 273-278 (2025).

(35) T. Enosawa, S. Yoshida, H. Takasu, Y. Kato: High reactivity and durability of silicone-supported magnesium chloride composite material for ammonia using thermochemical energy storage, *Prog. Nucl. Sci. Technol*., **7**, 279-285 (2025).

(36) K. Mochizuki, S. Funayama, M. Zamengo, H. Takasu, Y. Kato: Power-density enhancement of composite materials using open-cell foams for thermochemical energy storage, *Prog. Nucl. Sci. Technol*., **7**, 286–292 (2025).

(37) Naruki Shoji, Yoshihiko Oishi, Shou Osanai, Kenta Kusumoto, Hiroshige Kikura, Hideki Kawai: Assessment of silica sand behavior around rotating square rod in cylindrical container via ultrasonic velocity profiling; *Journal of Visualization*, Volume **28**, pp 279–290, (2025.1.25)

(38) Wongsakorn Wongsaroj, Natee Thong-un, Jirayut Hansot, Weerachon Treenuson, Jirasak Chanwutitum, Hiroshige Kikura: Low-cost ultrasonic measurement for estimation of liquid leakage point; *Journal of Mechanical Science and Technology*, Volume **39** Issue**1**, pp249-258(2025,1.4).

(39) Wongsakorn Wongsaroj, Natee Thong-un, Jirayut Hansot, Naruki Shoji, Weerachon Treenusorn, Hiroshige Kikura: The Application of Ultrasonic Measurement and Machine Learning Technique to Identify Flow Regime in a Bubble Column Reactor; *Sensors International*, Volume **6**, (Version of Record 2024.9.5).

(40) Natee Thong-un, Piyathat Panthong, Wongsakorn Wongsaroj, Hideharu Takahashi, Hiroshige Kikura: Development of an Automatic Paddle Wheel Aerator and Remote Movement Water Quality Monitoring for Use in a Marine Shrimp Farm; *Instrumentation Mesure Metrologie*, **23(2)**, pp. 79‑92(2024.4.26).

(41) Chonglin Shi, Zhi Li, Yuxing Liu, and Yoshinao Kobayashi: Activity of Chromium Oxide in CaO-SiO_2-MgO-Al_2O_3-MnO-CaF_2-CrO_x Slag for Chromium Reducing Process: *ISIJ International*, Volume 64, Issue 6, Page 893-900, Apr. 2024.

(42) N. Hirota, H. Nakano, Y. Fujita, T. Takeuchi, K. Tsuchiya, M. Demura, and Y. Kobayashi: Effect of dissolved oxygen concentration on dynamic strain aging and stress corrosion cracking of SUS304 stainless steel under high temperature pressurized water, *AIP Conference Proceedings* 3020, 030007 (2024) 1-6.

(43) Noriaki Hirota, Hiroko Nakano, Ryoma Takeda, Hiroshi Ide, Kunihiko Tsuchiya and Y. Kobayashi: Effect of Grain Refinement on Transgranular Stress Corrosion Cracking in SUS304L under Boiling Water Reactor conditions; *Material Science and Technology of Japan*, Vol. 61, No. 6 (2024) pp.248-252.

(44) Makoto Yamada, Ryota Nakazawa, Ayumi Itoh, Shintaro Yasui, Yoshinao Kobayashi and Taichi Abe: Oxygen Solubility in Molten Sm–La–O Alloys and Equilibrated Oxide Phases; *J. Japan Inst. Met. Mater.* Vol. 88, No. 10 (2024), pp. 245–251

(45) M. Kondo, Y. Kano, N. Chijiwa, M. Oh: Novel fiber reinforced concrete based on liquid metal technology toward resource recycling society; *Progress in Nuclear Science and Technology,* **7** (2025) 243-249. https://doi.org/10.15669/pnst.7.243.

(46) T. Horikawa, M. Kondo: Novel seawater desalination technology with liquid metal fluid; *Progress in Nuclear Science and Technology*, **7** (2025) 250-256, https://doi.org/10.15669/pnst.7.25.

(47) T. Horikawa, M. Masuda, M. Oh, M. Kondo: Liquid metal technology for collection of metal resources from seawater desalination brine and polluted groundwater; Water Reuse **15** (2025) 109–120, https://doi.org/10.2166/wrd.2025.100.

(48) M. Kondo, S. Hatakeyama, N. Oono-Hori, Y. Kitamura, K. Sakamoto, T. Tanaka, Y. Hishinuma: Chemical and structural durability of α-Al2O3 and γ-$LiAlO_2$ layers formed on ODS FeCrAl alloys in liquid lithium lead stirred flow; *Corros. Sci.,* **240** (2024) 112459. https://doi.org/10.1016/j.corsci.2024.112459.

(49) R. Muto, M. Kondo, T. Endo, R. Nishio, T. Tanaka: Growth of α-Al_2O_3 layer involving abnormal oxides in FeCrAl alloy tube fabricated

by WEDM process and electrical insulating performance in fusion reactor blanket; *Surface and Coatings Technology*, **493** (2024) 131250, https://doi.org/10.1016/j.surfcoat.2024.131250.

(50) B.A. Pint, Y.F. Su, M. Romedenne, J. Jun, M. Kondo, N. Oono, K. Sakamoto, Y. Hatano: Liquid metal compatibility of pre-oxidized FeCrAl in flowing Sn; *Fusion Engineering and Design,* **202** (2024) 114377, https://doi.org/10.1016/j.fusengdes.2024.114377

(51) Shimada M, Hirayama R, Matsumoto Y: Dimethyl sulfoxide attenuates ionizing radiation-induced centrosome overduplication and multipolar cell division in human-induced pluripotent stem cells; *Radiation Research*, Vol. **202**(4), pp.719-725 (2024).

(52) Imamichi S, Matsumoto Y, Matsuda T, Nakamura S, Shimada M, Yamanishi H, Masutani M, Suzuki M: Radiobiological characterization of neutron irradiation field of UTR-KINKI for the research utility toward boron neutron capture therapy: Cell killing effect and its enhancement by 4-borono-L-phenylalanine; Progress in Nuclear Science and Technology, Vol. **7**, pp.377-380 (2025).

(53) Tsukada K, Imamura R, Miyake T, Saikawa K, Saito M, Kase N, Fu L, Ishiai M, Matsumoto Y, Shimada M: CDKs-mediated phosphorylation of PNKP is required for end processing of single-strand DNA gaps on Okazaki Fragments and genome stability; *eLife*, Vol. **14**, pp.e99217 (2025).

(54) Shimada M, Matsumoto Y: Antioxidants ameliorates ionizing radiation-induced microcephaly in cerebral organoid derived from human-induced pluripotent stem cells; *Radiation Research*, Vol. **203**, pp.410-420 (2025).

(55) T. Kitano, S. Goto, X. Wang, T. Kamihara, Y. Sei, Y. Kondo, T. Sannomiya, H. Uekusa, Y. Murakami: 2.5-dimensional covalent organic frameworks; *Nature Communications*, Vol. **16**, Article Number 280 (10 pages), 2025.

(56) T. Tsukahara, K. Takao, M. Nakase, T. Ohnuki, A. Masuda, T. Hara, T. Kitagaki, T. Sumita, Y. Dotsuta, Y. Satou, L. Jiang, N. Kurosawa, M. Kanno: Study on degradation of fuel debris by combined effects of radiological, chemical, and biological functions; *JAEA-Review2024-026*(2024).

(57) K. Minowa, S. Watanabe, M. Nakase, Y. Takahatake, Y. Miyazaki, Y. Ban, H. Matsuura: Using X-ray absorption near edge structure to evaluate adsorption properties of rare earths and nitrogen by difference of their interactions; *Nuclear Instruments and Methods in Physics Research Section B*, **Vol.556**, 165496(2024).

(58) M. Nakase, S. Watanabe, H. Asano, T. Sakuragi, M. Harigai, R. Hamada, S. Hara, R. Maki, H. Kikunaga, T. Kobayashi: Challenge of Novel Hybrid-waste-solidification of Mobile Nuclei Generated in Fukushima Nuclear Power Station and Establishment of Rational Disposal Concept and Its Safety Assessment; *JAEA-Review2024-012*(2024).

(59) T. Obara, R. Horikoshi, S. Odmaa, J. Nishiyama: Small modular reactor concept sustainable in a carbon-neutral society; *Progress in Nuclear Science and Technology*, **7** (2025) 1-4. https://doi.org/10.15669/pnst.7.1

(60) T. Amarjargal, J. Nishiyama, T. Obara: Coolant void coefficient in a sodium-cooled rotational fuel-shuffling breed-and-burn fast reactor; *Progress in Nuclear Science and Technology*, **7** (2025) 5-8. https://doi.org/10.15669/pnst.7.5

(61) X. Zhao, J. Nishiyama, T. Obara: Comparison of burnup performance between lead coolant and LBE coolant in Rotational Fuel-shuffling Breed-and-Burn fast reactor; *Progress in Nuclear Science and Technology*, **7** (2025) 9-13. https://doi.org/10.15669/pnst.7.9

(62) O. Sambuu, V. K. Hoang, T. Amarjargal, T. Obara: Fuel cycle features of RFBB fast reactor with advanced fuel; *Journal of Nuclear Science and Technology*, **62** (2025) 562-572. https://doi.org/10.1080/00223131.2025.2455051

(63) K. Fukuda, T. Obara, K. Suyama: Neutronics–Thermal-Hydraulics–Coupled Transient Analysis for Reactor Power Change in an Inclined Offshore Floating Boiling Water Reactor; *Nuclear Technology*, **211** (2024) 963-973. https://doi.org/10.1080/00295450.2024.2368966

(64) T. Amarjargal , J. Nishiyama , T. Obara: Small rotational fuel-shuffling breed-and-burn sodium-cooled and nitride-fueled fast reactor with LBE reflectors; *Annals of Nuclear Energy*, **201** (2024) 110445. https://doi.org/10.1016/j.anucene.2024.110445

(65) A. C. Stafie, J. Nishiyama, T. Obara: Practical Design of a Breed-and-Burn Lead-Cooled Fast Reactor with Rotational Fuel Shuffling Strategy; *Nuclear Science and Engineering*, **199** (2025) 266-279. https://doi.org/10.1080/00295639.2024.2347716

(66) Eva M. Lisowski, Hiroshi Sagara, "Increased ^{238}Pu Production in Proliferation-Resistant U-10Zr Fuel Produced from Reprocessed Uranium Containing Unseparated ^{237}Np," Nuclear Technology, Volume 211, Issue 8, 2025. DOI: https://doi.org/10.1080/00295450.2024.2425914

(67) Kim Wei Chin, Hiroshi Sagara, Jun-ichi Hori, Yoshiyuki Takahashi, "Measurement System Requirements for Photofission Signal Detection with Coincidence Neutron Counting Method," Progress in Nuclear Science and Technology, Vol. 7, pp. 91-96, DOI: 10.15669/pnst.7.91, March, 2025.

(68) Hong Fatt Chong, Hiroshi Sagara, "Once-through High Burnup Fuel Management Strategy with Dual Neutron Energy Spectrum Core in HTGR," Progress in Nuclear Science and Technology, Vol. 7, pp. 47-52, DOI: 10.15669/pnst.7.47, March, 2025.

(69) Hiroshi Sagara, Masatoshi Kawashima, Koji Morita, Wei Liu, Tatsumi Arima, Yuji Arita, Isamu Sato, Haruaki Matsuura, Yoshihiro Sekio, "Development of a Passive Safety Shutdown Device to Prevent Core Damage Accidents in Fast Reactors (2) Performance of the Device in Reactivity Control and Nuclear Material Management," Progress in Nuclear Science and Technology, Vol. 7, pp. 34-40, DOI: 10.15669/pnst.7.34, March, 2025.

(70) Taketeru Nagatani, Hiroshi Sagara, Yoshihiro Kosuge, Takayoshi Nohmi, Keisuke Okumura, "Development of a Method for the Determination of Spontaneous Fission Nuclides in Irradiated Fuel and Applicability to Pu quantification in Fuel Debris by Dual Time Neutron Measurements," Progress in Nuclear Science and Technology, Vol. 7, pp. 41-46, DOI: 10.15669/pnst.7.41., March, 2025

(71) Natsumi Mitsuboshi, Hiroshi Sagara, "Evaluation for Proliferation Resistance of small and medium modular LWR with U3Si2 fuel," Progress in Nuclear Science and Technology, Vol. 7, pp. 318-323, DOI: 10.15669/pnst.7.318, March, 2025.

(72) Daisuke Hara, Hiroshi Sagara, "Proliferation Resistance Analysis of Offshore Floating Nuclear Power Plant," Progress in Nuclear Science and Technology, Vol. 7, pp. 324-330, DOI: 10.15669/pnst.7.324, March, 2025.

(73) Kosuke Tanabe, Masao Komeda, Yosuke Toh, Hiroshi Sagara, "Characterization of water Cherenkov neutron detector with high efficiency, availability and affordability for nuclear security," Progress in Nuclear Science and Technology, Vol. 7, pp. 67-73, DOI: 10.15669/pnst.7.67, March, 2025.

(74) Akito Oizumi, Hiroshi Sagara, "Safeguards Approach and Design of Transuranium Fuel Cycle with Accelerator-driven System based on Material Attractiveness," Progress in Nuclear Science and Technology, Vol. 7, pp. 331-337, DOI: 10.15669/pnst.7.331, March, 2025.

(75) Haruka Okazaki, Masatoshi Kawashima, Hiroshi Sagara, "Safety and proliferation resistance of small and medium-sized sodium-cooled fast reactors with passive shutdown devices," Progress in Nuclear Science and Technology, Vol. 7, pp. 338-344, DOI: 10.15669/pnst.7.338, March, 2025.

(76) Katsuyoshi TSUCHIYA, Hiroshi SAGARA, Chi Young HAN, "Development of Passive Neutron Emission Tomography Robust to Its Various Inhibiting Factors and Its Applicability to Nuclear Safeguards," Progress in Nuclear Science and Technology, Vol. 7, pp. 110-116, DOI: 10.15669/pnst.7.110, March, 2025.

(77) Kosuke Tanabe, Masao Komeda, Yosuke Toh, Yasunori Kitamura, Tsuyoshi Misawa, Ken'ichi Tsuchiya & Hiroshi Sagara, Compact and transportable system for detecting lead-shielded highly enriched uranium using 252Cf rotation method with a water Cherenkov neutron detector, Scientific Reports volume 14, Article number: 18828 (2024) https://doi.org/10.1038/s41598-024-69526-w

(78) D. Hara , H . Sagara, The Behavior of Hyper velocity Jet in the Water Generated by Shaped Charge", Journal of Nuclear Science and Technology; Volume 62, Issue 3, p. 278-287 https://doi.org/10.1080/00223131.2024.2424522, 2024

(79) Orino, T.; Cao, Y.; Tashiro, R.; Takeyama, T.; Gericke, R.; Tsushima, S.; Takao, K. "Utility of Interchangeable Coordination Modes of *N,N′*-

Dialkyl-2,6-Pyridinediamide Tridentate Pincer Ligands for Solvent Extraction of Pd(II) and Zr(IV) from High-level Radioactive Liquid Waste" *Inorg. Chem.* 2024, **63**, 24647-24661. DOI: 10.1021/acs.inorgchem.4c03844.

(80) Akashi, S.; Takao, K. "Reactivity of [3+1+1] Uranyl-DGA Complex as Lewis-acid Catalyst in Nucleophilic Acyl Substitution of Acid Anhydrides" *Inorganics*, 2024, **12**, 324. DOI: 10.3390/inorganics12120324 [Open Access].

(81) Takeyama, T.; Tsushima, S.; Takao, K. "Controlling Mixed-Valence States of Pyridyldiimino-bis(*o*-phenolato) Ligand Radical in Uranyl(VI) Complexes" *Dalton Trans.* 2024, **53**, 16671-16684. doi:10.1039/D4DT01821D.

(82) Tsushima, S.; Kretzschmar, J.; Doi, H.; Okuwaki, K.; Kaneko, M.; Mochizuki, Y.; Takao, K. "Towards tailoring hydrophobic interaction with uranyl(VI) oxygen for C-H activation", *Chem. Commun.* 2024, **60**, 4769-4772. DOI:10.1039/D4CC01030B.

(83) Takao. K.; Ouchi, K.; Komatsu, A.; Kitatsuji, Y.; Watanabe, M. "Securing Reversibility of $U^{V}O_2^{+}/U^{VI}O_2^{2+}$ Redox Equilibrium in [emim]T_f2N-Based Liquid Electrolytes towards Uranium Redox-Flow Battery" *Eur. J. Inorg. Chem.* 2024, **27**, e202300787. DOI:10.1002/ejic.202300787.

(84) Sejung JANG, Hiroaki TSUTSUI: Estimation of Plasma Vertical Position by Long-Short Term Memory Network with Time2Vec in a Small Tokamak Device PHiX; *Plasma and Fusion Research*, Vol.**19**, pp. 1403023 (2024).

(85) Donghwan Kim, Mizuki Uenomachi, Kenji Shimazoe, Hiroyuki Takahashi, Kei Kamada, Hideki Tomita: Imaging and Sensing of pH and Chemical State With Cascade Photons of ^{111}In Using Ring-Type Compton Camera; *IEEE Transactions on Radiation and Plasma Medical Sciences*, Vol.**9**, No.1, pp. 107-117(2024).

(86) Donghwan Kim, Linlin Yan, Kenji Shimazoe, Hiroyuki Takahashi, Kenichiro Ogane, Masao Yoshino, Kei Kamada, Mizuki Uenomachi: Demonstration of in-vivo simultaneous 3D imaging with 18F-FDG and Na131I using Compton–PET system; *Scientific Reports*, Vol. **14**, No.1, p.20946 (2024).

(87) M. Hamdan, B. Feng, K. Shimazoe, M. Nogami, K. Hitomi, H. Takahashi, M. Uenomachi, H. Toyokawa: Characterization of TlBr gamma detector based on electrical charge and Cherenkov light analysis; *Journal of Instrumentation*, Vol. **19**, No.11, p.C11017 (2024).

(88) Takuto Narita, Takeshi Go Tsuru, Mizuki Uenomachi, Tomonori Ikeda, Masamune Matsuda, Hiroyuki Uchida, Ayaki Takeda, Koji Mori, Masataka Yukumoto, Daisuke Izumi, Koyo Magata, Kenji Shimazoe, Hiroyuki Takahashi, Koichi Hagino, Ikuo Kurachi, Yasuo Arai, Takayoshi Kohmura, Takaaki Tanaka: Evaluation of the X-ray SOI pixel detector with the on-chip ADC; *X-Ray, Optical, and Infrared Detectors for Astronomy XI*, Vol. **13103**, pp.627-631 (2024).

(89) Hiroumi Matsuhashi, Kouichi Hagino, Aya Bamb,a Ayaki Takeda, Masataka Yukumoto, Koji Mori, Yusuke Nishioka, Takeshi Go Tsuru, Mizuki Uenomachi, Tomonori Ikeda, Masamune Matsuda, Takuto Narita, Hiromasa Suzuki Takaaki Tanaka Ikuo Kurachi Takayoshi Kohmura Yusuke Uchida Yasuo Arai Shoji Kawahito: Evaluation of the X-ray SOI pixel detector with the on-chip ADC; *Nuclear Instruments and Methods in Physics Research Section A: Accelerators, Spectrometers, Detectors and Associated Equipment*, Vol. **1064**, p.169426 (2024).

(90) Sou Yasuhara, Ayato Nakagawa, Kazuki Okamoto, Takahisa Shiraishi, Hiroshi Funakubo, Shintaro Yasui, Mitsuru Itoh, Takaaki Tsurumi, Takuya Hoshina: Evaluation of ferroelectricity in a distorted wurtzite-type structure of Sc-doped $LiGaO_2$; *RSC Adv.*, Vol. **14**, pp.13900-13904 (2024).

(91) Ayumi Itoh, Ryotaro Hagiwara, Shintaro Yasui, Yoshinao Kobayashi, Kan Sakamoto, Masato Mizokami, Mutsumi Hirai, Kenichi Ito: Microstructure evolution formed during early liquefaction stage between pre-oxidized Zircaloy 4 with SUS316 stainless steel at 1573 K; *Journal of Nuclear Science and Technology*, Vol. **61**(4), pp.530-540 (2024).

(92) Makoto Yamada, Ryota Nakazawa, Ayumi Itoh, Shintaro Yasui, Yoshinao Kobayashi, Taichi Abe: Oxygen Solubility in Molten Sm–La–O Alloys and Equilibrated Oxide Phases; *Journal of the Japan Institute of Metals*, Vol. **88**(10), pp.245-251 (2024).

(93) Haruto Takahashi, Shingo Maruyama, Hiroshi

Naganuma, Hiroki Taniguchi, Ryota Takahashi, Shintaro Yasui, Kenichi Kaminaga, Yuji Matsumoto: Ferroelectric polycrystalline Bi_2SiO_5 thin films on Pt-covered Si substrates prepared by pulsed laser deposition combined with post-annealing; *Journal of Alloys and Compounds*, Vol. **988**, pp.174195-174195 (2024).

(94) Sou Yasuhara, Akira Orio, Shintaro Yasui, Takuya Hoshina: Room temperature synthesis of $BaTiO_3$ nanoparticles using titanium bis(ammonium lactato) dihydroxide; *Japanese Journal of Applied Physics*, Vol. **63**(9), p.09SP16 (2024).

(95) Jinling Zhou, Hsin Hui Huang, Shunsuke Kobayashi, Shintaro Yasui, Ke Wang, Eugene A. Eliseev, Anna N. Morozovska, Pu Yu, Ichiro Takeuchi, Zijian Hong, Daniel Sando, Qi Zhang and Nagarajan Valanoor: An Emergent Quadruple Phase Ensemble in Doped Bismuth Ferrite Thin Films Through Site and Strain Engineering; *Advanced Functional Materials*, Vol. **34**(39), p.2403410 (2024).

(96) Daniel Sando, Florian Appert, Oliver Paull, Shintaro Yasui, Dimitrios Bessas, Abdeslem Findiki, Cécile Carrétéro, Vincent Garcia, brahim dkhil, Agnès Barthelemy, Manuel Bibes, Jean Juraszek and Nagarajan Valanoor: Finite Size Effects in Antiferromagnetic Highly Strained $BiFeO_3$ Multiferroic Films; *Advanced Physics Research*, Vol. **3**, p.2400068 (2024).

(97) Zerui Li, Taro Kuwano, Akitoshi Nakano, Manabu Hagiwara, Shintaro Yasui, Hiroki Taniguchi, Hiroko Yokota: Titanite-type solid solutions $(Ca,Pb)TiGeO_5$: a competition between triclinic and antiferroelectric distortions; *Journal of the Ceramic Society of Japan*, Vol. **133**(7), pp.275-280 (2025).

(98) Masaki Utsumi, Akihiko Fujiwara, Hidenori Goto, Hideki Okamoto, Nobuyuki Takeyasu, Yasunori Saitoh, Michihiro Suga, Yuichiro Takahashi, Hiroyuki Imanaka, Hiroki Taniguchi, Shintaro Yasui, Ritsuko Eguchi and Yoshihiro Kubozono: Biosensor Application of CMOS Inverter and Ring Oscillator with Organic Field-Effect Transistors; *ACS Applied Electronic Materials*, Vol. **7**, pp.1483-1492 (2025).

(99) Anna V. Gubarevich, Gen Homma, Katsumi Yoshida: Boron carbide with improved mechanical properties fabricated via rapid pressureless densification with electromagnetic induction assistance; *Scripta Materialia*, Vol.**238**, 115731 (2024).

(100) Yosuke Nishimura, Anna Gubarevich, Katsumi Yoshida, Avadhesh Kumar Sharma, Koji Okamoto: Kinetic modeling of IG-110 oxidation in inert atmosphere with low oxygen concentration for innovative high-temperature gas-cooled reactor applications; *Journal of Nuclear Science and Technology*, Vol. **61**, No. 6, pp. 802-809 (2024).

(101) Anna V. Gubarevich, Kenshin Miura, Katsumi Yoshida: Rapid synthesis of high-yield Ti_3AlC_2 MAX phase powders from $TiC_{0.67}$ and Al with induction heating assistance; *International Journal of Applied Ceramic Technology*, Vol. **21**, No.4, pp. 2712-2719 (2024).

(102) Yosuke Nishimura, Anna Gubarevich, Katsumi Yoshida, Avadhesh Kumar Sharma, Koji Okamoto: Modeling passive/active transition in high-temperature dry oxidation of reaction sintered SiC for innovative fuel matrix in high-temperature gas-cooled reactors; *Journal of European Ceramic Society*, Vol. **44**, No. 5, pp. 3031-3038 (2024).

(103) Katsumi Yoshida, Mayuko Kasakura, Anna Gubarevich, Masaki Kotani: Mechanical Properties of SiC_f/SiC Composites with h-BN Interphase Formed by Electrophoretic Deposition Method; *International Journal of Applied Ceramic Technology*, Vol. **21**, No.4, pp. 2730-2737 (2024).

(104) Atsuko Tanaka, Anna Gubarevich, Toshiyuki Nishimura, Katsumi Yoshida: Corrosion behavior of A_4SiC_4 ceramics exposed to molten calcium-magnesium-alumino-silicate at 1350°C in air; *International Journal of Applied Ceramic Technology*, Vol. **21**, No.4, pp. 2784-2795 (2024).

(105) Anna V. Gubarevich, Katsumi Yoshida: Fast Synthesis of Fine Boron Carbide Powders Using Electromagnetic Induction Synthesis Method; *Powders*, Vol. **3**, No.1, pp. 17-27 (2024).

(106) Yosuke Nishimura, Anna Gubarevich, Katsumi Yoshida, Koji Okamoto: An Innovative Fuel Design for HTGRs: Evaluating a 10-Hour High-Temperature Oxidation of the SiC Fuel Matrix During Air Ingress Accident Conditions; *Energies*, Vol. **17**, No. 21, 5366 (2024).

International Conference Proceedings

(1) Wataru Kikuchi, Yuya Yamashita, Atsushi Nezu, Hiroshi Akatsuka: Spectroscopic Measurement of Atmospheric-Pressure Non-Equilibrium Ar Plasma Based on Line Spectra with Undetected Level Densities; *50th EPS Conference on Plasma Physics*, July 8–12, 2024, Salamanca, Spain, P1-009.

(2) Yuya Yamashita, Kenta Doi, Tetsuji Kiyota, Shuhei Watanabe, Kazuki Shimatani, Wataru Kikuchi, Yuchen Ye, Atsushi Nezu, Hiroshi Akatsuka: Electron Temperature Diagnosis of CF_4/O_2 Plasma Based on Fluorine Atomic Corona Model by Tomographic Optical Emission Spectroscopic Measurement; *ESCAMPIG (Europhysics Conference on Atomic and Molecular Physics of Ionized Gases) XXVI*, July 9–13, 2024, Brno, Czech Republic, p2-P29.

(3) Wataru Kikuchi, Yuya Yamashita, Atsushi Nezu, Hiroshi Akatsuka: Spectroscopic Measurement of Atmospheric-Pressure Non-Equilibrium Ar Plasma Based on Continuum and Line Spectra with Weighted Analysis; *The 5th International Conference on Data-Driven Plasma Science (ICDDPS-5)*, August 12–16, 2024, Berkeley, USA, 2B.

(4) Shinji Yoshimura, Keren Lin, Wataru Kikuchi, Jun Enomoto, Motoshi Goto, Hiroshi Akatsuka: Development and Measurement of a Gas Temperature Controllable Atmospheric-Pressure Plasma Jet System for Plasma Bio Research; *77th Annual Gaseous Electronics Conference (77GEC)*, September 30 – October 4, 2024, San Diego, USA, HT4.00109.

(5) Hiroshi Akatsuka, Shuhei Watanabe, Kenta Doi, Tetsuji Kiyota, Yuta Yamashita, Wataru Kikuchi, Kenta Ishi, Yuchen Ye, Atsushi Nezu: Optical Emission Spectroscopic Measurement of Electron Temperature and Density of Oxygen ICP; *The 45th International Symposium on Dry Process (DPS2024)*, November 14–15, 2024, Chitose, Japan, P-24.

(6) Keren Lin, Shinji Yoshimura, Motoshi Goto, Wataru Kikuchi, Jun Enomoto, Hiroshi Akatsuka: Development and Measurement of a Gas Temperature Controllable Atmospheric-Pressure Plasma Jet System for Plasma Bio Research; *The 45th International Symposium on Dry Process (DPS2024)*, November 14–15, 2024, Chitose, Japan, P-44.

(7) Hiroshi Akatsuka, Shota Yamada, Yuki Morita, Atsushi Nezu: Spectroscopic Study of Rotational Temperatures CO-Excited States in Microwave Discharge CO_2 Plasma; *International Symposium on Green Transformation Initiative and Innovative Zero-Carbon Energy Systems, GXI-ZES*, January 14–16, 2025, Tokyo, Japan, 2P022.

(8) Keren Lin, Shinji Yoshimura, Motoshi Goto, Takayoshi Tsutsumi, Wataru Kikuchi, Jun Enomoto, Hiroshi Akatsuka: Development and Measurement of a Gas Temperature Controllable Atmospheric-Pressure Plasma Jet System for Plasma Bio Research; *ISPlasma2025/IC-PLANTS2025*, March 3–7, 2025, Kasugai, Japan, 05P-02.

(9) Yuchen Ye, Kenta Doi, Tetsuji Kiyota, Kazuki Shimatani, Ayaki Sakurai, Wentao He, Yuya Yamashita, Wataru Kikuchi, Atsushi Nezu, Hiroshi Akatsuka: Exploring Multiple Solutions of Electron Temperature and Density in the Argon Collisional-Radiative Model Using Monte Carlo Simulations; *ISPlasma2025/IC-PLANTS2025*, March 3–7, 2025, Kasugai, Japan, 05P-24.

(10) N. Yamano, T. Inakura, C. Ishizuka, S. Chiba: Crucial importance of correlation between cross sections and angular distributions in nuclear data of ^{28}Si; *JAEA-Conf 2024-002*, pp. 12–20 (2024).

(11) K. Kiatkongkaew, H. Sagara, K. Tanabe, T. Katabuchi, C. Ishizuka, R. Kunitomo: Photonuclear reaction detection using ^{7}Li(p,γ)^{8}Be gamma rays; *Proceedings of the 45th Annual Meeting of INMM Japan*, The University of Tokyo, Tokyo, Nov. 27–28, 2024.

(12) Nakazawa R., Itoh A., Kurata M., Kobayashi Y.: PHASE EQUILIBRIUM BETWEEN METALLIC LIQUID AND OXIDE IN CE-ZR-FE-O SYSTEM AS A SURROGATE SYSTEM OF METALLIC DEBRIS, *Proceedings of the International Topical Workshop on Fukushima Decommissioning Research 2024*.

(13) Itoh A., Inoue K., Mizokami M., Hirai M.,; PROGRESS IN DEVELOPMENT OF DECOMMISSIONING TECHNOLOGY IN TEPCO COLLABORATIVE RESEARCH CLUSTER FOR DECONTAMINATION AND DECOMMISSIONING FRONTIER

TECHNOLOGY CREATION (2) BORON DISTRIBUTION SCENARIO IN THE FDNPS UNIT 2 BASED ON THE EXPERIMENTAL STUDY AND ACCIDENT ANALYSIS, *Proceedings of the International Topical Workshop on Fukushima Decommissioning Research 2024*.

(14) T. Takeda, M. Stefanica: Study on Liquid Jet for Neutron Source of BNCT; *19th International Conference on Nuclear Engineering (ICONE20)*, October 24-25, 2012, Paris, France, ICONE20-45600.

(15) S. Funayama, T. Izaki, H. Saeki, K. Tomita, T. Sugiyama, K. Mochizuki, T. Kato, H. Takasu, Y. Kato: Hybrid thermal energy storage based on thermochemical energy storage and thermocline sensible thermal energy storage, *International Symposium on Green Transformation Initiative and Innovative Zero-Carbon Energy Systems (GXI-ZES)*, 2025/01/16, Tokyo.

(16) H. Saeki, T. Sugiyama, T. Izaki, K. Tomita, S. Tamano, S. Funayama, T. Kato, H. Takasu, Y. Kato: Numerical validation of calcium oxide-based composites in an indirect fixed-bed reactor for thermochemical energy storage, *International Symposium on Green Transformation Initiative and Innovative Zero-Carbon Energy Systems (GXI-ZES)*, 2025/01/15, Tokyo.

(17) T. Izaki, H. Saeki, T. Sugiyama, K. Tomita, K. Mochizuki, S. Funayama, T. Kato, H. Takasu, Y. Kato: Experimental evaluation of an indirect heated fixed-bed reactor with calcium hydroxide for thermal energy storage, *International Symposium on Green Transformation Initiative and Innovative Zero-Carbon Energy Systems (GXI-ZES)*, 2025/01/15, Tokyo.

(18) Y. Hozumi, R. Hamamura, S. Niwa, S. Funayama, H. Takasu, Y. Kato: Development of metal composite H2-permeable membranes by a reverse build-up method, *International Symposium on Green Transformation Initiative and Innovative Zero-Carbon Energy Systems (GXI-ZES)*, 2025/01/15, Tokyo.

(19) D. Moritomo, R. Miyazaki, Y. Ikeda, D. Teshima, Y. Kato, H. Takasu: Development of Metal-Supported Solid Oxide Electrolysis cell as carbon dioxide reduction technology for carbon recycling, *International Symposium on Green Transformation Initiative and Innovative Zero-Carbon Energy Systems (GXI-ZES)*, 2025/01/15, Tokyo.

(20) Y. Yugami, S. Funayama, H. Takasu, Y. Kato: Development of MgO-based carbon dioxide sorption material in presence of water vapor for Zero-Carbon Energy System, *International Symposium on Green Transformation Initiative and Innovative Zero-Carbon Energy Systems (GXI-ZES)*, 2025/01/15, Tokyo.

(21) K. Tomita, T. Izaki, Y. Guo, S. Funayama, H. Takasu, Y. Kato: Development of composite materials using calcium oxide for CO2 capture and storage applications, *International Symposium on Green Transformation Initiative and Innovative Zero-Carbon Energy Systems (GXI-ZES)*, 2025/01/15, Tokyo.

(22) H. Takasu, D. Moritomo, S. Funayama, Y. Kato: Carbon dioxide conversion technology at high temperatures using a metal-supported solid oxide electrolysis cell as a green transformation technology, *International Symposium on Green Transformation Initiative and Innovative Zero-Carbon Energy Systems (GXI-ZES),* 2025/01/15, Tokyo.

(23) S. Funayama, T. Sugiyama, K. Mochizuki, H. Takasu, Y. Kato: Development of composites for thermochemical energy storage based on calcium hydroxide and silicon-impregnated silicon carbide foams, *The Second Symposium on Carbon Ultimate Utilization Technologies for the Global Environment (CUUTE-2)*, 2024/11/13, Nara.

(24) K. Tomita, T. Iizaki, H. Saeki, T. Sugiyama, T. Kato, S. Funayama, H. Takasu, Y. Kato: Numerical investigation of an indirect heat fixed-bed reactor with multi reaction tubes for calcium oxide/water-based thermochemical energy storage, *The Second Symposium on Carbon Ultimate Utilization Technologies for the Global Environment (CUUTE-2)*, 2024/11/13, Nara.

(25) T. Izaki, T. Sugiyama, H. Saeki, K. Tomita, K. Mochizuki, T. Kato, S. Funayama, H. Takasu, Y. Kato: Performance evaluation of an indirect heated fixed-bed reactor using molten salt for thermochemical energy storage with calcium hydroxide, *The Second Symposium on Carbon Ultimate Utilization Technologies for the Global Environment (CUUTE-2)*, 2024/11/13, Nara.

(26) K. Fujii, S. Funayama, H. Takasu, Y. Kato, Numerical analysis of composite materials using

calcium hydroxide and ceramic honeycomb supports of silicon-impregnated silicon carbide, *The Second Symposium on Carbon Ultimate Utilization Technologies for the Global Environment (CUUTE-2)*, 2024/11/13, Nara.

(27) H. Saeki, T. Sugiyama, T. Izaki, K. Tomita, S. Tamano, S. Funayama, T. Kato, H. Takasu, Y. Kato: Thermochemical energy storage performance of an indirect fixed-bed reactor using calcium oxide-based composite, *The Second Symposium on Carbon Ultimate Utilization Technologies for the Global Environment (CUUTE-2)*, 2024/11/13, Nara, Poster

(28) Y. Hozumi, R. Hamamura, H. Takasu, Y. Kato: Development of PdCu composite H2-permeable membranes by a reverse build-up method, *The Second Symposium on Carbon Ultimate Utilization Technologies for the Global Environment (CUUTE-2)*, 2024/11/13, Nara.

(29) D. Moritomo, D. Teshima1, H. Takasu, Y. Kato: Effects of different cell layers on performance in solid oxide electrolysis cells for carbon dioxide reduction process in carbon recycling ironmaking system, *The Second Symposium on Carbon Ultimate Utilization Technologies for the Global Environment (CUUTE-2)*, 2024/11/13, Nara.

(30) S. Funayama, T. Sugiyama, T. Izaki, H. Saeki, K. Tomita, K. Fujii, S. Tamano, T. Kato, H. Takasu, Y. Kato: Thermal discharge performance of a composite foam in an indirect fixed-bed reactor for thermochemical energy storage, *ENERSTOCK 2024*, 2024/06/05, Lyon, France, Oral

(31) Fujitsuka Yuji, Kiyohara Ryosuke, Nagai Toshiya, Takahashi Hideharu, Hiroshige Kikura, Endo Gen: Elastic Telescopic Arm Extension/Contraction Mechanism Using a Helically Grooved Flexible Conduit; *Proceedings of 2025 IEEE/SICE International Symposium on System Integration (SII)*, January 21-24, 2025, Munich, Germany, IEEE, 12 February 2025.

(32) Kanichi Oyama, Makoto Hirose, Susumu Ozaki, Hiroshige Kikura: Study on Analytical Evaluation of Radiological Impacts due to Sabotage against Spent Nuclear Fuel Transport Package; *International Symposium on Green Transformation Initiative and Innovative Zero-Carbon Energy Systems, GXI-ZES*, January 14-16, 2025, Institute of Science Tokyo, 3S14-2.

(33) Tadashi Narabayashi, Hiroshige Kikura, Hideharu Takahashi, Eiji Toshima, Hiroshi Hattori, Seiichi Dono: Tokyo Tech's Collaboration Research with TEPCO for Decommissioning (5) Development of Air Purification System to Remove Radioactive Dust During Debris Cutting; *Proceedings of the International Topical Workshop on Fukushima Decommissioning Research 2024,* October 10-13, 2024, Naraha, Fukushima, 1097- 2024.

(34) Hiroshige Kikura, Gen Endo, Hideharu Takahashi, Nobuhiro Ishii, Shiro Takahira, Kenji Takeshita: Tokyo Tech's Collaboration Research with TEPCO for Decommissioning (4) Development of Leak Investigation Technology in Reactor Building; *Proceedings of the International Topical Workshop on Fukushima-Daiichi Decommissioning Research 2024,* October 10-13, 2024, Naraha, Fukushima,2024-1092.

(35) S. Oshima, N. Shoji, H. Kikura, H. Takahashi: BASIC RESEARCH ON ULTRASONIC SIGNAL RECEPTION SYSTEM USING LASER BEAM; *14th Pacific Symposium on Flow Visualization and Image Processing*, November 27-29, 2024, The University of Canterbury in Christchurch, New Zealand, ID-5

(36) Masataka Teshigawara, Hiroshige Kikura, Naruki Shoji, Hideki Kawai, Kazunori Takeuchi, Koji Mochizuki, Norio Tenma: Study on Multiphase flow Measurement in Large-diameter Metal Pipe using Ultrasonic Velocity Profiler; *10th World Conference on Experimental Heat Transfer, Fluid Mechanics and Thermodynamics*, August 26-30, 2024, Rhodes Island, Greece, V011T15A063.

(37) Chengzuo Ji, Yuan Chen, Christian Brice, Hiroshige Kikura, Hideharu Takahashi, Gen Endo: Remote Measurement by Robot Arm Equipped With Pauvp and Libs; *Proceedings of 31st International Conference on Nuclear Engineering (ICONE31)*, August 4-8, Prague, Czech Republic, ICONE31-135489, V011T15A063,7 pages.

(38) Yutaka Namiki, Naruki Shoji, Hiroshige Kikura: Fundamental Study of Development of Flow Visualization System Using Ultrasonic Velocity Profiler and Augmented Reality; *Proceedings of ASME2024 Fluids Engineering Division Summer Meeting*, September 10, 2024, Hilton Anaheim, CA.,U.SA, FEDSM2024-132203, V002T07A001, 7 pages.

(39) Seitaro Ueno, Yutaka Namiki, Masataka Teshigawara, Naruki Shoji,Hiroshige Kikura, Takahiko Tanahashi: Simulation and Evaluation of the Basic Equations Using the CubicDEL Method; *The third Asian Conference on Thermal Sciences (ACTS 2024)*, June 23-27, 2024, Shanghai Fuyue Hotel, Chaina, O-0603

(40) K. Kikuchi, T. Suzuki, N. Shoji, H. Kikura. Fundamental Research on a New Water Level Measurement Method using Clamp-On Ultrasonic Transducers. *Specialist Workshop on Advanced Instrumentation and Measurement Techniques for Nuclear Reactor Thermal-Hydraulics and Severe Accidents (SWINTH-2024)*, 2024.6/17-20, Dresden, Germany, A1-5.

(41) Tadashi Narabayashi, Hiroshige Kikura, Kazuhiko Kasai, Koji Endo: BWR-Type SMR with Load-Following Function, FCVS, and Seismic Isolation Device that Eliminates Location Requirements: *Proceedings of 2024 International Congress on Advances in Nuclear Power Plants (ICAPP),*Las Vegas, NV, June 16-19, 2024, Pages 1010-1023.

(42) Takao, K.; Mizumachi, T.; Sato, M.; Ito, K.; Nabata, R.; Kaneko, M.; Takeyama, T.; Tsushima, S. "Development of Water-Compatible N3O2-Pentadentate Planar Ligands for Uranium Harvesting from Seawater" *6th International ATALANTE Conference on Nuclear Chemistry for Sustainable Fuel Cycles (ATALANTE2024)*, Avignon, France (Sept 1-6, 2024). [Keynote Lecture].

(43) Ono, R.; Takeyama, T.; Gericke, R.; März, J.; Duckworth, T.; Tsushima, S.; Takao, K. "Molecular and Crystal Structures of Pu(IV)-Nitrato Complexes with Double-Headed 2-Pyrrolidone Derivatives in HNO_3(aq)" *6th International ATALANTE Conference on Nuclear Chemistry for Sustainable Fuel Cycles (ATALANTE2024)*, Avignon, France (Sept 1-6, 2024).

(44) Nojima, M.; Tsushima, S.; Takao, K. "Explolation of Predominant Factors of U(VI) Precipitation Formation in the Advanced Reprocessing Technology Using Diamide Ligands" *6th International ATALANTE Conference on Nuclear Chemistry for Sustainable Fuel Cycles (ATALANTE2024)*, ACT08, Avignon, France (Sept 1-6, 2024).

(45) Tashiro, R.; Tsushima, S.; Gericke, R.; Takao, K. "Feasibility Study on PUREX-NUMAP Hybrid Reprocessing: Precipitation-Based Recovery of U(VI) from Organic Phases with 30% TBP" 6th International *ATALANTE Conference on Nuclear Chemistry for Sustainable Fuel Cycles (ATALANTE2024)*, Avignon, France (Sept 1-6, 2024).

(46) Nabata, R.; Tsushima, S.; Takao, K. "Development of preorganized N_3O_2-pentadentate planar ligand for uranium harvesting from seawater" *45th International Conference on Coordination Chemistry (ICCC2024)*, Fort Collins, Colorado, USA, (Jul 28-Aug 3, 2024).

(47) Takeyama, T.; Tsushima, S.; Takao, K. "Utility of redox-active ligands for reversible multi-electron transfer in uranyl(VI) complexes" *45th International Conference on Coordination Chemistry (ICCC2024)*, Fort Collins, Colorado, USA, (Jul 28-Aug 3, 2024). [Invited Talk].

(48) Takao, K. "Coordination Chemistry of Actinide Nitrates with *N*-Substituted 2-Pyrrolidone Derivatives for Simple and Versatile Separation of U, Pu, and Th in Nuclear Fuel Recycling Scheme" *45th International Conference on Coordination Chemistry (ICCC2024)*, Fort Collins, Colorado, USA, (Jul 28-Aug 3, 2024). [Invited Talk].

Oral Presentation in international or domestic conferences

(1) Hiroshi Akatsuka: Practical Measurement of Plasma Electron Temperature and Density Using Optical Emission Spectroscopy and Machine Learning; *Japan Society for the Promotion of Science R052 DX Plasma Processing Committee 5th Research Meeting*, Tokyo, April 23, 2024.

(2) Yuya Yamashita, Kenta Doi, Tetsuji Kiyota, Yuchen Ye, Kazuki Shimatani, Wentao He, Hinata Hanyu, Wataru Kikuchi, Ayaki Sakurai, Atsushi Nezu, Hiroshi Akatsuka: Positional Distribution Diagnosis of Electron Temperature, Electron Density, and EEDF of CF_4/O_2/Ar plasma Based on Tomographic Optical Emission Spectroscopic Measurement and Argon Collisional-Radiative Model; *The 85th JSAP Autumn Meeting 2024*, Niigata, September 16–20, 2024, 20a-A32-5.

(3) Koji Kikuchi, Hiroshi Akatsuka: Discussion on Electron Temperatures of Non-Equilibrium Plasma Based on Principle of Maximum Tsallis and Rényi Entropy; *The 41st annual meeting of The Japan Society of Plasma Science and Nuclear Fusion Researc*h, Tokyo, November 17–20, 2024, 17Bp08.

(4) Yuchen Ye, Kenta Doi, Tetsuji Kiyota, Shuhei Watanabe, Kazuki Shimatani, Ayaki Sakurai, Yuya Yamashita, Wataru Kikuchi, Atsushi Nezu, Hiroshi Akatsuka: Electron Temperature and Density Diagnosis in Argon Dual-Frequency ICP by Tomographic Optical Emission Spectroscopy and Langmuir Probe Measurements; *The 41st annual meeting of The Japan Society of Plasma Science and Nuclear Fusion Researc*h, Tokyo, November 17–20, 2024, 17P02.

(5) Jun Enomoto, Wataru Kikuchi, Tomoya Taguchi, Yuya Yamashita, Atsushi Nezu, Hiroshi Akatsuka: Optical Emission Spectroscopy Measurement of Atmospheric Pressure Plasma Jet Considering Ionic Continuum Spectrum; *The 41st annual meeting of The Japan Society of Plasma Science and Nuclear Fusion Researc*h, Tokyo, November 17–20, 2024, 17P15.

(6) Koji Kikuchi, Hiroshi Akatsuka: Electron Temperature Analysis of Non-Equilibrium Plasmas Based on Nonextensive Statistical Mechanics; *2024 Annual Conference of the Institute of Engineers on Electrical Discharges in Japan*, On-Line, November 29, 2024, A-5. [Outstanding Paper Presentation Award]

(7) Hiroshi Akatsuka, Koji Kikuchi: Reexamination of the "Temperature" of Nonequilibrium Excited-State Distributions Based on Nonextensive Statistical Mechanics; *2024 NIFS Atomic Process Workshop*, Toki, December 9–11, 2024.

(8) Yuya Yamashita, Kenta Doi, Tetsuji Kiyota, Yuchen Ye, Wataru Kikuchi, Kazuki Shimatani, Wentao He, Hinata Hanyu, Ayaki Sakurai, Atsushi Nezu, Hiroshi Akatsuka: Diagnostics of CF_4/O_2/Ar Plasmas Based on Tomographic Emission Spectroscopy and Ar Collisional-Radiative Model--Influence of Excited-State Distributions of Other Atomic Species on Diagnostic Results; *2024 NIFS Atomic Process Workshop*, Toki, December 9–11, 2024.

(9) Yuchen Ye, Kenta Doi, Tetsuji Kiyota, Shuhei Watanabe, Kazuki Shimatani, Ayaki Sakurai, Yuya Yamashita, Wataru Kikuchi, Atsushi Nezu, Hiroshi Akatsuka: Detection of Two-Temperature Distributions of Argon ICP Using Collisional-Radiative Model and Tomographic Optical Emission Spectroscopy; *2024 NIFS Atomic Process Workshop*, Toki, December 9–11, 2024.

(10) Hiroshi Akatsuka, Wataru Kikuchi, Jun Enomoto, Keren Lin: Measurement of Atmospheric-Pressure Plasma by Line and Continuum Emissions; *34th Annual Meeting of MRS-J*, Yokohama, December 16–18, 2024, B4-I16-001. [Invited Talk]

(11) Hiroshi Akatsuka: Enhancement of Plasma Measurement Using Optical Emission Spectroscopy and Machine Learning; *4th Seminar of 2024 CGDP [Centre for Low-Temperature Plasma Science Research]*, Nagoya, December 20, 2024. [Invited Talk]

(12) Koji Kikuchi, Hiroshi Akatsuka: Redefinition of the Temperature of Nonequilibrium Excited-State Distributions Based on Non-Extensive Statistical Mechanics; *The 42nd Symposium on Plasma Processing*, Oita, January 28–30, 2025, 30p-2.

(13) Hiroshi Akatsuka: Advances in Measurements of Electron Temperature and Density in Low-pressure Plasmas Using Optical Emission Spectroscopy and Data Science Techniques; *257th Research Meeting Nano-Micro Fabrication Research Committee*, *Silicon Technology Subcommittee of the Japan Society of Applied*

Physics, Tokyo, February 27, 2025, (2). [Special Invited Lecture]

(14) Wataru Kikuchi, Yuya Yamashita, Yuchen Ye, Jun Enomoto, Hiroshi Akatsuka: Automated Line Spectrum Detection and Integration in Plasma; *The 72nd JSAP Spring Meeting 2025*, Noda, March 14–17, 2025, 17a-K303-1.

(15) Koji Kikuchi, Hiroshi Akatsuka: Review of Electron Temperature of Non-Equilibrium Plasma Using a Nonextensive Extension to the Gibbs Entropy; *The 72nd JSAP Spring Meeting 2025*, Noda, March 14–17, 2025, 17p-K303-2.

(16) Jun Enomoto, Wataru Kikuchi, Tomoya Taguchi, Atsushi Nezu, Hiroshi Akarsuka: Elucidation of the Nitrogen Blue Afterglow in Atmospheric Pressure Helium Plasma Jets; *The 72nd JSAP Spring Meeting 2025*, Noda, March 14–17, 2025, 17p-K303-4.

(17) Koji Kikuchi, Hiroshi Akatsuka: Self-consistent Redefinition of the Excitation Temperature of Non-Equilibrium Plasma Based on Nonextensive Statistical Mechanics; *The 2025 Annual Meeting IEE of Japan*, Tokyo, March 18–20, 2025, 1-048.

(18) Ayaki Sakurai, Yuya Yamashita, Yuchen Ye, Kazuki Shimatani, Koki Fukumoto, Atsushi Nezu, Hiroshi Akatsuka: Changes in Non-Equilibrium Properties Due to Argon Contamination of ICP Discharge Nitrogen Plasma, *The 2025 Annual Meeting IEE of Japan*, Tokyo, March 18–20, 2025, 1-049.

(19) Yosuke Shimada, Hiroshi Akatsuka: Examination of Steady State for the Excitation Process of Argon Plasma Using a Collisional-Radiative Model Using Malliavin Analysis, *The Physical Society of Japan 2025 Spring Meeting*, On-line, March 18–21, 2025, 21pB1-4.

(20) J. Hasegawa, K. Takayama, S. Takano, K. Okamura, T. Yoshimoto, and W. Jiang: Operating Principles and Hardware of a DC Induction Accelerator in a Circular Accelerator; *2024 National Institute for Fusion Science Joint Research - Latest Trends in Pulsed Power Technology Development and Its Application to Quantum Beam and Plasma Technology Development*, online, Jan. 6-7, 2025.

(21) T. Watanabe, K. Takahashi, T. Sasaki, T. Kikuchi, J. Hasegawa, K. Horioka, J. Tamura, and K. Takayama: Formation of Liquid Metal Targets in a Rotating Drum for Application to Laser Ion Sources; *2024 National Institute for Fusion Science Joint Research - Latest Trends in Pulsed Power Technology Development and Its Application to Quantum Beam and Plasma Technology Development*, online, Jan. 6-7, 2025.

(22) K. Arai, J. Hasegawa: Estimation of DD Fusion Reaction Region in a Compact IEC Fusion Neutron Source; *2024 National Institute for Fusion Science Joint Research - Latest Trends in Pulsed Power Technology Development and Its Application to Quantum Beam and Plasma Technology Development*, online, Jan. 6-7, 2025.

(23) Z. Wang, J. Hasegawa: Optimization of Highly Ionized Ion Charge Distribution Measurement Using an Electrostatic Analyzer; *41st Annual Meeting of the Japan Society of Plasma Science and Nuclear Fusion Research*, Edogawa, Nov. 17-20, 2024.

(24) K. Yokoi, J. Hasegawa: Effect of Guide Magnetic Field on Ion Momentum Distribution in Laser-Produced Plasma; *41st Annual Meeting of the Japan Society of Plasma Science and Nuclear Fusion Research*, Edogawa, Nov. 17-20, 2024.

(25) Y. Liu, J. Hasegawa: Numerical Analysis of a Coaxial Cylindrical Inertial Electrostatic Confinement Thruster; *41st Annual Meeting of the Japan Society of Plasma Science and Nuclear Fusion Research*, Edogawa, Nov. 17-20, 2024.

(26) S. Mukoda, K. Noguchi, J. Hasegawa: Development of Plasma Ion Implantation Method Using Laser-Produced Drift Plasma; *41st Annual Meeting of the Japan Society of Plasma Science and Nuclear Fusion Research*, Edogawa, Nov. 17-20, 2024.

(27) K. Noguchi, S. Mukoda, J. Hasegawa: PIC Simulation of Plasma Ion Implantation Using Drift Plasma; *41st Annual Meeting of the Japan Society of Plasma Science and Nuclear Fusion Research*, Edogawa, Nov. 17-20, 2024.

(28) K. Arai, J. Hasegawa: Monte Carlo Calculation of Neutron Irradiation Fields in a Linear Fusion Neutron Source; *41st Annual Meeting of the Japan Society of Plasma Science and Nuclear Fusion Research*, Edogawa, Nov. 17-20, 2024.

(29) Noriyosu Hayashizaki: Study on Legal Regulation and Safety Management for Fission Chambers; *Proceedings of the 45th Annual Meeting of INMM Japan Chapter*, Tokyo, November 27-28, 2025, #4522.

(30) T. Tan, N. Idota, T. Tsukahara: Stimuli-Responsive Separation of Lanthanides using Zwitterionic Polymer Brushes; *Global 2024*, Tokyo, October 6-9, 2024, 2B3-01-03.

(31) T. Xu, N. Idota, T. Tsukahara: A Microfluidic-based Approach to Investigate Dissolution Mechanism of Uranium in Simulated Fuel Debris; *Global 2024*, Tokyo, October 6-9, 2024, 2B3-01-03.

(32) X. Qian, N. Idota, T. Tsukahara: Development of Droplet Microfluidic Separation Processes using Deep Eutectic Solvents; *Global 2024*, Tokyo, October 6-9, 2024, 3B1-01-03

(33) T. Tan, N. Idota, T. Tsukahara: Development on Mutual Separation of Lanthanides by Stimuli-Responsive Binary Polymer Brushes; *International Symposium on Green Transformation Initiative and Innovative Zero-Carbon Energy Systems (GXI-ZES)*, Tokyo, January 14-16, 2025, 1S6-1.

(34) P. Kai, N. Idota, T. Tsukahara: Development of Spiropyran-Based Photoswitchable Adsorbents for Selective Recovery of Lanthanide ions; *International Symposium on Green Transformation Initiative and Innovative Zero-Carbon Energy Systems (GXI-ZES)*, Tokyo, January 14-16, 2025, 1S6-3.

(35) T. Xu, N. Idota, T. Tsukahara: Evaluation of Leaching Behavior of Uranium from Simulated Fuel Debris Using Microfluidic Devices; *International Symposium on Green Transformation Initiative and Innovative Zero-Carbon Energy Systems (GXI-ZES)*, Tokyo, January 14-16, 2025, 1S8-1.

(36) Y. Zhang, C. Chao, A. Pangiota, N. Idota, M. Pineda, E. Fraga, T. Tsukahara: Microfluidic Analysis of Aggregation and Dissolution Behaviour of Cerium Oxide Nanoparticles Generated from Nuclear Fuel Debris; *International Symposium on Green Transformation Initiative and Innovative Zero-Carbon Energy Systems (GXI-ZES)*, Tokyo, January 14-16, 2025, 1S8-2.

(37) X. Jiawei, N. Idota, T. Tsukahara: Creation of Graphene-Macrocycle Hybrid Nanomaterials and Its Application to Cesium Separation; *International Symposium on Green Transformation Initiative and Innovative Zero-Carbon Energy Systems (GXI-ZES)*, Tokyo, January 14-16, 2025, 1S9-2.

(38) X. Qian, N. Idota, T. Tsukahara: Microfluidic Approach for Efficient Cesium Separation Using Deep Eutectic Solvents; *International Symposium on Green Transformation Initiative and Innovative Zero-Carbon Energy Systems (GXI-ZES)*, Tokyo, January 14-16, 2025, 1S9-3.

(39) Shota Ikeda, Noriyosu Hayashizaki: RF simulation of a TE211 mode single hybrid cavity linear accelerator; 2024 Annual Meeting of Atomic Energy Society of Japan, Miyagi, September 11-13, 2024, 3A08.

(40) Chikako Ishizuka: Production of medical isotopes and evaluation of radiation dose for therapy; *2024 Fall Meeting of the Atomic Energy Society of Japan (AESJ)*, Tohoku University Kawauchi Campus, Sendai, September 12, 2024, [2F_PL].

(41) Chikako Ishizuka, Masaomi Ueno, Osamu Iwamoto, Satoshi Takeda: Construction of nuclear fission data using machine learning (1) Overview of the study; *2024 Fall Meeting of the Atomic Energy Society of Japan (AESJ)*, Tohoku University Kawauchi Campus, Sendai, September 12, 2024, [2F10].

(42) Jingde Chen, Yuta Mukobara, Satoshi Chiba, Naoki Yamano, Tatsuya Katabuchi, Chikako Ishizuka: Construction of nuclear fission data using machine learning (2) Prediction and evaluation of fission product yields by machine learning; *2024 Fall Meeting of the Atomic Energy Society of Japan (AESJ)*, Tohoku University Kawauchi Campus, Sendai, September 12, 2024, [2F11].

(43) Yuta Mukobara, Tsunenori Inakura, Akira Ono, Satoshi Chiba, Tatsuya Katabuchi, Chikako Ishizuka: Benchmark comparison for intermediate-energy range relevant to heavy-ion cancer therapy using Antisymmetrized Molecular Dynamics and PHITS calculations; *2024 Fall Meeting of the Atomic Energy Society of Japan (AESJ)*, Tohoku University Kawauchi Campus, Sendai, September 12, 2024, [2F16].

(44) Michio Yamawaki, Hiroyasu Mochizuki, Chikako Ishizuka, Masahiko Nakase, Hiroshi Mitachi, Yoichiro Shimazu, Yuji Arita, Masashi Koyama, Kenichi Fukumoto, Takuya Goto: Feasibility study of molten chloride salt fast reactors (IV) –

Overview of the study; *2024 Fall Meeting of the Atomic Energy Society of Japan (AESJ)*, Tohoku University Kawauchi Campus, Sendai, September 13, 2024, [3G06].

(45) Yoshihisa Tahara, Chikako Ishizuka: Feasibility study of molten chloride salt fast reactors (IV) – Analysis of burn-up characteristics; *2024 Fall Meeting of the Atomic Energy Society of Japan (AESJ)*, Tohoku University Kawauchi Campus, Sendai, September 13, 2024, [3G08].

(46) Chikako Ishizuka: Development of machine-learning models for nuclear fission data; *GXI-ZES International Conference on Zero-Carbon Energy Systems*, Tokyo Institute of Technology, Tokyo, January 2025, [G05].

(47) Yuta Mukobara, Akira Ono, Satoshi Chiba, Tatsuya Katabuchi, Chikako Ishizuka: Evaluation of momentum fluctuations of nucleon wave packets on cross sections in heavy-ion therapy; *2025 Annual Meeting of the Atomic Energy Society of Japan (AESJ)*, Online Conference (using Zoom), March 12, 2025, [1A03].

(48) Chikako Ishizuka, Yuta Mukobara, Satoshi Chiba, Tatsuya Katabuchi: Exploring the fission mechanism through trajectory analysis of the four-dimensional Langevin model; *2025 Annual Meeting of the Atomic Energy Society of Japan (AESJ)*, Online Conference (using Zoom), March 12, 2025, [1A11].

(49) Jingde Chen, Yuta Mukobara, Satoshi Chiba, Tatsuya Katabuchi, Chikako Ishizuka: Verification of energy dependence of fission product yields predicted by machine learning; *2025 Annual Meeting of the Atomic Energy Society of Japan (AESJ)*, Online Conference (using Zoom), March 12, 2025, [1A12].

(50) Yoshihisa Tahara, Chikako Ishizuka: Feasibility study of molten chloride salt fast reactors (V) – Applicability of point reactor kinetics equations to molten salt fast reactors; *2025 Annual Meeting of the Atomic Energy Society of Japan (AESJ)*, Online Conference (using Zoom), March 13, 2025, [2D06].

(51) Itoh A., Konashi K., Arita Y., Yaita T., Tanida H., Kobayashi T., Fukuda T., Kobata M.: Development of ultra-high temperature in-situ observation technique for nuclear fuel (4) Analysis of transient state during Zr-Y2O3 test at high temperatures; *2024 Autumn Meeting of Atomic Energy Society of Japan*, Miyagi, September 9-11, 2024, 1O09.

(52) Itoh A.: Elucidation of Fuel Debris Formation Mechanisms Using High-Temperature Synchrotron XAFS; *The 38th Annual Meeting of the Japan Synchrotron Radiation Society & Joint Symposium on Synchrotron Radiation Science*, Ibaraki, January 10-12, 2025.

(53) Itoh A., Konashi K., Arita Y., Yaita T., Sibata G.: Development of ultra-high temperature in-situ observation technique for nuclear fuel (8) Comparison analysis with thermodynamic phase diagram for the UO_2-ZrO_2 reaction at high temperatures.; *2025 Annual Meeting of Atomic Energy Society of Japan*, On-line, March 12-14, 2025, 2G03.

(54) M. Maloney, T. Katabuchi, C. Ishizuka, G. Li1, H. Kondo, J. Han, Z. Shao, G. Rovira, S. Endo, A. Kimura, S. Nakamura: Measurement of neutron capture cross sections of Tc-99 at ANNRI of J-PARC MLF; *2024 Fall Meeting of Atomic Energy Society of Japan*, Osaka, September 11-13, 2024, 2F01.

(55) Gerard Rovira, A. Kimura, S. Nakamura, S. Endo, O. Iwamoto, N. Iwamoto, T. Katabuchi: Neutron total and capture cross-section measurements of ^{nat}Er at ANNRI and resolved resonance analysis; *2024 Fall Meeting of Atomic Energy Society of Japan*, Osaka, September 11-13, 2024, 2F02.

(56) Jingde Chen, Yuta Mukobara, Satoshi Chiba, Naoki Yamano, Tatsuya Katabuchi, Chikako Ishizuka: Development of Fission Nuclear Data using Machine Learning (2) Fission Product Yield Prediction and Evaluation Using Machine Learning; *2024 Fall Meeting of Atomic Energy Society of Japan*, Osaka, September 11-13, 2024, 2F11.

(57) Yuta Mukobara, Tsunenori Inakura, Akira Ono, Satoshi Chiba, Tatsuya Katabuchi, Chikako Ishizuka: Intermediate energy benchmark comparison of Antisymmetrized Molecular Dynamics and PHITS; *2024 Fall Meeting of Atomic Energy Society of Japan*, Osaka, September 11-13, 2024, 2F16.

(58) Krittanai Kiatkongkaew, Hiroshi Sagara, Tatsuya Katabuchi, Chikako Ishizuka and Risa Kunitomo: Numerical Analysis of Photonuclear Reaction Detection using High Energy Gamma-ray from ^{7}Li(p,γ)^{8}Be reaction Triggered by Pelletron

Accelerator; *2024 Fall Meeting of Atomic Energy Society of Japan*, Osaka, September 11-13, 2024, 1O04.

(59) Yuta Mukobara, Akira Ono, Satoshi Chiba, Tatsuya Katabuchi, Chikako Ishizuka: The effect of momentum fluctuations in nucleon wave packets on cross-sections in heavy-ion therapy; *2025 Annuall Meeting of Atomic Energy Society of Japan*, Osaka, March 12-14, 2025, 1A03.

(60) Chikako Ishizuka, Yuta Mukobara, Satoshi Chiba, Tatsuya Katabuchi: Exploring fission mechanisms with four-dimensional Langevin trajectory analysis; *2025 Annuall Meeting of Atomic Energy Society of Japan*, Osaka, March 12-14, 2025, 1A11.

(61) Jingde Chen, Yuta Mukobara, Satoshi Chiba, Naoki Yamano, Tatsuya Katabuchi, Chikako Ishizuka: Development of Fission Nuclear Data using Machine Learning (2) Fission Product Yield Prediction and Evaluation Using Machine Learning; *2025 Annuall Meeting of Atomic Energy Society of Japan*, Osaka, March 12-14, 2025, 1A12.

(62) Tsushi Kimura, Tatsuya Katabuchi, Jun-ichi Hori, Osamu Iwamoto, Nobuyuki Iwamoto, Shoji Nakamura, Shinsuke Nakayama, Shunsuke Endo, Gerard Rovira, Chikako Ishizuka, Hiroshi Yashima, Kazushi Terada, and Yoshiyuki Takahashi: Improvement of accuracy of neutron-induced fission reaction data for MAs（I）; *2025 Annuall Meeting of Atomic Energy Society of Japan*, Osaka, March 12-14, 2025, 1A13.

(63) S. Funayama, H. Takasu, Y. Kato: Numerical investigation on composite materials using calcium hydroxide and silicon-impregnated silicon carbide foams for thermochemical energy storage, *The 61st National Heat Transfer Symposium*, 2024/05/30, Kobe.

(64) K. Fujii, S. Funayama, H. Takasu, Y. Kato: Optimization of calcium hydroxide composite material using silicon-impregnated silicon carbide honeycomb, *The 61st National Heat Transfer Symposium*, 2024/05/30, Kobe.

(65) H. Saeki, T. Sugiyama, T. Izaki, K. Tomita, S. Tamano, S. Funayama, T. Kato, H. Takasu, Y. Kato: Performance evaluation of an indirect fixed-bed reactor using calcium oxide/water-based thermochemical energy storage materials, *The 61st National Heat Transfer Symposium*, 2024/05/30, Kobe.

(66) Kikuchi Kohei, Sasa Daisuke, Suzuki Takeshi, Kikura Hiroshige Development of an Oblique-Incidence Ultrasonic Water Level Measurement Technique for Enhanced Safety in Severe Nuclear Accidents. *The 1st Asian Workshop on Flow Measurement Techniques using Ultrasound and UVP,* Hanoi, Vietnam, March 11-13, 2025.

(67) Masataka Teshigawara, Hiroshige Kikura, Naruki Shoji, Hideki Kawai: Application of UVP to Multiphase Flow Measurement in Large Diameter Metal Pipe; *The 1st Asian Workshop on Flow Measurement Techniques using Ultrasound and UVP* Hanoi, Vietnam, March 11-13, 2025.

(68) Seitaro Ueno, Masataka Teshigawara, Naruki Shoji, Koji Teramoto, Hideki Kawai and Hiroshige Kikura: Consideration of signal difference in each phase using UVP of solid-gas-liquid three-phase flow measurement; *The 1st Asian Workshop on Flow Measurement Techniques using Ultrasound and UVP*, Hanoi, Vietnam, 11-13, 2025.

(69) Yutaka Namiki, Hiroshige Kikura: Development of a flow velocity distribution visualization system in piping by integrating UVP, CFD simulation and AR technology; *The 1st Asian Workshop on Flow Measurement Techniques using Ultrasound and UVP,* Hanoi, Vietnam, 11-13, 2025.

(70) Lechen Lu, Hiroshige Kikura, Weichen Zhang: Fundamental research on Ultrasonic Measurement of High-temperature Fluid; *The 1st Asian Workshop on Flow Measurement Techniques using Ultrasound and UVP*, Hanoi, Vietnam, 11-13, 2025.

(71) Shuji OSHIMA, Naruki Shoji, Weichen Zhang, Hideki Kawai, Hideharu Takahashi, Hiroshighe Kikura, Nobuyoshi Tsuzuki: Basic research on the development of ultrasonic receiver sensors based on light deflection phenomena; *The 1st Asian Workshop on Flow Measurement Techniques using Ultrasound and UVP*, Hanoi, Vietnam, 11-13, 2025.

(72) Hibikki Kohama, Hiroshige Kikura, Takahiko Tanahashi, Seitaro Ueno, Yutaka Namiki, Masataka Teshigawara: Advanced First-Order Differential Modules and Detailed Error Verification Using CubicDEL Method: Toward Open Platform Implementation; *JASE Kanto Student Association The 64th Student Member*

Graduation Research Presentation, 932, Saitama Univercity, 2025.3.3.

(73) Shuji Oshima, Naruki Shoji, Weichen Zhang, Hideki Kawai, Hideharu Takahashi, Hiroshige Kikura, Nobuyoshi Tsuzuki: Fundamental research on the system development of ultrasonic receiver sensors utilizing the light deflection phenomena; *AESJ Kanto Koshinetsu Branch The 18th Student Research Presentation Meeting on Nuclear and Radiation Field* , A13, Tokyo, 2025.2.28.

(74) Yuan CHEN, Lechen LU, Yuaki KAMIMURA, Takumi NANBA, Hiroshige KIKURA: Fundamental study of the UVP flow measurement of narrow gap flow; *JASME 102nd Fluid Engineering Division Meeting,* OS04-07,Nagaoka, 2024.11.20.

(75) Shuji Oshima, Naruki Shoji, Hiroshige Kikura, Hideharu Takahashi: Fundamental Research on an Ultrasonic Signal Reception System Utilizing Laser Beam Displacement; *JASME 102nd Fluid Engineering Division Meeting,* OS04-07, Nagaoka, 2024.11.20.

(76) Weichen Zhang, Hiroshige Kikura, Yutaka Tamaura, Tadashi Kawamoto: Investigation of Radiation Effects on All-Solid-State Battery Performance; *AESJ The 23rd Young Researchers' Presentation*, Tokyo, 2024 11.8

(77) Weichen Zhang, Hiroshige Kikura, Yutaka Tamaura, Tadashi Kawamoto: Performance Evaluation of All-Solid-State Batteries in a Radiation Environment; 2O17,*AESJ 2024 Fall Meeting*, Tohoku Univ., 2024.9.11-13.

(78) Yuki Kamimura, Seigo Kai, Hideharu Takahashi, Hayato Taniguchi, Akihiko Kawashima, Takeshi Sugiura, Hiroshi Takahashi, Keisuke Jinza, Hiroshige Kikura:Fundamental Study on Mechanism of Blasting Decontamination Device for Small Diameter Pipe (Part 7); 3L04,*AESJ 2024 Fall Meeting*, Tohoku Univ., 2024.9.11-13.

(79) Masataka Teshigawara, Hioroshige Kikura, Naruki Shoji, Takeshi Suzuki, Daisuke Sasa: Evaluation of Applicability of Flowmeter based on Ultrasonic Velocity Profiler Method to Nuclear Power Plant; 2I14, *AESJ 2024 Fall Meeting*, Tohoku Univ., 2024.9.11-13.

(80) Shuji Oshima, Kazuya Yasui, Hiroshige Kikura, Hideharu Takahashi: Development of a Pipe Gas Leakage Detection System Using Ultrasonic Wave;2I13, *AESJ 2024 Fall Meeting*, Tohoku Univ., 2024.9.11-13.

(81) Daisuke Sasa, Takeshi Suzuki, Kohei Kikuchi, Hiroshige Kikura: Clamp-On Ultrasonic Measurement for Reactor Pressure Vessel Water Level Monitoring; *JASME 2024 Annual Conference,* S018-03, Ehime Univ., 2024.9.9.

(82) Shuji Oshima, Kazuya Yasui, Hiroshige Kikura, Hideharu Takahashi: Visualization of Gas Leaks in Pipe Using Ultrasound; *The 52nd Visualization Symposium*, Okinawa Industry Support Center, 2024.7.19-21.

(83) Daisuke Sasa, Takeshi Suzuki, Kohei Kikuchi, Hiroshige Kikura: Ultrasound Propagation Simulation for the Development of a New Water Level Measurement Method Using Clamp-on Ultrasonic Transducers (2); *The 52nd Visualization Symposium*, Okinawa Industry Support Center, 2024.7.19-21.

(84) Masataka Teshigawara, Kohei Kikuchi, Yutaka Namiki, Lu Lechen, Hideharu Takahashi, C, Ryosuke Akagi, Takashi Enomoto, Taiki Yoshinaka, Shinji Hirakane: Study on Ultrasonic Propagation Characteristics of Molten Glass using Buffer Rod; *The 52nd Visualization Symposium*, Okinawa Industry Support Center, 2024.7.19-21.

(85) Hideki Kawai, Naruki Syoji, Yoshihiko Oishi, Hiroshige Kikura: UVP Measurement of Turbulent Stresses in Slurry Flow within Photosynthetic Algae Bioreactors; *The 52nd Visualization Symposium*, Okinawa Industry Support Center, 2024.7.19-21.

(86) Daisuke Sasa, Takeshi Suzuki, Kohei Kikuchi, Hiroshige Kikura: Fundamental Research on the Application of Clamp-On Ultrasonic Water Level Measurement Techniques in Power Plants; *The 28th Symposium on Power and Energy Technology*, C214, Kyoto, 2024.6.17.

(87) Yuxing Liu, Shintaro Yasui, Yoshinao Kobayashi: Modification of Alumina Inclusions in Molten Steel by Calcium Treatment, *International Symposium on Green Transformation Initiative and Innovative Zero-Carbon Energy Systems; GXI-ZES*, 14 - 16 January 2025, Tokyo, Japan, Jan. 2025.

(88) Yoshinao Kobayashi and Keisuke Nagase: Approach for smelting reduction process by carbon neutral reducing gas; *International*

Symposium on Green Transformation Initiative and Innovative Zero-Carbon Energy Systems, GXI-ZES, 14 - 16 January 2025, Tokyo, Japan

(89) Yoshinao Kobayashi: Effects of Cooling Rate on Precipitation of Copper Sulfide in Low Carbon Steels; *The Second Symposium on Carbon Ultimate Utilization Technologies for the Global Environment, CUUTE-2*, November 15th, 2024

(90) Koki Imabayashi, Shintaro Yasui, Yoshinao Kobayashi. Evaluation of Cathode α-$NaFeO_2$ for Sodium-Ion Batteries; *PRiME2024*, Oct. 2024.

(91) Ryota Nomura, Shintaro Yasui, and Yoshinao Kobayashi: Preparation of Amorphous SiO_2 Coated $Li_4Ti_5O_{12}$ Anode and Their High Cycleability, *PRiME2024*, Oct. 2024.

(92) Yuxing Liu, Yoshinao Kobayashi and Shintaro Yasui: Modification of alumina inclusions in molten steel by calcium treatment; *The 188th ISIJ Meeting* Sep. 2024

(93) Yota Koike, Sota Hagiwara, Masatoshi Kondo: Chemical behaviors of ODS FeCrAl alloys in liquid lead bismuth eutectic stirred flow at 1173K; 2025 Annual Meeting of Atomic Energy Society of Japan, Online, March 12-14, 2025, 2G11.

(94) Shota Futami, Masatoshi Kondo, Effect of solidification shrinkage of liquid LiPb on exfoliation of α-Al2O3 layer formed on FeCrAl alloys; 2025 Annual Meeting of Atomic Energy Society of Japan, Online, March 12-14, 2025, 2I14.

(95) Kaoru Omiya, Johzaki Tomoyuki, Kanta Utsumi, Kazuki Matsuo, Masatoshi Kondo: Tritium breeding scenario of laser inertial fusion reactor with limited tritium fuel; 2025 Annual Meeting of Atomic Energy Society of Japan, Online, March 12-14, 2025, 2I07.

(96) Yoshiki Kitamura, Atsushi Kawarai, Masatoshi Kondo, Shigeru Saito, Hironari Obayashi: Adhesion strength of Al-rich oxide layer on FeCrAl alloy in flowing lead-bismuth eutectic; 2025 Annual Meeting of Atomic Energy Society of Japan, Online, March 12-14, 2025, 2G10.

(97) Kanta Utsumi, Kaoru Omiya, Masatoshi Kondo: Study on tritium breeding performance of various liquid metal breeders for laser inertial fusion reactors; 2024 Fall Meeting of Atomic Energy Society of Japan, Tohoku University Kawauchi Kita Campus, September 11-13, 2024, 3B11.

(98) Humam, Susumu Hatakeyama, Masatoshi Kondo: Metallurgical study on corrosion of 304 stainless steel accelerated by electromigration in liquid metal pool; 2024 Fall Meeting of Atomic Energy Society of Japan, Tohoku University Kawauchi Kita Campus, September 11-13, 2024, 2B02.

(99) Ryuhei Muto, Takashi Endo, Masatoshi Kondo, Study on growth behavior of abnormal oxides in FeCrAl alloy tube machined by WEDM process and mitigation methodology; 2024 Fall Meeting of Atomic Energy Society of Japan, Tohoku University Kawauchi Kita Campus, September 11-13, 2024, 2B03.

(100) Masatoshi Kondo, Kaoru Omiya, Kanta Utsumi, Tomoyuki Jozaki, Yoshitaka Mori, Kazuki Matsuo: Feasibility study on Laser inertial fusion Tritium Production Reactor (LTPR); 2024 Fall Meeting of Atomic Energy Society of Japan, Tohoku University Kawauchi Kita Campus, September 11-13, 2024, 3B10.

(101) Yoshiki Kitamura, Masatoshi Kondo: Effect of thermal cycling on adhesion of protective α-Al2O3 layer formed on ODS FeCrAl alloys; 2024 Fall Meeting of Atomic Energy Society of Japan, Tohoku University Kawauchi Kita Campus, September 11-13, 2024, 2B11.

(102) Bo Zhang, Yoshihisa Matsumoto: Regulatory roles of miR-20-5p and miR-424-5p in association with ZNF384 in colon adenocarcinoma deciphered through integrated network analysis and machine learning; *61st Annual Meeting of Radiation Biology Group, Japanese Society for Radiation Oncology*, Maebashi, May 17, 2024, G3-1.

(103) Yoshihisa Matsumoto: Molecular Mechanisms for DNA Damage Recognition and Cellular Response; *20th AMO Forum*, Wako, June 8, 2024 (Invited).

(104) Yoshihisa Matsumoto: Radiation sensitivity of Shin-Godzilla: From the aspect of DNA; *28th Research Workshop, International Association for Sensitization of Cancer Treatment*, Miyakojima, June 29, 2024, OS2.

(105) Yoshihisa Matsumoto: Research on the molecular mechanisms for the recognition and repair of DNA double-strand breaks and its application to cancer therapy; *67th Annual Meeting of Japanese Radiation Research Society*, Kitakyushu, September 25-28, 2024, Award Lecture.

(106) Yoshihisa Matsumoto: Radiation science education in elementary and junior high schools:

Passing correct knowledge, interest and importance of radiation science on to the future; *67th Annual Meeting of Japanese Radiation Research Society*, Kitakyushu, September 25-28, 2024, SY6-1.

(107) Rikiya Imamura, Mizuki Saito, Mikio Shimada, Yoshihisa Matsumoto: OGG1-dependent DNA single-strand breaks underline PARP inhibitor sensitivity of XRCC1-deficient cells; *67th Annual Meeting of Japanese Radiation Research Society*, Kitakyushu, September 25-28, 2024, AS2-4.

(108) Hisanori Tazuru, Rikiya Imamura, Mukesh Sharma, Mikio Shimada, Yoshihisa Matsumoto: Analysis of Phosphorylation in XRCC4 Extremely C-terminal Region in DNA Double-Strand Break Repair; *67th Annual Meeting of Japanese Radiation Research Society*, Kitakyushu, September 25-28, 2024, AS3-2.

(109) Mikio Shimada, Kensuke Otsuka, Yoshihisa Matsumoto: Live cell imaging by Focicle reporter in human iPS cells revelas DNA damage response alteration during neural development; *67th Annual Meeting of Japanese Radiation Research Society*, Kitakyushu, September 25-28, 2024, OS3-1.

(110) Yumin Huang, Tetsuya Sakashita, Yasuhiro Ohshima, Yoshihisa Matsumoto: Study on Non-uniformity of Single-Cell Dose Distribution in Targeted Alpha Therapy; *4th Annual Meeting of Japanese Society for Quantum Medical Science*, Chiba, December 6-7, 2024, O-3.

(111) Yumin Huang, Tetsuya Sakashita, Yasuhiro Ohshima, Ichiro Sasaki, Noriko S. Ishioka, Yoshihisa Matsumoto: Optimizing Dose Evaluation of Targeted Alpha Therapy with Experiments and Simulation; *International Symposium on Green Transformation Initiative and Innovative Zero-Carbon Energy Systems*, Tokyo, January 14-16, 2025, 1S8-3.

(112) Lingyan Fu, Rikiya Imamura, Tomoko Miyake, Kaima Tsukada, Yoshihisa Matsumoto, Mikio Shimada: Deciphering the mechanisms of PNKP regulation toward improvement of cancer radiotherapy; *International Symposium on Green Transformation Initiative and Innovative Zero-Carbon Energy Systems*, Tokyo, January 14-16, 2025, 1S9-4.

(113) Kazuki Yoshida, Mikio Shimada, Yoshihisa Matsumoto: Analysis of single nucleotide polymorphism of DNA double-strand break repair gene XRCC4 in EBV-immortalized lymphocyte from Japanese; *25th Sugahara-Ohnishi Memorial Symposium for Sensitization of Cancer Treatment*, Sagamihara, February 1-2, 2025, O2-6.

(114) Yoshihisa Matsumoto: Introduction and the "Cell Death"; *15th Radiation Biology Seminar*, Tokyo, March 1, 2025.

(115) Y. Murakami, X. Wang, S. Mitsui: Elucidations of the microstructure and the melting point lowering mechanism of the solid-state heat storage materials made by impregnating mannitol into covalent organic framework; *HTSJ International Heat Transfer Symposium*, Okinawa, May 14-17, 2025.

(116) Y. Murakami, Y. Ikeda, Y. Cho: LIQUID-TEHRMOELECTRICS — THERMO-ELECTROCHEMICAL POWER GENERATION AND THE FORCED-FLOW THERMOCELL; *The Third Asian Conference on Thermal Sciences (ACTS 2024)*, Shanghai, China, June 23-27, 2024.

(117) Xiaohan Wang, Shoma Mitsui, Shiori Nakagawa, Hiroki Fujisawa, Meguya Ryu, Junko Morikawa, Yoichi Murakami: DEVELOPMENT OF HEAT STORAGE MATERIAL USING COVALENT ORGANIC FRAMEWORK IMPREGNATED WITH SUGAR ALCOHOLS; *The Third Asian Conference on Thermal Sciences (ACTS 2024)*, Shanghai, China, June 23-27, 2024.

(118) Yoichi Murakami, Shoma Mitsui, Shiori Nakagawa, Xiaohan Wang, Hiroki Fujisawa, Meguya Ryu, Junko Morikawa: NEW HEAT STORAGE COMPOSITE USING SUGAR ALCOHOL IMPREGNATED IN COVALENT ORGANIC FRAMEWORKS AND THE THERMAL PROPERTIES; *The Third Pacific Rim Thermal Engineering Conference (PRTEC2024)*, Honolulu, Hawaii, USA, December 15-19, 2024.

(119) Yoichi Murakami, Shoma Mitsui, Shiori Nakagawa, Xiaohan Wang, Hiroki Fujisawa, Meguya Ryu, Junko Morikawa: NEW HEAT STORAGE COMPOSITE USING SUGAR ALCOHOL IMPREGNATED IN COVALENT ORGANIC FRAMEWORKS AND THE THERMAL PROPERTIES; *The Third Pacific Rim Thermal Engineering Conference (PRTEC2024)*, Honolulu, Hawaii, USA, December 15-19, 2024.

(120) Riku Enomoto, Yoichi Murakami: HIGHLY EFFICIENT PHOTON UPCONVERSION SOLID-SOLUTION CRYSTALS ENABLED BY LONG DISTANCE INTER-MOLECULAR

ENERGY TRANSFER FOR EFFICIENT SOLAR SPECTRUM UTILIZATION; *The Third Pacific Rim Thermal Engineering Conference (PRTEC2024)*, Honolulu, Hawaii, USA, December 15-19, 2024.

(121) M. Nakase, T. Okamura, T. Nishihara: [Invited] Optimizing the Fuel Cycle and Advancing Deep Geological Repositories with Digital Twins and Innovative Technologies; *Seventh International Conference on Geological Repositories (ICGR-7)*, Korea, Busan, May 27-31, 2024.

(122) M. Nakase, T. Nishihara, F. H. Ikhwan, T. Okamura, K. Matsui: Development of integrated actinide chemistry application, AACE, for acceleration of actinide chemistry experiments; *6th International Conference on Nuclear Chemistry for Sustainable Fuel Cycles (Atalante2024)*, France, Avignon, September 1-6, 2024.

(123) T. Okamura, R. Takahashi, T. Shimada, M. Nakase, T. Yamamura, K. Takeshita: Research on Sustainable Nuclear Energy Use with Actinide Management: Scenario Study on High-Level Waste Generation with MA Separation and Intermediate Storage Technology Implementation; *6th International Conference on Nuclear Chemistry for Sustainable Fuel Cycles (Atalante2024)*, France, Avignon, September 1-6, 2024.

(124) M. Yamawaki, H. Mochizuki, C. Ishizuka, M. Nakase, K. Mitachi, Y. Shimazu, Y. Arita, T. Koyama, K. Fukumoto, T. Goto: Feasibility Study of Integral Molten Chloride Salt Fast Reactor (IV)(1) Outline of the Study; *Atomic Energy Society of Japan 2024 Autumn Meeting*, Japan, Sendai, September 11-13, 2024.

(125) M. Nakase: Feasibility Study of Integral Molten Chloride Salt Fast Reactor (IV)(4) Consideration of waste disposal methods; *Atomic Energy Society of Japan 2024 Autumn Meeting*, Japan, Sendai, September 11-13, 2024.

(126) T. Suzuki, T. Okamura, M. Nakase, K. Nishihara, T. Abe: Development of Detailed Japanese Models for Quantitative Evaluation in Nuclear Power Generation Scenarios; *Atomic Energy Society of Japan 2024 Autumn Meeting*, Japan, Sendai, September 11-13, 2024.

(127) T. Yamamura, T. Shimada, T. Okamura, M. Nakase, K. Takeshita, H. Konishi, K. Nishimura, T. Tsukamoto, H. Ishida, Y. Ban: Investigation on Fuel Cycle based on Actinide Management Towards Sustainable Use of Nuclear Energy(1)Challenges of LWR fuel cycle and Research Overview; *Atomic Energy Society of Japan 2024 Autumn Meeting*, Japan, Sendai, September 11-13, 2024.

(128) T. Okamura, M. Nakase, K. Takeshita, T. Shimada, H. Konishi, K. Nishimura, H. Ishida, T. Yamamura: Investigation on Fuel Cycle based on Actinide Management Towards Sustainable Use of Nuclear Energy(2)Analysis of the necessity and usefulness of MA temporary storage technology for the sustainable nuclear fuel cycle; *Atomic Energy Society of Japan 2024 Autumn Meeting*, Japan, Sendai, September 11-13, 2024.

(129) M. Nakase: Current Status and Next Development of Fuel Cycle Analysis Technique for the Future Scenarios(5)Considerations for Benchmark of Future Nuclear Fuel Cycle Technologies; *Atomic Energy Society of Japan 2024 Autumn Meeting*, Japan, Sendai, September 11-13, 2024.

(130) K. Takeshita, T. Okamura, M. Nakase: Impacts of the Introduction of Metal-Fuel Fast Reactor Cycle on the Sustainable Use of Nuclear Energy; *Atomic Energy Society of Japan 2024 Autumn Meeting*, Japan, Sendai, September 11-13, 2024.

(131) K. Takeshita: Current Status and Next Development of Fuel Cycle Analysis Technique for the Future Scenarios(1)Significance of Fuel Cycle Analysis and Purpose of Establishment of the Committee; *Atomic Energy Society of Japan 2024 Autumn Meeting*, Japan, Sendai, September 11-13, 2024.

(132) T. Okamura: Current Status and Next Development of Fuel Cycle Analysis Technique for the Future Scenarios(2)Domestic and International Activities of Fuel Cycle Analysis; *Atomic Energy Society of Japan 2024 Autumn Meeting*, Japan, Sendai, September 11-13, 2024.

(133) K. Nishihara: Current Status and Next Development of Fuel Cycle Analysis Technique for the Future Scenarios(3)Current status and Issues of Fuel Cycle Analysis Technique; *Atomic Energy Society of Japan 2024 Autumn Meeting*, Japan, Sendai, September 11-13, 2024.

(134) M. Nakase: Current Status and Next Development of Fuel Cycle Analysis Technique for the Future

Scenarios(5)Considerations for Benchmark of Future Nuclear Fuel Cycle Technologies; *Atomic Energy Society of Japan 2024 Autumn Meeting*, Japan, Sendai, September 11-13, 2024.

(135) K. Shirasaki, M. Nakase: Effects of Competing Complexation with Crown Ethers in Sr(II) Solvent Extraction; *The 68th Symposium of the Radiochemistry Society of Japan*, Japan, Shizuoka, September 23-25, 2024.

(136) T. Miyawaki, K. Shirasaki, M. Nakase: Evaluation of extraction behavior of 228Ac by D2EHPA under pH region; *The 68th Symposium of the Radiochemistry Society of Japan*, Japan, Shizuoka, September 23-25, 2024.

(137) M. Nakase: [Invited] Chemical Experiments and Chemoinformatic Approach in Actinide Separation Chemistry; *Institute for Materials Research, Tohoku University Oarai / Alpha Joint meeting*, Japan, Sendai, September 25-27, 2024.

(138) T. Okamura, T. Nishihara, M. Nakase: An Inventory-Driven Approach to Optimizing Glassified Waste Loading in Vitrified Wasteforms; *The 6th Meeting on Nuclear Waste Glasses and Related Materials*, Japan, Chiba, September 27, 2024.

(139) K. Takeshita, T. Okamura, M. Nakase, K. Nishihara, T. Abe: Impact of Metal Fuel Fast Reactor Cycle Implementation on Back-end System including Final Disposal; *GLOBAL2024*, Japan, Tokyo, October 6-10, 2024.

(140) M.Nakase, S.Watanabe, Y.Sano, M.Takeuchi: Extraction chromatography technology for MA(III) recovery from spent MOX fuel(5)Column operation simulation; *GLOBAL2024*, Japan, Tokyo, October 6-10, 2024.

(141) T. Okamura, M. Nakase, K. Takeshita, T. Shimada, Y. Konishi, K. Nishimura, H. Ishida, T. Yamamura: Investigation on Fuel Cycle based on Actinide Management Towards Sustainable Use of Nuclear Energy(2)Analysis of the necessity and usefulness of MA temporary storage technology for the sustainable nuclear fuel cycle; *GLOBAL2024*, Japan, Tokyo, October 6-10, 2024.

(142) F. H. Ikhwan, M. Nakase, K. Konashi, C. Abe, A. R. Putra, T. Suzuki: Separation Behavior of Am/Cm on DGA Resin in Hydrochloric Acid Aqueous Solution; *GLOBAL2024*, Japan, Tokyo, October 6-10, 2024.

(143) T. Yamamura, T. Shimada, T. Okamura, M. Nakase, K. Takeshita, Y. Konishi, K. Nishimura, T. Tsukamoto, H. Ishida, Y. Ban, T. Sato, Y. Tsubata: Investigation on Fuel Cycle based on Actinide Management Towards Sustainable Use of Nuclear Energy(1)Challenges of LWR fuel cycle and Research Overview; *GLOBAL2024*, Japan, Tokyo, October 6-10, 2024.

(144) T. Shimada, T. Okamura, M. Nakase, K. Takeshita, R. Takahashi, H. Ishida, Y. Konishi, K. Nishimura, K. Hibi, H. Gima, T. Yamamura: Investigation on Fuel Cycle based on Actinide Management Towards Sustainable Use of Nuclear Energy(3)Policies of Actinides Management; *GLOBAL2024*, Japan, Tokyo, October 6-10, 2024.

(145) Y. Konishi, T. Shimada, H. Ishida, K. Nishimura, Y. Ban, Y. Tsubata, T. Sato, M. Nakase, K. Hibi, H. Gima, T. Yamamura: Investigation on Fuel Cycle based on Actinide Management Towards Sustainable Use of Nuclear Energy(4)Cycle Concept with ACM; *GLOBAL2024*, Japan, Tokyo, October 6-10, 2024.

(146) Y. Sano, S. Watanabe, M. Takeuchi, H. Fukumoto, T. Arai, S. Kim, M. Nakase, T. Tsukahara: Extraction chromatography technology for MA(III) recovery from spent MOX fuel (1) Overview of the research project; *GLOBAL2024*, Japan, Tokyo, October 6-10, 2024.

(147) K. Takeshita: Tokyo Tech‘s Collaboration Research with TEPCO for Decommissioning (1) Purpose of Establishing Collaborative Research Cluster and Its Research Activities; *International Topical Workshop on Fukushima-Daiichi Decommissioning Research 2024 (FDR2024)*, Japan, Fukushima, October 10-13, 2024.

(148) M. Nakase, R. Maki, S. Maruyama, T. Sakuragi, S. Tanaka, M. Harigai, H. Asano, T. Kobayashi, H. Kikunaga: Tokyo Tech's Collaboration Research with TEPCO for Decommissioning (8) Development of rapid solidification technology for 1F waste using advanced sintering methods; *International Topical Workshop on Fukushima-Daiichi Decommissioning Research 2024 (FDR2024)*, Japan, Fukushima, October 10-13, 2024.

(149) T. Okamura, T. Nishihara, M. Nakase: Tokyo Tech's Collaboration Research with TEPCO for Decommissioning (9) NEUCHAIN-F: Development of data management system for diversified 1F waste; *International Topical*

Workshop on Fukushima-Daiichi Decommissioning Research 2024 (FDR2024), Japan, Fukushima, October 10-13, 2024.

(150) F. H. Ikhwan, H. Kazama, C. Abe, K. Konashi, M. Nakase, T. Suzuki: Chromatographic Separation of Actinides High Accurate Mass Spectrometric Analyses; *International Topical Workshop on Fukushima-Daiichi Decommissioning Research 2024 (FDR2024)*, Japan, Fukushima, October 10-13, 2024.

(151) A. Gubarevich, R. Kubo, K. Yoshida, S. Yasui, M. Nakase, K. Takeshita, R. Masuda, K. Asano, A. Chiba, T. Sakai: Tokyo Tech's Collaboration Research with TEPCO for Decommissioning (6) Stable Solidification Technique for ALPS Sediment Wastes; *International Topical Workshop on Fukushima-Daiichi Decommissioning Research 2024 (FDR2024)*, Japan, Fukushima, October 10-13, 2024.

(152) H. Kikura, G. Endo, H. Takahashi, N. Ishii, S. Takahira, K. Takeshita: Tokyo Tech's Collaboration Research with TEPCO for Decommissioning (4) Development of Leak Investigation Technology in Reactor Building; *International Topical Workshop on Fukushima-Daiichi Decommissioning Research 2024 (FDR2024)*, Japan, Fukushima, October 10-13, 2024.

(153) M. Nakase: [Invited, International Advisory Panel] Socio-tech ecosystem & orchestration for accomplish disruptive nuclear innovation; *NEA Steering Committee meeting*, OCECD headquarter, France, Paris, October 24, 2024.

(154) M. Nakase, T. Nishihara, T. Rattanasirimaneewate, F. H. Ikhwan, T. Okamura, K. Matsui, A. S. M. Saleh: Exploration of Minor Actinide Extraction–Separation Systems Using Machine-Learning Approaches; The 37th Symposium on Japan Society of Ion Exchange, *The 43th Symposium on Solvent Extraction of Japan Association of Solvent Extraction*, Japan, Ibaraki, October 31-November 1, 2024.

(155) M. Nakase, T. Nishihara, T. Okamura, S. Watanabe, Y. Sano, M. Takeuchi: Development of an Efficient Parameter-Search Environment for Extraction Chromatography Calculations Using ANSYS Fluent and Python; The 37th Symposium on Japan Society of Ion Exchange, *The 43th Symposium on Solvent Extraction of Japan Association of Solvent Extraction*, Japan, Ibaraki, October 31-November 1, 2024.

(156) S. Ozawa, Y. Shiozawa, Y. Saijo, T. Miyajima, D. Matsumura, T. Tsuji, M. Nakase, T. Maehara: Elucidation of Redox Behavior of Cerium Ions in Glass Melts by In-situ Time-Resolved Ce K-edge DXAFS; *The 65th Symposium on Glass and Photonic Materials*, Japan, Fukuoka, November 7-8, 2024.

(157) M. Nakase: R & D activities related to digital technology, waste and knowledge management in Nakase lab; *Discussion with the IAEA on knowledge management*, Austria, Vienna, November 29, 2024.

(158) M. Nakase, T. Okamura, T. Nishihara: [Invited Lecture] Applicability of Machine Learning and Digital Technologies to Back-End Nuclear Fuel Cycle R&D — Activities at the Nakase Laboratory, Tokyo University of Science —; *Japan Atomic Energy Agency Academic Lecture*, Japan, Ibaraki, December 6, 2024.

(159) T. Okamura, T. Nishihara, M. Nakase: [Invited Lecture] NEUChain: Toward a Digital Twin of the Nuclear Industry Starting from Inventories; *Japan Atomic Energy Agency Academic Lecture,* Japan, Ibaraki, December 6, 2024.

(160) M. Nakase, R. Maki, S. Maruyama, T. Sakuragi, S. Tanaka, M. Harigai, H. Asano, H. Kikunaga, T. Kobayashi, H. Tanida: Development of Artificial Rockified Wasteforms for Stable Immobilization of Fuel Debris and Evaluation by Micro-XAFS; *The 38th Annual Meeting of the Japanese Society for Synchrotron Radiation Research Joint Symposium on Synchrotron Radiation Science*, Japan, Ibaraki, January 10-12, 2025.

(161) K. Takeshita, T. Okamura, N. Aizawa, M. Nakase, T. Shimada, K. Nishihara: Current Status and Next Development of Fuel Cycle Analysis Technique for the Future Scenarios: Research Committee on Fuel Cycle Analysis Technique for FutureNuclear Scenarios in Atomic Energy Society; *International Symposium on Green Transformation Initiative and Innovative Zero-Carbon Energy Systems, GXI-ZES*, Japan, Tokyo, January 14-16, 2025.

(162) T. Okamura, T. Abe, T. Suzuki, M. Nakase, K. Takeshita, K. Nishihara: Three Years of NMB4.0: A Driving Force Toward Nuclear Innovation

Through Open Access Nuclear Fuel Cycle Simulator Development; *International Symposium on Green Transformation Initiative and Innovative Zero-Carbon Energy Systems, GXI-ZES*, Japan, Tokyo, January 14-16, 2025.

(163) K. Takeshita: Sustainable Use of Nuclear Energy through Introduction of Fast Reactors and Fast Reactor Fuel Cycles; *NPO Innovative Nuclear Reactor Promotion Council Symposium: Thinking about the Future of Energy*, Japan, Fukui, February 15, 2025.

(164) K. Takeshita: [Special Lecture] Significance of Introducing Fast Reactor Fuel Cycles for Back-End Systems Including Final Disposal; *35th Nuclear Facility Decommissioning Technology Seminar*, Japan, Tokyo, February 17, 2025.

(165) M. Nakase: Screening of Fluorinated Super-Solvents for MA Extraction; *FY2024 Nuclear Energy Systems Research and Development Project Results Reporting Session*, Online, March 3, 2025.

(166) M. Nakase: Student Activity Report (2nd Cohort) — International Deployment of Nuclear R&D from the Zero-Carbon Institute Nakase Laboratory; *Science Tokyo, Institute of Integrated Research, Center for Fundamental Research, Research Results Presentation 2024*, Japan, Tokyo, March 4, 2025.

(167) M. Nakase: Application of Machine Learning in Actinide Separation Science — Toward Breaking the Impasse; *FY2024 Special Research Group on Actinide Chemistry and Its Applications, and RI Production for Medical Irradiation by Nuclear Reactors*, Online, March 5-6, 2025.

(168) T. Ohnuki, S. Utsunomiya, M. Nakase, M. Takano, T. Dohi: Experimental Elucidation of Cs and I Behavior within CsMP (Cesium-bearing Microparticles); *Atomic Energy Society of Japan 2025 Spring Annual Meeting*, Online, Japan, March 12-14, 2025.

(169) M. Nakase, T. Okamura, Y. Tahara, H. Mochizuki, T. Murakami, T. Koyama: Feasibility Study of Chloride Molten Salt Fast Reactors (V) — Evaluation of Quantities for Molten Salt Fast Reactors; *Atomic Energy Society of Japan 2025 Spring Annual Meeting*, Online, Japan, March 12-14, 2025.

(170) T. Abe, T. Suzuki, T. Okamura, M. Nakase, K. Nishihara, K. Takeshita: Implementation of an Ideal Centrifugal-Separation Cascade Enrichment Model into NMB4 and Quantitative Assessment of Scenarios Using Recovered Uranium; *Atomic Energy Society of Japan 2025 Spring Annual Meeting*, Online, Japan, March 12-14, 2025.

(171) T. Yamamura, M. Harigai, T. Shimada, T. Okamura, M. Nakase, K. Takeshita, Y. Konishi, K. Nishimura, T. Tsukamoto, Y. Ban: Research on Fuel Cycles with Actinide Management for Sustainable Nuclear Use (3) — Overview of Research and Processes and TRL Setting for Social Implementation; *Atomic Energy Society of Japan 2025 Spring Annual Meeting*, Online, Japan, March 12-14, 2025.

(172) T. Shimada, T. Yamamura, M. Harigai, M. Nakase, K. Takeshita, T. Okamura, Y. Ban, H. Tsukamoto, K. Nishimura, H. Gima: Research on Fuel Cycles with Actinide Management for Sustainable Nuclear Use (4) — Fundamental Policy and KPIs for Actinide Management in Fuel Cycles; *Atomic Energy Society of Japan 2025 Spring Annual Meeting*, Online, Japan, March 12-14, 2025.

(173) T. Okamura, M. Nakase, K. Takeshita, T. Shimada, K. Hibi, Y. Konishi, K. Nishimura, H. Ishida, T. Yamamura: Research on Fuel Cycles with Actinide Management for Sustainable Nuclear Use (5) — Quantitative Assessment of Actinide Management Functions during the LF Coexistence Phase; *Atomic Energy Society of Japan 2025 Spring Annual Meeting*, Online, Japan, March 12-14, 2025.

(174) T. Tsukamoto, Y. Konishi, K. Nishimura, T. Shimada, Y. Ban, Y. Tsubata, M. Nakase, T. Yamamura: Research on Fuel Cycles with Actinide Management for Sustainable Nuclear Use (7) — Development of MA Separation and Direct Conversion Processes Using Low-Vapor-Heat Diluent; *Atomic Energy Society of Japan 2025 Spring Annual Meeting*, Online, Japan, March 12-14, 2025.

(175) F. H. Ikhwan, M. Nakase, T. Nishihara, T. Okamura, K. Takeshita, T. Tsukamoto, K. Nishimura, T. Shimada, T. Yamamura: Investigation on Fuel Cycle based on Actinide Management Towards Sustainable Use of Nuclear Energy(8) Separation of minor actinide by using DGA derivatives and diluent with low heat of Vaporizatio; *Atomic Energy Society of Japan 2025 Spring Annual Meeting*, Online, Japan, March 12-

14, 2025.

(176) Hiroshi Sagara, Discussion on the 3S for Peaceful Use of Nuclear Energy for Future Generations (2) Concept of Nuclear Security and its implementation, AESJ 2024 Fall Mtg 2024. (Invited)

(177) Hong Fatt Chong, Hiroshi Sagara, Safety Properties of High-Temperature Gas-Cooled Reactor Core Layouts to Directly Reuse HALEU Spent Fuel, 1S4-1, International Symposium on Green Transformation Initiative and Innovative Zero-Carbon Energy Systems(GXI-ZES), Tokyo, 14th-16th January, 2025

(178) Chi Young HAN, Hiroshi SAGARA, Hidekazu ASANO, Material Balance in MA Separation and Recycling for Environmental Load Reduction in Nuclear Fuel Cycle, 1S6-3, International Symposium on Green Transformation Initiative and Innovative Zero-Carbon Energy Systems(GXI-ZES), Tokyo, 14th-16th January, 2025

(179) Mori Yusuke, Sagara Hiroshi, Chong Hong Fatt, Impact of Uranium-silicide fuels on simultaneous enhancement of nuclear safety-security features and fuel lifetime extension in large scale LWRs, 2P06, International Symposium on Green Transformation Initiative and Innovative Zero-Carbon Energy Systems(GXI-ZES), Tokyo, 14th-16th January, 2025 (Poster)

(180) Eva Lisowski, Hiroshi Sagara, Recycling RepU Containing Unseparated Np-237 to Improve the Sustainability and Proliferation-Resistance of Sodium-Cooled Fast Reactor Fuel Cycles, 1S4-2, International Symposium on Green Transformation Initiative and Innovative Zero-Carbon Energy Systems(GXI-ZES), Tokyo, 14th-16th January, 2025

(181) Krittanai Kiatkongkaew, Hiroshi Sagara, Kosuke Tanabe, Tatsuya Katabuchi, Chikako Ishizuka, Risa Kunitomo, Numerical Analysis of Photonuclear Reaction Detection using High Energy Gamma-ray from 7Li(p,g)8Be Triggered by Proton Accelerator, 3S12-2, International Symposium on Green Transformation Initiative and Innovative Zero-Carbon Energy Systems(GXI-ZES), Tokyo, 14th-16th January, 2025.

(182) Koji Tsutsui, Hiroshi Sagara, Evaluation of Measures for Enhancing the Efficiency of International Safeguards Activities Applied to SMRs, 1S15-3, International Symposium on Green Transformation Initiative and Innovative Zero-Carbon Energy Systems(GXI-ZES), Tokyo, 14th-16th January, 2025

(183) Shotaro Terayama, Hiroshi Sagara, Lisowski Eva, Safeguards by design of sodium-cooled fast reactor with online re-fueling function, 2P010, International Symposium on Green Transformation Initiative and Innovative Zero-Carbon Energy Systems(GXI-ZES), Tokyo, 14th-16th January, 2025 (Poster)

(184) Hayato Sato, Hiroshi Sagara, Chi Young Han, Yoshiki Kimura, Kosuke Tanabe, Estimating the origin of reprocessed Pu for Nuclear Forensics, 2P017, International Symposium on Green Transformation Initiative and Innovative Zero-Carbon Energy Systems(GXI-ZES), Tokyo, 14th-16th January, 2025 (Poster)

(185) Aya Eguchi, Hiroshi Sagara, Natsumi Mitsuboshi, Taketeru Nagatani, Applicability of passive neutron non-destructive assay technique -DDSI method- for Pu quantification in advanced fuels, 2P019, International Symposium on Green Transformation Initiative and Innovative Zero-Carbon Energy Systems(GXI-ZES), Tokyo, 14th-16th January, 2025 (Poster)

(186) Mori Yusuke, Hiroshi Sagara, Chong Hong Fatt, Performance analysis of large scale LWRs loaded with uranium-silicide fuels for enhancement of nuclear safety and security features, Proc. 45th Annual Mtg. INMMJ, P4551, Tokyo, 2024.

(187) Kusaka Yuto, Hiroshi Sagara, CHONG HONG FATT, Mori Yusuke, Enhancement of Core Lifetime and Safety Performance of Reduced-Moderation Water Reactors with Accident Tolerant HALEU Fuel -Research Plan-, Proc. 45th Annual Mtg. INMMJ, P4552, Tokyo, 2024.

(188) Nozomi Takechi , Hiroshi Sagara, Survey Research on Feasibility and 3S Characteristics of Off-grid Next-generation Small Module Reactors Satisfying Demand of Energy and Green Transformation in Industry Sector, Proc. 45th Annual Mtg. INMMJ, P4553, Tokyo, 2024

(189) Hayato SATO, Hiroshi SAGARA, Chi Young HAN , Yoshiki KIMURA, Kosuke TANABE, Estimating the origin of reprocessed Pu for

Nuclear Forensics(2) Identification of Key Signature Nuclides, Proc. 45th Annual Mtg. INMMJ, P4554, Tokyo, 2024

(190) Aya EGUCHI , Hiroshi SAGARA , Natsumi MITSUBOSHI, and Taketeru NAGATANI, Applicability of passive neutron non-destructive assay technique for Pu quantification in advanced fast fuels, Proc. 45th Annual Mtg. INMMJ, P4558, Tokyo, 2024

(191) Shotaro Terayama, Hiroshi Sagara, Lisowski Eva, Safeguards by design of sodium-cooled fast reactor with online re-fueling function, Proc. 45th Annual Mtg. INMMJ, P4557, Tokyo, 2024

(192) Krittanai Kiatkongkaew, Hiroshi Sagara, Kosuke Tanabe, Tatsuya Katabuchi, Chikako Ishizuka, Risa Kunitomo, Numerical Analysis of Photonuclear Active Interrogation Demonstration based on 7Li(p,γ)8Be Gamma-rays Triggered by Pelletron Accelerator, Proc. 45th Annual Mtg. INMMJ, P4559, Tokyo, 2024

(193) Eva Lisowski, Hiroshi Sagara, Neutronics and Proliferation Resistance Assessment of U-10Zr Fuel Containing Unseparated Np-237, Proc. 45th Annual Mtg. INMMJ, P4562, Tokyo, 2024

(194) Takato Ishii , Hiroshi Sagara, Vital Areas Identification Evaluation of Sodium Cooled Fast Reactors with New Threat Definition, Proc. 45th Annual Mtg. INMMJ, P4563, Tokyo, 2024

(195) Hong Fatt Chong, Hiroshi Sagara, Once-through High Burnup Fuel Management Strategy with Dual Neutron Energy Spectrum Core in HTGR(III) Analysis of Reactivity Insertion Accident, Proc. 45th Annual Mtg. INMMJ, #4501, Tokyo, 2024

(196) Tatsuya Katabuchi, ＊Risa Kunitomo, Hiroshi Sagara, Chikako Ishizuka, Krittanai Kiatkongkaew, Kosuke Tanabe, Development of a Detection Technique for Nuclear Materials Using the Proton-Lithium Nuclear Reaction as a Photon Source, Proc. 45th Annual Mtg. INMMJ, #4506, Tokyo, 2024

(197) Chi Young HAN, Hiroshi SAGARA, Yoshihisa MATSUMOTO, Noriyosu HAYASHIZAKI, Takehiko TSUKAHARA, Masako IKEGAMI, Tatsuya KATABUCHI, Hiroshige KIKURA, Koichiro TAKAO, Katsumi YOSHIDA, Hiroki TAKASU, and Satoshi MATSUURA, The Program of NRA Human Resource Development“Advanced Nuclear 3S Education and Training in Cyber-Physical Space (ANSET-CP)” (3) FY2024 Implementation Status, Proc. 45th Annual Mtg. INMMJ, #4515, Tokyo, 2024

(198) Takao, K.; Mizumachi, T.; Sato, M.; Ito, K.; Nabata, R.; Kaneko, M.; Takeyama, T.; Tsushima, S. "Development of Water-Compatible N3O2-Pentadentate Planar Ligands for Uranium Harvesting from Seawater" *6th International ATALANTE Conference on Nuclear Chemistry for Sustainable Fuel Cycles (ATALANTE2024)*, Avignon, France (Sept 1-6, 2024). [Keynote Lecture].

(199) Ono, R.; Takeyama, T.; Gericke, R.; März, J.; Duckworth, T.; Tsushima, S.; Takao, K. "Molecular and Crystal Structures of Pu(IV)-Nitrato Complexes with Double-Headed 2-Pyrrolidone Derivatives in HNO_3(aq)" *6th International ATALANTE Conference on Nuclear Chemistry for Sustainable Fuel Cycles (ATALANTE2024)*, Avignon, France (Sept 1-6, 2024).

(200) Nojima, M.; Tsushima, S.; Takao, K. "Explolation of Predominant Factors of U(VI) Precipitation Formation in the Advanced Reprocessing Technology Using Diamide Ligands" *6th International ATALANTE Conference on Nuclear Chemistry for Sustainable Fuel Cycles (ATALANTE2024)*, ACT08, Avignon, France (Sept 1-6, 2024).

(201) Tashiro, R.; Tsushima, S.; Gericke, R.; Takao, K. "Feasibility Study on PUREX-NUMAP Hybrid Reprocessing: Precipitation-Based Recovery of U(VI) from Organic Phases with 30% TBP" *6th International ATALANTE Conference on Nuclear Chemistry for Sustainable Fuel Cycles (ATALANTE2024)*, Avignon, France (Sept 1-6, 2024).

(202) Nabata, R.; Tsushima, S.; Takao, K. "Development of preorganized N_3O_2-pentadentate planar ligand for uranium harvesting from seawater" *45th International Conference on Coordination Chemistry (ICCC2024)*, Fort Collins, Colorado, USA, (Jul 28-Aug 3, 2024).

(203) Takeyama, T.; Tsushima, S.; Takao, K. "Utility of redox-active ligands for reversible multi-electron transfer in uranyl(VI) complexes" *45th International Conference on Coordination Chemistry (ICCC2024)*, Fort Collins, Colorado,

USA, (Jul 28-Aug 3, 2024). [Invited Talk].

(204) Takao, K. "Coordination Chemistry of Actinide Nitrates with *N*-Substituted 2-Pyrrolidone Derivatives for Simple and Versatile Separation of U, Pu, and Th in Nuclear Fuel Recycling Scheme" *45th International Conference on Coordination Chemistry (ICCC2024)*, Fort Collins, Colorado, USA, (Jul 28-Aug 3, 2024). [Invited Talk].

(205) WANG Jingting, TSUTSUi Hiroaki: Relations of Multi-layers Method and Magnetohydrodynamics; *2025 Annual Meeting Record, I.E.E. Japan*, Tokyo, March 18-20, 2025. 7-46

(206) K. Kurashima, H. Tsutsui: Analysis of Plasma Discharge Footage in Tokamak Device PHiX using Dynamic Mode Decomposition; *2024 Annual Meeting of The Japan Society of Plasma Science and Nuclear Fusion Research*, Tokyo, November 17-20, 2025, 17P06.

(207) H. Kamasawa, H. Tsutsui: Fast Reconstruction of Plasma Emission Distribution on Poloidal Cross Section from Camera Imaging of Plasma in QUEST; *2024 Annual Meeting of The Japan Society of Plasma Science and Nuclear Fusion Research*, Tokyo, November 17-20, 2025, 18P55.

(208) Mizuki Uenomachi: Development of novel nuclear medicine technology through simultaneous multi-photon and multi-nuclide measurement; *The 72nd JSAP Sprint Meeting 2025*, Chiba, Japan, March 14-17, 2025.

(209) Mizuki Uenomachi, Mom Hamdan, Boyu Feng, Kenji Shimazoe, Mitsuhiro Nogami, Keitaro Hitomi, Ayaki Takeda, Hidenori Toyokawa: Development of pixelated TlBr detectors with self-trigger pixel ASICs for Compton-PET hybrid camera; *2024 IEEE Nuclear Science Symposium, Medical Imaging Conference, and Room-Temperature Semiconductor Detectors Symposium*, Tampa, USA, October 26-November 2, 2024.

(210) Mizuki Uenomachi, Kenji Shimazoe, Mohammad Hamdan, Setsuo Sato, Ayaki Takeda, Daisuke Matsunaga, Yuji Okubo, Makoto Motoyoshi: Development of fine-pitch hybrid silicon pixel detectors with self-trigger function for electron tracking Compton imaging; *International Workshop on Radiation Imaging Detectors 2024*, Lisbon, Portugal, June 30-July 4, 2024.

(211) Mizuki Uenomachi: Development of Quantum Imaging via Nuclear Spin for Nuclear Medicine Applications; *The 6th Annual Meeting of the Quantum Life Science Society*, Tokyo, Japan, May 30-31, 2024.

(212) Yosuke Nishimura, Avadahesh K. Sharma, Anna Gubarevich, Katsumi Yoshida, Koji Okamoto: V&V of nuclear fuel oxidation behavior in sleeveless SiC-matrix during air ingress accident; *The 11th European Review Meeting on Severe Accident Research (ERMSAR2024)*, Stockholm, Sweden, May 14, 2024.

(213) Sakakibara Daichi, Anna Gubarevich, Masaki Kotani, Katsumi Yoshida: Effect of BN Interphase Formed by EPD Method on Mechanical Behavior of SiC_f/SiC Composites Fabricated by PIP Method; *10th International Congress on Ceramics (ICC10)*, Montreal, Canada, July 15, 2024, ICC-SYM1-007-2024.

(214) Yosuke Nishimura, Avadahesh Sharma, Anna Gubarevich, Katsumi Yoshida, Koji Okamoto: V&V of Accident Behaviors in Silicon Carbide Fuel Matrices for High-Temperature Gas-Cooled Reactors; *31st International Conference on Nuclear Engineering (ICONE 31)*, Prague, Czech Republic, August 8, 2024, ICONE31-135182.

(215) Ryotaro Kubo, Anna Gubarevich, Katsumi Yoshida: Investigation of immobilization process of Sr in whitlockite by cold sintering; *The Fourteenth International Conference on the Science and Technology for Advanced Ceramics (STAC14)*, Kanagawa, Japan, October 8, 2024, P18.

(216) Genki Hirano, Anna Gubarevich, Katsumi Yoshida: Synthesis of Cr_2AlB_2 by combustion synthesis process; *The Fourteenth International Conference on the Science and Technology for Advanced Ceramics (STAC14)*, Kanagawa, Japan, October 8, 2024, P19.

(217) Yu Nakano, Anna Gubarevich, Katsumi Yoshida: Reaction sintering of B_4C ceramics using induction heating; *The Fourteenth International Conference on the Science and Technology for Advanced Ceramics (STAC14)*, Kanagawa, Japan, October 10, 2024, 3B04.

(218) Alin Yoshida, Anna Gubarevich, Katsumi Yoshida: Sintering Behavior and Polytype Transformation of SiC Ceramics Influenced by Induction Heating; *The Fourteenth International Conference on the Science and Technology for*

Advanced Ceramics (STAC14), Kanagawa, Japan, October 10, 2024, 3B05.

(219) Haruki Setogawa, Anna Gubarevich, Katsumi Yoshida: The effect of SiC particle size and uniaxial pressure on cold sintering of SiC ceramics; *The Fourteenth International Conference on the Science and Technology for Advanced Ceramics (STAC14)*, Kanagawa, Japan, October 10, 2024, 3B06.

(220) Yosuke Nishimura, Anna Gubarevich, Katsumi Yoshida, Koji Okamoto: High temperature oxidation behavior of silicon-rich silicon carbide fuel matrices for innovative high-temperature gas-cooled reactors (HTGRs); *The Nuclear Materials Conference (NuMat2024)*, Singapore, October 16, 2024, 2A.C.29.

(221) Taketo Sawaki, Shun Narita, Anna Gubarevich, Katsumi Yoshida, Kento Matsukura, Yoshiaki Tazaki: Thermal stability and phase transition of $(Y, Gd, Yb)_5O_4F_7$; *The 38th International Japan-Korea Seminar on Ceramics*, Fukuoka, Japan, November 1, 2024, 1SC-06.

(222) Ryoto Takizawa, Katsumi Yoshida: Surface reaction of zirconia coating with different Y_2O_3 content prepared by AD method during sliding test; *The 38th International Japan-Korea Seminar on Ceramics*, Fukuoka, Japan, November 1, 2024, 1SC-12.

(223) Daisuke Kawai Anna Gubarevich, Katsumi Yoshida: Synthesis of B_6Si Ceramics by Induction Heating; *The 38th International Japan-Korea Seminar on Ceramics*, Fukuoka, Japan, November 1, 2024, 1SC-14.

(224) Katsumi Yoshida, Mizuki Sueda, Anna Gubarevich, Masaki Kotani: Formation of Ti_3SiC_2 interphase for SiC_f/SiC composites by electrophoretic deposition method and their mechanical properties; *The 38th International Japan-Korea Seminar on Ceramics*, Fukuoka, Japan, November 2, 2024, 2SC-14.

(225) Ryoto Takizawa, Katsumi Yoshida: Evaluation of sliding surface reaction of nano crystal structured zirconia coating with different Y_2O_3 content prepared by AD method; *10th Tsukuba International Coating Symposium (TICS 10)*, Tsukuba, Japan, December 10, 2024, S2-2.

(226) Tatsunori Ide, Hajime Kiyono, Tohru Suzuki, Kiyoshi Kobayashi, Tetsuo Uchikoshi, Anna Gubarevich, Katsumi Yoshida: Thermal shock resistance of crystallographic orientated Al_2O_3 fabricated by slip casting in strong magnetic field; *The Ceramic Society of Japan Annual Meeting 2024*, Kumamoto, March 14, 2024, 1P09.

(227) Ryoto Takizawa, Katsumi Yoshida: Mechanical, thermal and sliding properties of Nano-crystal structured Zirconia coating by AD method; *The Ceramic Society of Japan Annual Meeting 2024*, Kumamoto, March 15, 2024, 2M26.

(228) Anna Gubarevich, Katsumi Yoshida: Combustion synthesis and reactive sintering of boron carbide with electromagnetic induction assistance; *The Ceramic Society of Japan Annual Meeting 2024*, Kumamoto, March 16, 2024, 3K02.

(229) Katsumi Yoshida, Anna Gubarevich, Yukio Tachibana, Kuniyoshi Takamatsu, Shoichiro Okita, Yosuke Nishimura, Koji Okamoto: Investigation of fabrication process of SiC matrix fuel compacts for high temperature gas-cooled reactors by reaction sintering; *The Ceramic Society of Japan Annual Meeting 2024*, Kumamoto, March 16, 2024, 3M04.

(230) Yosuke Nishimura, Anna Gubarevich, Katsumi Yoshida, Kuniyoshi Takamatsu, Koji Okamoto: Multiphysics Behavior in HTGRs with High Power Density (1) Accident Behaviors of Fuel Matrices; *Atomic Energy Society of Japan 2024 Annual Meeting*, Osaka, March 27, 2024, 2E14.

(231) Taketo Sawaki, Shun Narita, Anna Gubarevich, Katsumi Yoshida, Kento Matsukura, Yoshiaki Tazaki: Fabrication of $(Y, Gd, Yb)_5O_4F_7$ ceramics and their mechanical and thermal properties; *The 37th Fall Meeting of The Ceramic Society of Japan*, Nagoya, September 11, 2024, 2N04.

(232) Daisuke Kawai, Anna Gubarevich, Katsumi Yoshida: Investigation of fast and low temperature synthesis of B_6Si ceramics using induction heating; *The 37th Fall Meeting of The Ceramic Society of Japan*, Nagoya, September 11, 2024, 2N17.

(233) Mizuki Sueda, Katsumi Yoshida, Anna Gubarevich, Masaki Kotani: Investigation of Ti_3SiC_2 interphase formation process for SiC_f/SiC composites by electrophoretic deposition method; *The 37th Fall Meeting of The Ceramic Society of Japan*, Nagoya, September 11, 2024, 2N22.

(234) Daichi Sakakibara, Anna Gubarevich, Masaki Kotani, Katsumi Yoshida: Formation process of

BN coating on SiC fibers by pulsed DC electrophoretic deposition method; *The 37th Fall Meeting of The Ceramic Society of Japan*, Nagoya, September 11, 2024, 2N23.

(235) Ryoto Takizawa, Katsumi Yoshida: Wear mechanism of zirconia coating by AD method by sliding test; *The 37th Fall Meeting of The Ceramic Society of Japan*, Nagoya, September 12, 2024, 3N07.

(236) Alin Yoshida, Katsumi Yoshida, Anna Gubarevich: Effect of induction heating on fast sintering behavior and polytype transformation of SiC; *The 37th Fall Meeting of The Ceramic Society of Japan*, Nagoya, September 12, 2024, 3R20.

BULLETIN OF THE
LABORATORY FOR ZERO-CARBON ENERGY

Vol.4 2025

2025年12月　印刷

編集兼
発行者　東京科学大学総合研究院
ゼロカーボンエネルギー研究所
責任者　加　藤　之　貴
〒152-8550 東京都目黒区大岡山2丁目12-1
電話　03－5734－3052
FAX　03－5734－2959

印刷所　昭和情報プロセス㈱
東京都港区三田5－14－3

Printed by
SHOWA JOHO PROCESS
Minato-ku, Tokyo, Japan